QUANTUM ENTANGLEMENT: GEOMETRIC QUANTIFICATION AND APPLICATIONS TO MULTI-PARTITE STATES AND QUANTUM PHASE TRANSITIONS

BY

TZU-CHIEH WEI

B.S., National Taiwan University, 1994
M.S., National Taiwan University, 1996

DISSERTATION

Submitted in partial fulfillment of the requirements
for the degree of Doctor of Philosophy in Physics
in the Graduate College of the
University of Illinois at Urbana-Champaign, 2004

Urbana, Illinois

QUANTUM ENTANGLEMENT: GEOMETRIC QUANTIFICATION AND APPLICATIONS TO MULTI-PARTITE STATES AND QUANTUM PHASE TRANSITIONS

Tzu-Chieh Wei, Ph.D.
Department of Physics
University of Illinois at Urbana-Champaign, 2004
Prof. Paul M. Goldbart, Advisor

The degree to which a pure quantum state is entangled can be characterized by the distance or angle to the nearest unentangled state. This geometric measure of entanglement is explored for bi-partite and multi-partite pure and mixed states. It is determined analytically for arbitrary two-qubit mixed states, generalized Werner, and isotropic states, and is also applied to certain multi-partite mixed states, including two distinct multi-partite bound entangled states. Moreover, the ground-state entanglement of the XY model in a transverse field is calculated and shown to exhibit singular behavior near the quantum critical line. Along the way, connections are pointed out between the geometric measure of entanglement, the Hartree approximation, entanglement witnesses, correlation functions, and the relative entropy of entanglement.

To my parents.

Acknowledgments

The person to whom I owe the greatest thanks is my advisor, Prof. Paul Goldbart. This thesis originated back to the early days of QUISS seminars here in UIUC, when once he described a simple geometric picture of entanglement. Under his insight and guidance, I was able to carry out his ideas further and they evolved into this thesis. In addition to working with him on quantum information science, I was and still am very fortunate to learn a lot of condensed matter physics from him.

Paul is not only a mentor for my scientific career, but is also a very caring friend in my everyday life. He and his wife, Jenny, treat me like a member of their family. While I was visiting him in Boulder, Colorado, where he spent his sabatical leave, they invited me to their house for dinner every night. I enjoyed staying with them and playing with their children Ollie and Greta, and I felt like at home. I also want to thank Jenny and the children for sharing their family time as Paul often invited me to their house for a cup of tea and then we worked till very late, sometimes after midnight.

Another mentor that I am very fortunate to have is Prof. Paul Kwiat. I want to thank him for bringing the science of quantum information to this campus and for building up a forum—the Quantum Information Science Seminar—to discuss quantum information science. The discussions with him and his group—Kwiat's Clan—have been very stimulating and enlightening. The Kwiat Clan has included Dave Branning, Daryl Achilles, Joe Altepeter, Julio Barreiro, Marie Ericsson, Mike Goggin, Onur Hosten, Evan Jeffrey, Nick Peters, Matt Rakher, and Aaron VanDevender. They are the people responsible for my involvement and interest in experimental quantum information processing. They taught me a lot about their experiments on quantum optics, and they even allowed me to adjust their waveplates! It is my privilege to work with them.

In addition to Paul and Paul, I would like to express my earnest thanks to Prof. Tony Leggett

and Prof. Mike Weissman for serving in both my Preliminary Exam and thesis committees and for many inspiring and stimulating discussions, which have greatly helped to shape my scientitific and intellectual outlook.

I am grateful to Smitha Vishveshwara, who is another source of insipration for me. She has educated me on a lot of science, including Luttinger liquids, bosonization, superfluid and Mott insulator transitions, shot noise, and critical dynamics. Her exuberant spirit is always an encouragement to me. She is also a very caring friend.

I would like to thank Prof. Brian DeMarco for educating me on optical lattices and atomic physics, as well as for showing me the coolest stuff in the Midwest, and Prof. Jim Eckstein for educating me on electro-optic frequency shifters. It is also a great pleasure for me to thank Prof. Alexey Bezryadin and Ulas Coskun, who kindly taught me a lot about carbon nanotube physics and shared with me many results of their beautiful research.

I am very grateful to Prof. Mike Stone and Prof. Eduado Fradkin for many insightful and enlightening discussions, which have greatly helped some of my projects.

I would like to thank other people in ESB: my office-mate and collaborator Swagatam Mukhopadyay for many stimulating discussions; David Pekker for teaching me the physics of Fiske modes; Dyutiman Das for collaboration and for helping me with numerical work; and Eun-Ah Kim, my former office-mate in Loomis Laboratory, for many useful suggestions and references.

I am also thankful to many people who have contributed to our Quantum Information Science Study Group: Julio Barreiro, Bryan Clark, David Ferguson, Richard Kassman, Nick Peters, Yu Shi, Smitha Vishveshwara, Xiangjun Xing, Guojun Zhu, and the many others who have particpated in our discussions.

I thank Yuli Lyanda-Geller for educating me on mesoscopic physics, when he was in Urbana. I also thank Mohit Randeria and Nandini Trivedi for useful discussions during their stay here.

It is a pleasure of me to thank several colleagues outside the University of Illinois: Marie Ericsson, Daniel James, Bill Munro, Frank Verstraete, and Andrew White, with whom I have had fruitful collaboration.

I also benefited a great deal from many enlightening discussions with Ivan Deutsch, Rosario Fazio, Pawel Horodecki, Gerardo Ortiz, Vlatko Vedral, and Lorenza Viola. I acknowledge useful

discussions with people that I met in Benasque: Howard Barnum, Dagmar Bruß, Ignacio Cirac, Wolfgang Dür, Jens Eisert, Otfried Gühne, Artur Ekert, L.-C. Kwek, Debbie Leung, Chiara Macchiavello, Kiran Manne, and Güfre Vidal, some of whom I have had the fortune to meet on several occasions.

I would also like to thank the directors, organizers, and participants of the Les Houches summer school on Nanoscopic Quantum Physics, where I enjoyed the intellectual stimulation of the scientific activities, as well as the breath-taking views of nature explored during my stay at the school.

During my graduate career here at the University of Illinois at Urbana-Champaign I have been supported in part by the Department of Physics, the U.S. Department of Energy, Division of Material Sciences under Award No. DEFG02-96ER45434, through the Federick Seitz Materials Research Laboratory at the University of Illinois at Urbana-Champaign, and the National Science Foundation under Grant No. EIA01-21568. I also acknowledge the receipt of a Mavis Memorial Fund Scholarship (2002), a Harry G. Drickamer Graduate Fellowship (2003), and a John Bardeen Award for graduate research (2004).

Finally, I dedicate this thesis to my parents, who have always been the strongest support behind me.

Table of Contents

List of Figures

List of Abbreviations

CHSH Clauser-Horne-Simony-Holt

CNOT Controlled-NOT

EPR Einstein-Podolsky-Rosen

GHZ Greenberger-Horne-Zeilinger

GME Geometric Measure of Entanglement

LHV Local Hidden Variables

LOCC Local Operations and Classical Communication

MREGS Minimal Reversible Entanglement Generating Set

NPT Negative Partial Transpose

PPT Positive Partial Transpose

QDC Quantum Data Compression

REE Relative Entropy of Entanglement

UPB Unextendible Product Bases

Chapter 1

Introduction to quantum entanglement

The superposition principle—one of the several postulates of quantum mechanics—produces consequences that deviate from the predictions of classical mechanics. Consider, e.g., a pair of spin-1/2 particles, each of which can inhabit an up ($|\uparrow\rangle$) or down ($|\downarrow\rangle$) spin state relative to some spin quantization axis or any linear combination of $|\uparrow\rangle$ and $|\downarrow\rangle$. Then two spin-1/2 particles can, e.g., be in a state $|\uparrow\downarrow\rangle$ or $|\downarrow\uparrow\rangle$, in which each spin has a definite direction. However, they are also allowed to be in the singlet state

$$|\Psi^-\rangle \equiv \frac{1}{\sqrt{2}}\left(|\uparrow\downarrow\rangle - |\downarrow\uparrow\rangle\right), \tag{1.1}$$

in which neither spin possesses a definite direction. States such as $|\Psi^-\rangle$ are said to be entangled, a term coined by Erwin Schrödinger in 1935. The two spins, which we shall call A and B, can be spatially far from each other, even—in principle—at galactic separations.

Suppose that a Stern-Gerlach measurement is performed on A and the result $|\uparrow\rangle$ is obtained. Then the spin state of B is in a definite state $|\downarrow\rangle$. However, if the result $|\downarrow\rangle$ is obtained for A then B, as required by quantum mechanics, is in the state $|\uparrow\rangle$. Quantum mechanics appears to imply a nonlocal correlation between the two spins. More specifically, if one consider observables for the state $|\Psi^-\rangle$, such as σ_A^z and σ_B^z, one obtains the following predictions from quantum mechanics:

$$\langle\sigma_A^z \otimes \sigma_B^z\rangle = -1, \quad \langle\sigma_A^z\rangle = \langle\sigma_B^z\rangle = 0. \tag{1.2}$$

Therefore, quantum mechanics can have the consequence that the expectation value of the product of the two observables is not necessarily equal to the product of the expectation values of the two observables, e.g.,

$$\langle \sigma_A^z \otimes \sigma_B^z \rangle \neq \langle \sigma_A^z \rangle \langle \sigma_B^z \rangle. \tag{1.3}$$

Actually, the results in Eq. (1.2) can be easily explained by a classical theory, e.g., the ensemble of the pairs of spins in the measurement is a statistical equal mixture of $\uparrow\downarrow$ and $\downarrow\uparrow$. The question of whether quantum mechanics can predict something that cannot be explained by classical theories remained unanswered until in 1964, when John S. Bell came up with an inequality that all classical local theories (usually called local hidden variable [LHV] theories; local in the sense that the measurement outcome on one side should not influence the other side) obey, whereas it can be violated by quantum mechanics. Clauser, Horne, Shimony, and Holt (CHSH) [1] later derived an inequality based on correlations, such as that in Eq. (1.2), that all classical local theories must satisfy:

$$\left| \langle \vec{\sigma} \cdot \vec{a} \otimes \vec{\sigma} \cdot \vec{b} \rangle + \langle \vec{\sigma} \cdot \vec{a} \otimes \vec{\sigma} \cdot \vec{b'} \rangle + \langle \vec{\sigma} \cdot \vec{a'} \otimes \vec{\sigma} \cdot \vec{b} \rangle - \langle \vec{\sigma} \cdot \vec{a'} \otimes \vec{\sigma} \cdot \vec{b'} \rangle \right| \leq 2, \tag{1.4}$$

where $\vec{a}$ and $\vec{a'}$ ($\vec{b}$ and $\vec{b'}$) are unit vectors, representing pairs of different orientations of the Stern-Gerlach apparatus at A (B). This Bell-CHSH inequality can be violated by the singlet state $|\Psi^-\rangle$, with the maximum value of the left-hand side being $2\sqrt{2}$ (see Appendix A for more details). The violation has been demonstrated experimentally, e.g., using photon polarization states [2, 3].

So far, we have been discussing the singlet state. What about other entangled states? Gisin [4] showed that any non-product two-spin-1/2 state indeed violates the CHSH inequality. This non-product, unfactorizable property of wavefunctions is entanglement, the characteristic trait of quantum mechanics, and is responsible for the deviation from classical theories.

Although entanglement was initially associated with a rather philosophical debate over the foundations of quantum mechanics, it has recently been discovered to be a useful resource. For example, for quantum cryptography Ekert [5] found that violation of the CHSH inequality can be used as a test of security in the process of the random key distribution via a spin singlet state. Bennett and Wiesner [6] found that transmission of a two-level quantum state (i.e., qubit), which is initially maximally entangled with another two-level system at the receiving end, can encode

classical information of two bits ("super dense-coding"). Bennett and co-workers [7] further found that with the shared maximal entanglement (i.e., a singlet state), an unknown two-level state can be faithfully reconstructed via communication of only two classical bits ("quantum teleportation"). All these tasks are made possible by entanglement. Although it is not yet clear whether entanglement is necessary for the speed-up of quantum algorithms, such as Shor's factoring [8] and Grover's searching [9], it has been established that entanglement does enable quantum computation. This is well illustrated by the so-called one-way quantum computer, due to Rossendorf and Brigel [10], in which an initial highly entangled state (specifically, a "cluster" state), together with subsequent local measurements alone, allows efficient execution of quantum computation.

Although violation of Bell inequalities is a necessary and sufficient signature of entanglement in the pure-state setting, the situation is more subtle in the setting of mixed states. What do we mean by a mixed state? When is a mixed state entangled? Let us begin with a familiar setting for density matrices, quantum statistical mechanics, where a Hamiltonian $\mathcal{H}$ leads to the density matrix ρ, given by

$$\rho = Z^{-1} e^{-\beta \mathcal{H}} = \sum_n \frac{e^{-\beta E_n}}{Z} |n\rangle\langle n|, \tag{1.5}$$

where $Z = \mathrm{Tr}(e^{-\beta \mathcal{H}})$, $\beta = 1/k_B T$, and $|n\rangle$ is the energy eigenstate with energy eigenvalue E_n. A more general description of a system than by wavefunctions is thus provided by a density matrix, which can be regarded as a probabilistic mixture of pure states, hence, the name mixed state:

$$\rho = \sum_i p_i |\psi_i\rangle\langle\psi_i|, \tag{1.6}$$

with $0 \leq p_i \leq 1$ and $\sum_i p_i = 1$. Both a wavefunction $|\psi\rangle$ and a density matrix ρ will hereafter be simply referred to as a state. The density a matrix description is necessary when the system interacts with an environment or when we only have access to part of a larger system. We remark that the decomposition in Eq. (1.6) is by no means unique. For example, the "white" distribution $\frac{1}{2}\mathbb{1}$ can be expressed as

$$\frac{1}{2}|\uparrow\rangle\langle\uparrow| + \frac{1}{2}|\downarrow\rangle\langle\downarrow| \tag{1.7}$$

or

$$\frac{1}{2}|+\rangle\langle+| + \frac{1}{2}|-\rangle\langle-|, \tag{1.8}$$

where $|\pm\rangle \equiv (|\uparrow\rangle \pm |\downarrow\rangle)/\sqrt{2}$. Furthermore, there is no requirement that the pure states in the decomposition be orthogonal to one another.

The idea of a *mixed* entangled state of two or more parties is naturally extended from the pure-state case as a state that allows *no* decomposition into a mixture of factorizable pure states. If a mixed state does have such a decomposition, it is said to be separable or unentangled. Despite its seemingly innocuous definition, the question of whether or not a mixed state is entangled turns out to present deep mathematical challenges. There have been proposed several useful criteria (usually called separability criteria) that can (but not always) determine whether or not a given state is entangled. It has been found that certain mixed states, although entangled, do not violate any Bell inequality and, even more surprisingly, allow a classical, local description [11]. Thus we see that entanglement in the mixed-state scenario is a much richer and subtler phenomenon than it is for pure states.

As Bell inequalities do not, in general, completely reveal entanglement for mixed entangled states, other approaches to quantifying entanglement have emerged. These include (i) entanglement as a quantifiable resource: entanglement of distillation and entanglement cost; (ii) information-theoretic considerations: relative entropy of entanglement and related measures; and (iii) other, mathematical approaches, including the central theme of this dissertation. Approach (i) is perhaps the most natural way to quantify entanglement. However, as we shall see later, it has so far been limited to the settings of two parties (i.e., bi-partite systems), and there are major difficulties in extending it to multi-paritite systems. Approaches (ii) and (iii) are thus seen as indispensible for providing a better understanding of entanglement in various settings, especially multi-partite ones. Although the measure that we shall focus on for most of this dissertation belongs to the mathematical approach, later we shall show that it is nevertheless related to other entanglement and physical properties.

As one of the central themes in the entanglement theory is to quantity the degree of entanglement, in the following, we shall introduce several important, standard measures of entanglement. We shall conclude this chapter with an overview of the dissertation.

1.1 Separability and entanglement

Let us define precisely whether a state is entangled or not. A state is entangled if it is not separable. A bi-partite state, describing parties A and B, $\rho_{\rm s}^{\rm AB}$ is separable (or unentangled) if and only if $\rho_{\rm s}^{\rm AB}$ can be expressed as

$$\rho_{\rm s}^{\rm AB} = \sum_i p_i \, \rho_i^{\rm A} \otimes \rho_i^{\rm B}, \tag{1.9}$$

where the $\{\rho_i^{A(B)}\}$'s are local states of A(B), which can be either pure or mixed, and $\{p_i\}$'s are probabilities with $0 \leq p_i \leq 1$ and $\sum_i p_i = 1$. Such a sum, in which the weights are non-negative, is called a convex sum. The generalization to multi-partite states involves including more parties:

$$\rho_{\rm s}^{\rm AB\cdots K} = \sum_i p_i \, \rho_i^{\rm A} \otimes \rho_i^{\rm B} \otimes \cdots \otimes \rho_i^{\rm K}. \tag{1.10}$$

In the present chapter we shall focus on bi-partite states. If a bi-partite state cannot be written as a convex sum of direct products of density matrices then it is entangled. However, this definition does not offer a practical way of determining separability or entanglement.

Peres [12] proposed a very simple but useful criterion for separability. As a density matrix is Hermitian and positive semi-definite, its transpose is still a valid density matrix. If we take the transpose of the matrices $\{\rho_i^{\rm B}\}$'s in Eq. (1.9), the resulting matrix, denoted by $\rho_{\rm s}^{\rm T_B}$, still contains non-negative eigenvalues. The operation is called partial transpose and can be defined for any bi-partite state:

$$\rho = \sum_{i,j,k,l} \rho_{ij;kl} |e_i^{\rm A} \otimes e_j^{\rm B}\rangle\langle e_k^{\rm A} \otimes e_l^{\rm B}| \longrightarrow \rho^{\rm T_B} \equiv \sum_{i,j,k,l} \rho_{i\underline{l};k\underline{j}} |e_i^{\rm A} \otimes e_j^{\rm B}\rangle\langle e_k^{\rm A} \otimes e_l^{\rm B}|, \tag{1.11}$$

where $|e_i^{\rm A} \otimes e_j^{\rm B}\rangle \equiv |e_i^{\rm A}\rangle \otimes |e_j^{\rm B}\rangle$ is the product basis used to represent the density matrix, and the underscores are used to highlight the changes under the partial transpose. Thus we have that if the state is separable, its partially transposed matrix has non-negative eigenvalues (usually called PPT). Said equivalently, if the state is not PPT under the partial transpose, the state must be entangled[1]. This is the Peres positive partial transpose (PPT) criterion for separability [12].

[1] In general, if a state has PPT, no entanglement can be distilled out from it [19]. But the state can be either unentangled or entangled. When the state has PPT and is also entangled, it is called a bound entangled state.

Let us examine the example of a singlet state $|\Psi^-\rangle$. When written in the form of density matrix in the basis $\{|\uparrow\uparrow\rangle, |\uparrow\downarrow\rangle, |\downarrow\uparrow\rangle, |\downarrow\downarrow\rangle\}$, it corresponds to the density matrix

$$|\Psi^-\rangle\langle\Psi^-| \longleftrightarrow \begin{pmatrix} 0 & 0 & 0 & 0 \\ 0 & \frac{1}{2} & -\frac{1}{2} & 0 \\ 0 & -\frac{1}{2} & \frac{1}{2} & 0 \\ 0 & 0 & 0 & 0 \end{pmatrix}. \tag{1.12}$$

The partial transpose takes it to

$$\begin{pmatrix} 0 & 0 & 0 & -\frac{1}{2} \\ 0 & \frac{1}{2} & 0 & 0 \\ 0 & 0 & \frac{1}{2} & 0 \\ -\frac{1}{2} & 0 & 0 & 0 \end{pmatrix}, \tag{1.13}$$

which has one negative eigenvalue, $-1/2$. Thus, via the PPT criterion we see that $|\Psi^-\rangle$ is entangled.

In general, this PPT criterion is necessary but not sufficient for establishing separability. However, it was shown by Horodecki and co-workers [13] that PPT is sufficient in the cases of $C^2 \otimes C^2$ (two-qubit) and $C^2 \otimes C^3$ (qubit-qutrit) systems: if two-qubit or qubit-qutrit states obey PPT, they are separable. On the other hand, if PPT is violated, the state is entangled. The extent to which a state violates PPT is manifested in the negative eigenvalues of the partially transposed density matrix, and can be used as a measure (not just an identifier) of entanglement; this measure is called the *negativity* [14, 15]. Following Życzkowski and co-workers [14], we define the negativity $\mathcal{N}$ to be twice the absolute value of the sum of the negative eigenvalues:

$$\mathcal{N}(\rho) = 2\max(0, -\lambda_{\text{neg}}), \tag{1.14}$$

where λ_{neg} is the sum of the negative eigenvalues of ρ^{T_B} and the factor of two is a normalization chosen such that the singlet state $|\Psi^-\rangle$ has $\mathcal{N} = 1$.

1.2 Entanglement of distillation

The notion of the entanglement of distillation was introduced by Bennett and co-workers [16, 17] to give an operational definition of the degree of entanglement. Suppose ρ represents the state of two particles possessed by two parties (usually referred to as Alice and Bob) separated by some distance. A way to envisage the degree of entanglement that ρ has is to ask how useful ρ is compared to a standard state, such as any of the four Bell states:

$$|\Psi^{\pm}\rangle \equiv \frac{1}{\sqrt{2}}(|01\rangle \pm |10\rangle), \quad |\Phi^{\pm}\rangle \equiv \frac{1}{\sqrt{2}}(|00\rangle \pm |11\rangle). \tag{1.15}$$

Here $\{|0\rangle, |1\rangle\}$ represents an orthonormal basis of a two-level system, for instance, the z-component of the spin of a spin-1/2 particle, or the polarization of a photon. More specifically, given n copies of the state ρ shared between Alice and Bob, how many pairs, say k, of Bell states can be obtained if each of Alice and Bob is allowed to (i) perform any local operations (including measurement) on the particles he or she possesses and (ii) share with the other party classical information, e.g., the outcome of some measurements. These operations are called local operations and classical communication (LOCC). The asymptotic limit

$$E_{\rm D}(\rho) \equiv \lim_{n\to\infty}(k/n), \tag{1.16}$$

is called the entanglement of distillation [16, 17]. In it, k is the average number of Bell states taken over different possibilities (due to measurement) of an optimal procedure. $E_{\rm D}$ quantifies the entanglement as a resource, using Bell states as a standard ruler.

Let us illustrate the idea with an example. Suppose ρ is a pure state corresponding to the ket

$$|\psi_\theta\rangle = \cos\theta|00\rangle + \sin\theta|11\rangle, \tag{1.17}$$

with $\theta \in [0, \pi/2]$. For $\theta = 0$ or $\pi/2$, it is not entangled. For the intermediate range of θ, the state is entangled, and maximally so at $\theta = \pi/4$. Suppose that two copies of non-maximally entangled

$|\psi_\theta\rangle$ are shared between Alice and Bob:

$$\begin{aligned}|\psi_\theta\rangle_{12}\otimes|\psi_\theta\rangle_{34} &= (\cos\theta|0_1 0_2\rangle+\sin\theta|1_1 1_2\rangle)\otimes(\cos\theta|0_3 0_4\rangle+\sin\theta|1_3 1_4\rangle)\\ &= \cos^2\theta|0_1 0_2 0_3 0_4\rangle+\sqrt{2}\cos\theta\sin\theta\frac{1}{\sqrt{2}}(|0_1 0_2 1_3 1_4\rangle+|1_1 1_2 0_3 0_4\rangle)+\sin^2\theta|1_1 1_2 1_3 1_4\rangle,\end{aligned}$$

where Alice has particles 1 and 3, whereas Bob has 2 and 4. Their joint goal is to extract a Bell state under LOCC.

Both parties can perform any local operations allowed by quantum mechanics. A possible operation is to measure the number of his/her particles in state $|1\rangle$ (e.g., the z-component of total angular momentum). If Alice measures the number of 1's of her particles to be 0 or 2 then the resulting state ($|0_1 0_2 0_3 0_4\rangle$ or $|1_1 1_2 1_3 1_4\rangle$) is unentangled. She needs to tell Bob to abort the operation, as there is now no entanglement to extract. But with probability $2\cos^2\theta\sin^2\theta$ she gets the state

$$|\psi\rangle=\frac{1}{\sqrt{2}}(|0_1 0_2 1_3 1_4\rangle+|1_1 1_2 0_3 0_4\rangle), \tag{1.18}$$

which is evidently entangled. But how do they establish from this a Bell state, say, $|\Phi^+\rangle$?

This time, Alice proceeds to perform a unitary transformation U on her particles and contacts Bob (which is when the classical communication takes place) and asks him to perform the same unitary transformation on *his* particles. Suppose that the unitary transformation they agree to perform is (also known as a CNOT operation)

$$U=\begin{pmatrix}1&0&0&0\\0&1&0&0\\0&0&0&1\\0&0&1&0\end{pmatrix} \tag{1.19}$$

in the basis of $\{|00\rangle,|01\rangle,|10\rangle,|11\rangle\}$. In particular, for it we have

$$U_{13}|0_1 1_3\rangle=|0_1 1_3\rangle,\ U_{13}|1_1 0_3\rangle=|1_1 1_3\rangle,\ U_{24}|0_2 1_4\rangle=|0_2 1_4\rangle,\ U_{24}|1_2 0_4\rangle=|1_2 1_4\rangle. \tag{1.20}$$

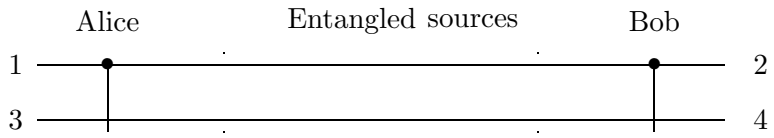

Figure 1.1: Entanglement of distillation.

Then the joint state after the transformations becomes

$$\begin{aligned} U_{13}U_{24}|\psi\rangle &= U_{13}U_{24}\left(\frac{1}{\sqrt{2}}(|0_1 0_2 1_3 1_4\rangle + |1_1 1_2 0_3 0_4\rangle)\right) \\ &= \frac{1}{\sqrt{2}}(|0_1 0_2 1_3 1_4\rangle + |1_1 1_2 1_3 1_4\rangle) \\ &= \frac{1}{\sqrt{2}}(|0_1 0_2\rangle + |1_1 1_2\rangle) \otimes |1_3 1_4\rangle. \end{aligned} \tag{1.21}$$

As particles 3 and 4 are not entangled with 1 and 2, what now needs to be done is that Alice throws away her particle 3 and Bob throws away his particle 4. Finally, they have distilled one maximally entangled pair $\frac{1}{\sqrt{2}}(|0_1 0_2\rangle + |1_1 1_2\rangle)$ out of two non-maximally entangled pairs. The probability P of success is $2\cos^2\theta \sin^2\theta$, i.e., on average they can distill $k/n = \frac{1}{2}P = \cos^2\theta \sin^2\theta$ Bell pairs per initial pair.

The above discussion involves Alice and Bob dealing with two pairs at a time. In fact, it can be extended to the case where they can manipulate n copies at a time [16]. The average number of Bell pairs per initial pair can be dervied to be

$$\overline{E}(n) = \frac{1}{n}\sum_{k=0}^{n} P(k)E_k = \frac{1}{n}\sum_{k=0}^{n} P(k)\log_2(C_k^n), \tag{1.22a}$$

$$P(k) \equiv (\cos^2\theta)^{n-k}(\sin^2\theta)^k C_k^n, \tag{1.22b}$$

where $C_k^n \equiv n!/[k!(n-k)!]$. As the number n of copies approaches infinity,

$$\lim_{n\to\infty} \overline{E}(n) \to E_{\rm D} = S(\rho_{\rm A}), \tag{1.23}$$

where $\rho_A \equiv {\rm Tr}_{\rm B}|\psi_\theta\rangle\langle\psi_\theta|$, and $S(\rho) \equiv -{\rm Tr}\rho\log_2\rho$ is the von Neumann entropy of ρ. In the case of $|\psi_\theta\rangle$, its entanglement of distillation is $E_{\rm D} = h(\cos^2\theta)$, where $h(x) \equiv -x\log_2(x) - (1-x)\log_2(1-x)$,

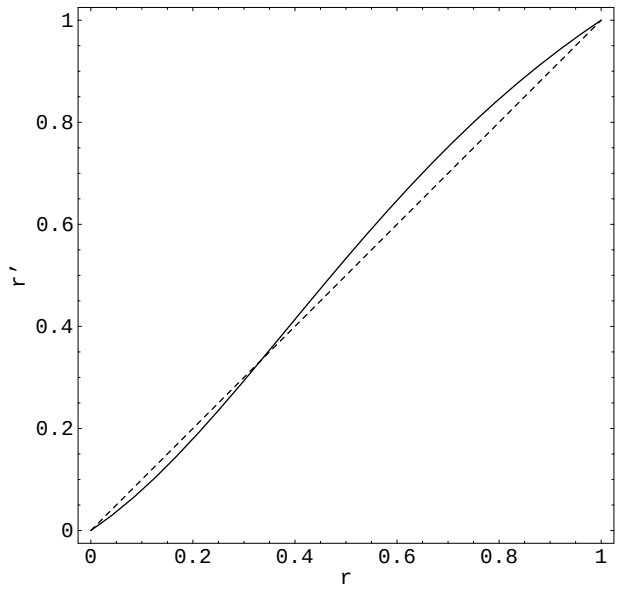

Figure 1.2: Mixed state distillation for Werner state $\rho_{\mathrm{W}+}(r)$. States above the dashed line (i.e., $r > 1/3$) can be distilled by the procedure.

i.e., is the Shannon entropy. The result

$$E_{\mathrm{D}} = -\mathrm{Tr}\big(\rho_A \log_2(\rho_A)\big), \tag{1.24}$$

is valid for *any* bi-partite pure state.

In Fig. 1.1 we show a distillation scheme slightly modified from the two-pair example. In this modified scheme, Alice and Bob both perform the CNOT operation *before* the measurement. This transforms the initial state $|\psi_\theta\rangle_{12} \otimes |\psi_\theta\rangle_{34}$ as follows:

$$|\psi_\theta\rangle_{12}\otimes|\psi_\theta\rangle_{34} \to (\cos^2\theta|0_1 0_2\rangle + \sin^2\theta|1_1 1_2\rangle)|0_3 0_4\rangle + \sqrt{2}\cos\theta\sin\theta\frac{1}{\sqrt{2}}(|0_1 0_2\rangle + |1_1 1_2\rangle)|1_3 1_4\rangle. \tag{1.25}$$

If Alice and/or Bob then measures the third and/or fourth qubit, respectively, and the outcome is $|1\rangle$, they immediately obtain a Bell state shared between particles 1 and 2. If the outcome is $|0\rangle$, they get a slightly less entangled state, which they can store for a second trial of distillation. What we mean by this is that two pairs of the states

$$\frac{1}{\sqrt{\cos^4\theta + \sin^4\theta}}\big(\cos^2\theta|00\rangle + \sin^2\theta|11\rangle\big), \tag{1.26}$$

although less entangled than the original pairs of Eq. (1.17), is distillable. Thus, this modified scheme performs slightly better than the original two-pair scheme.

For mixed entangled states, there are very few cases for which $E_{\rm D}$ is known. No general optimal distillation procedure is known for generic states. But a similar set-up to the one shown in Fig. 1.1 (except that the measurement is performed in a different basis) does provide a way (although not optimal) to distill very general two-qubit states. For example, Bennett and co-workers [17] have shown that after one step of the mixed-state distillation procedure, two initial pairs of the state (which is usually called the Werner state)

$$\rho_{\rm W+}(r) \equiv r|\Psi^+\rangle\langle\Psi^+| + \frac{1-r}{4}\mathbb{1}, \tag{1.27}$$

will be transformed into one pair with a new parameter (see Fig. 1.2)

$$r' = \frac{2r(1+2r)}{3(1+r^2)}. \tag{1.28}$$

Note that the larger the parameter r is, the higher entanglement the Werner state possesses. If $r' > r$, i.e., when $r > 1/3$ or equivalently the fidelity $F \equiv \langle\Psi^+|\rho_{\rm W}|\Psi^+\rangle > 1/2$, the entanglement is said to be increased. Horodecki and co-workers [18] further showed that any entangled two-qubit state can be transformed into a state $\rho_{\rm W+}(r)$ with $r > 1/3$, and hence can be distilled via the scheme of Bennett and co-workers (also known as the BBPSSW scheme) [17].

However, the procedure is not optimal for an arbitrary state ρ, and it is generally rather difficult to compute $E_{\rm D}(\rho)$. Nevertheless, if $E_{\rm D}(\rho) > 0$ we say that the state ρ is *distillable*. We remark that there is a connection between the PPT criterion and the distillability of a bi-partite state. Horodecki and co-workers [19] found that if a state has PPT then it cannot be distilled. But the converse is not generally true. In fact, there is still no simple criterion to determine whether or not a state is distillable.

1.3 Entanglement cost and entanglement of formation

The distillation is a process for concentrating entanglement from a large number of pairs with less entanglement into a small number of pairs with more (and ultimately maximal) entanglement. On the other hand, we can consider the converse process, which is usually called *dilution*. Given k pairs of Bell states shared between Alice and Bob, how many pairs n of a given state ρ can be obtained by local operations (including adding unentangled particles) and classical communication? The goal is to maximize the number n of copies of the output state ρ. The optimal ratio defines the *entanglement cost* [20]:

$$E_{\rm C}(\rho) \equiv \lim_{k\to\infty} (k/n). \tag{1.29}$$

As with $E_{\rm D}$, $E_{\rm C}$ is very difficult to calculate for general mixed states, and is only known for a very few special cases.

However, for pure states such as the state $|\psi_\theta\rangle$ discussed previously, $E_{\rm C} = -{\rm Tr}\big(\rho_A \log_2(\rho_A)\big)$, which equals $E_{\rm D}$. The optimal way to realize this dilution process for the pure state is to utilize two techniques: (i) quantum teleportation, which we have introduced at the beginning and which simply says that a Bell state shared between two parties can be used to tranfer an unknown qubit state with certainty, and (ii) *quantum data compression* [21], which basically states that a large message consistive of say n qubits, with each qubit on average being described by a density matrix $\rho_{\rm A}$, can be compressed into a possibly smaller number $k = nS(\rho_{\rm A}) \leq n$ of qubits; and one can faithfully recover the whole message, as long as n is large enough. For more detail of quantum data compression, see Appendix B.

With these two tools in hand, Alice can first prepare n copies of $|\psi_\theta\rangle$ ($2n$ qubits in total) locally, compress the n qubits to k qubits that she will "send" to Bob, and teleport the compressed k qubits to Bob using the shared k Bell states. Bob then decompresses the k qubits back to the uncompressed n qubits, which belong to half of the n copies of the entangled state $|\psi_\theta\rangle$. Thus, Alice and Bob establish n pairs of $|\psi_\theta\rangle$. This describes the optimal procedure for the dilution process for a pure state.

The entanglement of distillation and entanglement cost are defined asymptotically, i.e., both

processes involve an infinite number of copies of the initial states. For pure states, $E_{\rm C} = E_{\rm D}$ [16], which means that the two processes are reversible asymptotically. Yet, for mixed states, both quantities are very difficult to calculate. Nevertheless, it is expected that $E_{\rm C}(\rho) \geq E_{\rm D}(\rho)$, viz. that one can not distill more entanglement than is put in.

However, as we now explain, there is a modification of $E_{\rm C}$, obtained by averaging $E_{\rm C}$ over pure states, and it is called the *entanglement of formation* $E_{\rm F}$ [20, 22]. Any mixed state ρ can be decomposed into mixture of pure states $\{p_i, |\psi_i\rangle\langle\psi_i|\}$ as in Eq. (1.6), although the decomposition is far from unique. To construct the mixed state via mixing pure states in this way will cost, on average, $\sum_i p_i E(|\psi_i\rangle\langle\psi_i|)$ pairs of Bell states. The entanglement of formation for a mixed state ρ is thus defined as the *minimal* average number of Bell states needed to realize an ensemble described by ρ, i.e.,

$$E_{\rm F}(\rho) \equiv \min_{\{p_i,\psi_i\}} \sum_i p_i \, E_{\rm C}(|\psi_i\rangle\langle\psi_i|), \tag{1.30}$$

where the minimization is taken over those probabilities $\{p_i\}$ and pure states $\{\psi_i\}$ that, taken together, reproduce the density matrix $\rho = \sum_i p_i |\psi_i\rangle\langle\psi_i|$. Such a construction is usually called a *convex hull* construction. Furthermore, the quantity $E_{\rm C}(|\psi_i\rangle\langle\psi_i|)$ is the entropy of entanglement of pure state $|\psi_i\rangle$, viz. the expression in the right-hand side of Eq. (1.24). However, $E_{\rm F}$ is, in general, also difficult to calculate for mixed states, as it involves a minimization over all possible decompositions. So far, there has been more analytic progress for $E_{\rm F}$ than forn $E_{\rm C}$ and $E_{\rm D}$. Notable cases include (i) Wootters' formula for arbitary two qubits [22] (or see Appendix C); (ii) Terhal and Vollbrecht's formula [23] for *isotropic* states for two qu-*dit*s (d-level parties); and (iii) Vollbrecht and Werner's formula [24] for generalized Werner states of two qu-dits.

One of the central issues in entanglement theory is the so-called *additivity* of entanglement, i.e., whether the entanglement of formation, defined as an average quantity, equals the entanglement cost, which is defined asymptotically. Recently, Shor [25] has established that the additivity problem of entanglement of formation is equivalent to three other additivity problems: the strong superadditivity of the entanglement of formation, the additivity of the minimum output entropy of a quantum channel, and the additivity of the Holevo classical capacity of a quantum channel. However, further discussion of these additivity problems is beyond the scope of this dissertation.

1.4 Entanglement via a distance measure

As any mixture of separable density matrices is still, by definition, separable, any separable state can be expressed as a sum of two separable states

$$\rho_s = p\,\rho_s^1 + (1-p)\rho_s^2, \tag{1.31}$$

unless it is the extremal point, viz. a pure product state. Thus we see that the set of separable states is a *convex* set. This leads to another type of entanglement measure: the shortest "distance" $E(\rho)$ from an entangled state to the convex set $D_{\rm s}$ of separable mixed states [26], i.e., $E(\rho) \equiv \min_{\sigma\in D_{\rm s}} d(\rho||\sigma)$. One example of such an entanglement measure is the relative entropy of entanglement,

$$E_{\rm R}(\rho) \equiv \min_{\sigma\in D_{\rm s}} {\rm Tr}\left(\rho\log\rho - \rho\log\sigma\right), \tag{1.32}$$

where the distance measure d is defined to be the relative entropy of two states:

$$d(\rho||\sigma) \equiv {\rm Tr}\big[\rho\log\rho - \rho\log\sigma\big]. \tag{1.33}$$

We remark that the relative entropy is non-negative, but it is also not symmetric, i.e., $d(\rho||\sigma) \neq d(\sigma||\rho)$. For pure states this definition of entanglement reduces to the entropy of entanglement.

Another example is the Bures metric of entanglement $E_{\rm B}(\rho)$, defined via

$$E_{\rm B}(\rho) \equiv \min_{\sigma\in D_{\rm s}} \big[2 - 2F(\rho,\sigma)\big], \tag{1.34}$$

where $F(\rho,\sigma) \equiv \left({\rm Tr}\sqrt{\sqrt{\sigma}\rho\sqrt{\sigma}}\right)^2$ is called the *fidelity* and *is* symmetric. For two pure states $\rho = |\psi\rangle\langle\psi|$ and $\sigma = |\phi\rangle\langle\phi|$, the distance $d(\rho||\sigma) \equiv \big(2 - 2F(\rho,\sigma)\big)$ reduces to $2(1-|\langle\psi|\phi\rangle|^2)$.

We shall give more discussion of the relative entropy of entanglement later on.

1.5 A simple model

Let us illustrate how mixed states arise naturally and study the entanglement properties of the mixed states. Consider the Hamiltonian $\mathcal{H} = -J\vec{\sigma}^1\cdot\vec{\sigma}^2$. The eigenstates are $|\uparrow\uparrow\rangle$, $|\downarrow\downarrow\rangle$, $|\Psi^+\rangle =$

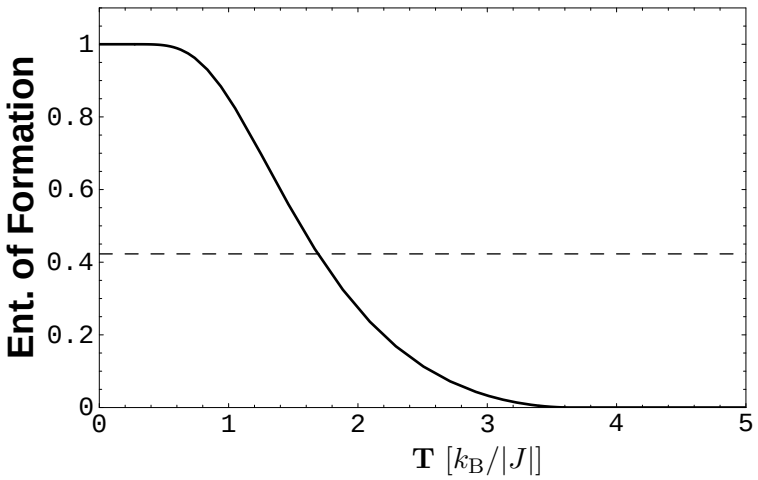

Figure 1.3: Entanglement vs. temperature. The dashed line represents the threshold of entanglement above which there is a violation of Bell's inequality.

$(|\uparrow\downarrow\rangle + |\downarrow\uparrow\rangle)/\sqrt{2}$, and $|\Psi^-\rangle = (|\uparrow\downarrow\rangle - |\downarrow\uparrow\rangle)/\sqrt{2}$ with respective eigenvalues $-J$, $-J$, $-J$ and $+3J$.

At a temperature $T = 1/(k_B\beta)$ the two-spin system is described by a density matrix

$$\rho = \frac{e^{\beta J}}{Z}(|\Phi^+\rangle\langle\Phi^+| + |\Phi^-\rangle\langle\Phi^-| + |\Psi^+\rangle\langle\Psi^+|) + \frac{e^{-3\beta J}}{Z}|\Psi^-\rangle\langle\Psi^-| = r|\Psi^-\rangle\langle\Psi^-| + \frac{1-r}{4}\mathbb{1}, \quad (1.35)$$

where $Z = 3e^{\beta J} + e^{-3\beta J}$ and $r \equiv (e^{-3\beta J} - e^{\beta J})/(3e^{\beta J} + e^{-3\beta J})$. This happens to be a Werner state. Using the Peres-Horodecki separability criterion, we find that if $J > 0$ the state is separable, as $r < 1/3$. On the other hand, if $J < 0$, there is a transition from being entangled to separable as the temparature is increased [29]. This can be seen from the entanglement of formation for the state as a function of temperature; see Fig. 1.3. In fact, Werner [11] found that such a state violates the Bell-CHSH inequality if $r > 1/\sqrt{2}$. Thus, there is a finite region between being entangled ($r > 1/3$) and violating the Bell-CHSH inequality. Moreover, Werner found that for $r \leq 1/2$ the state can be described by a classical local theory. The interval has recently been extended to $r \leq 2/3$ by Terhal and co-workers [30]. Even more interestingly, as we have seen previously, two pairs of Werner states with $r > 1/2$ can be distilled into a single Werner state of higher r, viz. higher entanglement. Thus, given a sufficient supply of Werner states, each of which does not violate any Bell inequality, a highly entangled Werner state can be distilled to violate a Bell inequality. This nonlocal quantum feature hidden in the initial states is thus revealed by the distillation process [17, 31].

This toy system demonstrates an interesting behavior of entanglement of canonical ensembles as the temperature is varied. Later in this dissertation we shall study a more realistic model of

large number of spins but at zero temperature. The model that we shall discuss exhibits quantum phase transitions as some system parameters vary.

1.6 Overview of the dissertation

One of the goals of this thesis is to develop an entanglement theory applicable to many-body (multi-partite) systems. But before we apply to more realistic models of many bodies, in Chapter 2 we examine the theory in the context of more familiar bi-partite systems, where corresponding results for other entanglement measures are already known. We then apply our entanglement measure to several nontrivial families of multi-partite states. Connections of our entanglement measure to other topics, such as the Hartree approximation, entanglement witnesses, and correlation functions are also discussed along the way. In Chapter 3 we discuss in detail the connection between the geometric measure of entanglement to the relative entropy of entanglement. In Chapter 4 we compute the multi-partite measure for two distinct peculiar states, i.e., the so-called bound entangled states. Finally, in Chapter 5 we apply our measure to the ground state of the XY quantum spin chain model in a transverse magnetic field. The behavior of the entanglement near the quantum critical points is found to be dictated by the universality classes of the model.

Chapter 2

Geometric measure of entanglement for multi-partite states

2.1 Introduction

Only recently, after more than half a century of existence, has the notion of entanglement become recognized as central to quantum information processing. As a result, the task of characterizing and quantifying entanglement have emerged as one of the prominent themes of quantum information theory. There have been many achievements in this direction, primarily in the setting of *bi-partite* systems. Among these, one highlight is Wootters' formula [22] for the entanglement of formation for arbitrary two-qubit mixed states. This formula enables discussions of entanglement between any pair of two-level systems, which are quite common in various physical systems (or idealizations of them). Other achivements include corresponding results for highly symmetrical states of higher-dimensional systems [23, 24].

The success of bi-partite entanglement theories, such as the entanglement of distillation and formation, hinges on the reversible interconvertibility of pure entangled states. To be more precise, any bi-partite pure entangled states can be, via local operations and classical communication, transformed into Bell states, asymptotically and reversibly. This means that there is only one type of pure entangled state and one can use Bell states as a "standard ruler" to quantify the degree of entanglement. As a result. the entanglement cost E_{C} equals the entanglement of distillation E_{D} for pure states.

However, things become more delicate in the multi-partite settings. For example, in the case of three qubits, two of the qubits can be entangled whilst the third one is separable from (not entangled

with) with them. This kind of entanglement is nothing more than the bi-partite entanglement we already know. But there are two other extreme types of entangled states. One is the so-called GHZ state: $|\mathrm{GHZ}\rangle \equiv (|000\rangle + |111\rangle)/\sqrt{2}$, and the other is the W state: $|W\rangle \equiv (|001\rangle + |010\rangle + |100\rangle)/\sqrt{3}$. It was found by Dür and co-workers [32] that, given a single copy of GHZ state, there is no way via local operations and classical communication (LOCC), not even probabilistically, that it can be transformed into a W state, or vice versa. GHZ and W states have different types of entanglement.

The GHZ state can be rewritten as

$$|\mathrm{GHZ}\rangle = \frac{1}{2}|00\rangle\otimes(|+\rangle+|-\rangle)+\frac{1}{2}|11\rangle\otimes(|+\rangle-|-\rangle) = \frac{1}{2}(|00\rangle+|11\rangle)\otimes|+\rangle+\frac{1}{2}(|00\rangle-|11\rangle)\otimes|-\rangle, \quad (2.1)$$

where $|\pm\rangle \equiv (|0\rangle \pm |1\rangle)/\sqrt{2}$. If one of the parties, e.g., the third one, performs measurement in the $\{\pm\}$ basis, and if the outcome is $|+\rangle$, the other two parties have the entangled state $|\Phi^+\rangle$. If the outcome is $|-\rangle$, the other two parties have the entangled state $|\Phi^-\rangle$. Therefore, two of the three parties can establish a Bell state. Thus, given two copies of GHZ states, they can establish a Bell state shared between say A and B, and another Bell state shared between A and C. A can locally prepares a W state

$$|\mathrm{W}\rangle = \frac{1}{\sqrt{3}}(|0_1 0_2 1_3\rangle + |0_1 1_2 0_3\rangle + |1_1 0_2 0_3\rangle). \quad (2.2)$$

As she has one Bell state shared with B and the other with C, she can use quantum teleportation to teleport the state of particle 2 of the W state to B and that of particle 3 to C. Thus two copies of GHZ states can achieve a copy of the W state.

On the other hand, if the three parties share a W state and one of them makes a measurement in the $\{0/1\}$ basis, 2/3 of the time the other two parties can establish a Bell state. The other 1/3, they fail to do so. If they are given 2 copies of W states, 4/9 of the time they can establish one Bell state between, say, A and B, and the other Bell state between A and C. A can use the same trick of teleportation such that they end up with a GHZ state. So two copies of W states can achieve 4/9 copy of GHZ state.

However, it is still not yet clear whether or not given some number of copies of GHZ states, they can be transformed into as many copies of W states and then transformed back to the original number of GHZ states. Namely, it is not yet known that whether the process is asymptotically

reversible.

Bennett and co-workers have come up with the notion of a finite minimal reversible entanglement generating set (MREGS) [33]. Such a set should include different types of "ruler" states. But the numer of states in this set should be finite, otherwise, it is not practical to use an infinite number of different rulers to "measure" the property of entanglement. For example, the minimal set might contain $\{|\text{Bell}\rangle_{12}, |\text{Bell}\rangle_{13}, |\text{Bell}\rangle_{23}, |\text{GHZ}\rangle\}$. Perhaps a large number of any three-qubit pure state can be transformed reversibly into, say, x_1 copies of $|\text{Bell}\rangle_{12}$, x_2 copies of $|\text{Bell}\rangle_{13}$, x_3 copies of $|\text{Bell}\rangle_{23}$, and x_4 copies of $|\text{GHZ}\rangle$? Or perhaps the minimal set might contain $\{|\text{Bell}\rangle_{12}, |\text{Bell}\rangle_{13}, |\text{Bell}\rangle_{23}, |\text{GHZ}\rangle, |\text{W}\rangle\}$? Then the entanglement could be defined as some kind of vector. However, this MREGS problem has not been solved yet. The situation gets even worse beyond three qubits. Verstraete and co-workers [34] have found that there are nine inequivalent classes of four-qubit entangled states. As the dimensions and the number of parties grow, the number of states in MREGS, if such a set exists, is expected to grow considerably large.

The above considerations complicate the task of extending measures such as the entanglement of distillation [16] and formation [20, 22] to multi-partite systems. Moreover, we have seen that the characterization of general multi-partite entanglement remains incomplete, as the number of the *types* of entanglement grows with the number of parties and the dimensions of Hilbert space. The issue of entanglement for multi-partite states hence poses an even greater challenge than bi-partite states. On the other hand, one can quantify multi-partite entanglement via other measures, such as the relative entropy of entanglement, the Bures metric [26, 27], and the Schmidt measure [35], which are naturally extendible to multi-partite settings.

In this chapter, we present an attempt to quantify multi-partite entanglement by developing and investigating a certain geometric measure of entanglement (GME), first introduced by Shimony [36] in the setting of bi-partite pure states and generalized to the multi-partite setting (via projection operators of various ranks) by Barnum and Linden [37]. In Sec. 2.2 we begin by examining this geometric measure in pure-state settings and establishing a connection with entanglement witnesses, Hartree approximations, and correlation functions. In Sec. 2.3 we extend the measure to mixed states, showing that it satisfies certain criteria required of good entanglement measures. In Sec. 2.4 we examine the GME for several families of mixed states of bi-partite systems: (i) arbitrary two-

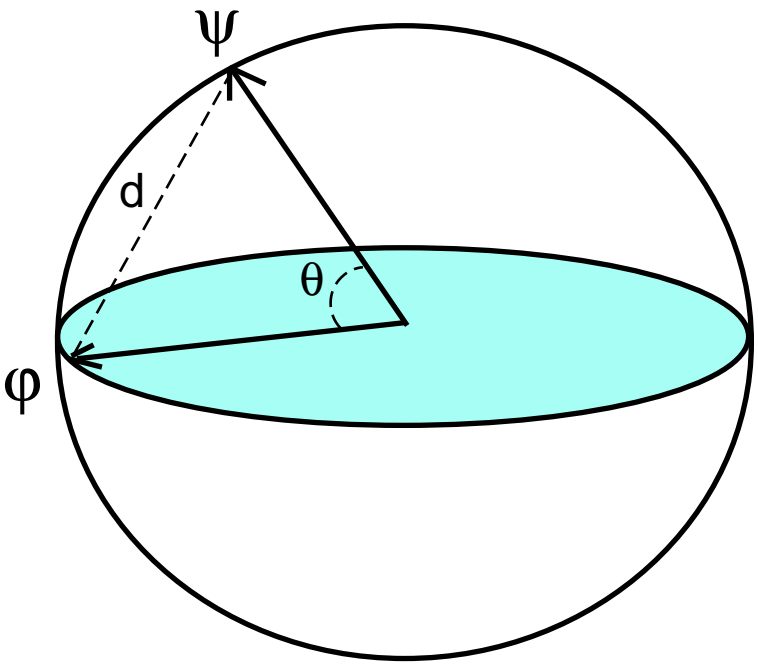

Figure 2.1: The schematic picture of the geometric measure. Imagine all pure states lie on the sphere and all separable pure states $|\phi\rangle$'s lie on the equator. The degree of entanglement for $|\psi\rangle$ is reflected in the shortest distance to the set of separable states.

qubit mixed, (ii) generalized Werner, and (iii) isotropic states in bi-partite systems, as well as (iv) certain mixtures of multi-partite symmetric states. In Sec. 2.5 we give a detailed application of the GME to arbitrary mixtures of three-qubit GHZ, W and inverted-W states. In Sec. 2.6 we discuss some open questions and further directions. The discussion in this chapter is based on Ref. [38]

It is not our intention to cast aspersions on existing approaches to entanglement; rather we simply wish to add one further element to the discussion. Our discussion focuses on quantifying multi-partite entanglement rather than characterizing it.

2.2 Basic geometric ideas and application to pure states

We begin with an examination of entangled *pure* states, and of how one might quantify their entanglement by making use of simple ideas of Hilbert space geometry. Let us start by developing a quite general formulation, appropriate for multi-partite systems comprising n parts, in which

each part can have a distinct Hilbert space. Consider a general n-partite pure state

$$|\psi\rangle = \sum_{p_1 \cdots p_n} \chi_{p_1 p_2 \cdots p_n} |e^{(1)}_{p_1} e^{(2)}_{p_2} \cdots e^{(n)}_{p_n}\rangle, \tag{2.3}$$

where $\{e^{(k)}_{p_k}\}$ is the local basis of the k-th party, e.g., the spin $\uparrow$ or $\downarrow$. One can envisage a geometric definition of its entanglement content via the distance

$$d = \min_{|\phi\rangle} \| \, |\psi\rangle - |\phi\rangle \| \tag{2.4}$$

between $|\psi\rangle$ and the nearest of the separable states $|\phi\rangle$ (or equivalently the angle between them). Here

$$|\phi\rangle \equiv \otimes_{i=1}^{n} |\phi^{(i)}\rangle = |\phi^{(1)}\rangle \otimes |\phi^{(2)}\rangle \otimes \cdots \otimes |\phi^{(n)}\rangle \tag{2.5}$$

is an arbitrary separable (i.e., Hartree) n-partite pure state, the index $i = 1 \ldots n$ labels the parties, and a state vector of part i is written as

$$|\phi^{(i)}\rangle \equiv \sum_{p_i} c^{(i)}_{p_i} \, |e^{(i)}_{p_i}\rangle. \tag{2.6}$$

It seems natural to assert that the more entangled a state is, the further away it will be from its best unentangled approximant (and, correspondingly, the wider will be the angle between them). We emphasize that we only compare the entangled pure state to the set of *pure* unentangled state. We shall extend to mixed states via the so-called convex-hull construction in Sec. 2.3. Another approach one might take is to compare any entangled state to the set of unentalged states, including both pure and mixed. The Bures measure, introduced in Sec. 1.4, is such an example.

To actually find the nearest separable state, it is convenient to minimize, instead of d, the quantity d^2, i.e.,

$$\| |\psi\rangle - |\phi\rangle \|^2, \tag{2.7}$$

subject to the constraint $\langle\phi|\phi\rangle = 1$. In fact, in solving the resulting stationarity condition one may restrict one's attention to the subset of solutions $|\phi\rangle$ that obey the further condition that each factor $|\phi^{(i)}\rangle$ obeys its own normalization condition $\langle\phi^{(i)}|\phi^{(i)}\rangle = 1$. Thus, by introducing a Lagrange

mulitplier Λ to enforce the constraint $\langle\phi|\phi\rangle = 1$, differentiating with respect to the independent amplitudes, and then imposing the further condition $\langle\phi^{(i)}|\phi^{(i)}\rangle = 1$, one arrives at the *nonlinear eigenproblem* for the stationary $|\phi\rangle$:

$$\sum_{p_1\cdots\widehat{p_i}\cdots p_n} \chi^*_{p_1 p_2\cdots p_n} c^{(1)}_{p_1} \cdots \widehat{c^{(i)}_{p_i}} \cdots c^{(n)}_{p_n} = \Lambda\, c^{(i)*}_{p_i}, \tag{2.8a}$$

$$\sum_{p_1\cdots\widehat{p_i}\cdots p_n} \chi_{p_1 p_2\cdots p_n} c^{(1)*}_{p_1} \cdots \widehat{c^{(i)*}_{p_i}} \cdots c^{(n)*}_{p_n} = \Lambda\, c^{(i)}_{p_i} \ , \tag{2.8b}$$

where the eigenvalue Λ is associated with the Lagrange multiplier enforcing the constraint $\langle\phi|\phi\rangle = 1$, and the symbol $\widehat{\ }$ denotes the exclusion of the corresponding term or factor. In a form independent of the choice of basis within each party, Eqs. (2.8) read

$$\langle\psi|\Big(\bigotimes_{j(\neq i)}^{n} |\phi^{(j)}\rangle\Big) = \Lambda\langle\phi^{(i)}|, \tag{2.9a}$$

$$\Big(\bigotimes_{j(\neq i)}^{n} \langle\phi^{(j)}|\Big)|\psi\rangle = \Lambda|\phi^{(i)}\rangle. \tag{2.9b}$$

From Eqs. (2.8) or (2.9), e.g., by taking inner product of both sides of Eq. (2.9a) with $|\phi^{(i)}\rangle$ one readily sees that

$$\Lambda = \langle\psi|\phi\rangle = \langle\phi|\psi\rangle \tag{2.10}$$

and thus the eigenvalues Λ are real, in $[-1, 1]$, and independent of the choice of the local basis $\{|e^{(i)}_{p_i}\rangle\}$. Hence, the spectrum Λ is the cosine of the angle between $|\psi\rangle$ and $|\phi\rangle$; the largest, $\Lambda_{\max}$, which we call the *entanglement eigenvalue*, corresponds to the closest separable state and is equal to the maximal overlap

$$\Lambda_{\max} = \max_{\phi} ||\langle\phi|\psi\rangle||, \tag{2.11}$$

where $|\phi\rangle$ is an arbitrary separable pure state.

Although, in determining the closest separable state, we have used the squared distance between the states, there are alternative (basis-independent) candidates for entanglement measures which are related to it in an elementary way: the distance, the sine, or the sine squared of the angle θ between them (with $\cos\theta \equiv \mathrm{Re}\,\langle\psi|\phi\rangle$). We shall adopt $E_{\sin^2} \equiv 1 - \Lambda^2_{\max}$ as our entanglement measure because, as we shall see, when generalizing $E_{\sin^2}$ to mixed states we have been able to

show that it satisfies a set of criteria demanded of entanglement measures.

In bi-partite applications, the eigenproblem (2.8) is in fact *linear*, and solving it is actually equivalent to finding the Schmidt decomposition [36]. Moreover, the entanglement eigenvalue is equal to the maximal Schmidt coefficient. To be more precise, in bi-partite systems the stationarity conditions (2.8) reduce to the linear form

$$\sum_{p_1} \chi^*_{p_1 p_2} c^{(1)}_{p_1} = \Lambda\, c^{(2)*}_{p_2}, \tag{2.12a}$$

$$\sum_{p_1} \chi_{p_1 p_2} c^{(1)*}_{p_1} = \Lambda\, c^{(2)}_{p_2}, \tag{2.12b}$$

$$\sum_{p_2} \chi^*_{p_1 p_2} c^{(2)}_{p_2} = \Lambda\, c^{(1)*}_{p_1}, \tag{2.12c}$$

$$\sum_{p_2} \chi_{p_1 p_2} c^{(2)*}_{p_2} = \Lambda\, c^{(1)}_{p_1}. \tag{2.12d}$$

Eliminating $c^{(2)}_p$ between Eqs. (2.12a) and (2.12d) and, similarly, eliminating $c^{(1)}_p$ between Eqs. (2.12b) and (2.12c) gives

$$\sum_{p'_1\, p_2} \chi_{p_1 p_2} \chi^*_{p'_1 p_2} c^{(1)}_{p'_1} = \Lambda^2\, c^{(1)}_{p_1}, \tag{2.13a}$$

$$\sum_{p_1\, p'_2} \chi_{p_1 p_2} \chi^*_{p_1 p'_2} c^{(2)}_{p'_2} = \Lambda^2\, c^{(2)}_{p_2}, \tag{2.13b}$$

or equivalently

$$\mathrm{Tr}_2\big(|\psi\rangle\langle\psi|\big)|\phi^{(1)}\rangle = \Lambda^2\,|\phi^{(1)}\rangle, \tag{2.14a}$$

$$\mathrm{Tr}_1\big(|\psi\rangle\langle\psi|\big)|\phi^{(2)}\rangle = \Lambda^2\,|\phi^{(2)}\rangle. \tag{2.14b}$$

Now, solving the above equations is equivalent to finding the Schmidt decomposition for $|\psi\rangle$. To see this, first recall that Schmidt decomposability guarantees that an arbitrary pure bi-partite state

$$|\psi\rangle = \sum_{p_1 p_2} \chi_{p_1 p_2} |e^{(1)}_{p_1}\rangle \otimes |e^{(2)}_{p_2}\rangle \tag{2.15}$$

in the (product) Hilbert space $\mathcal{H}_1 \otimes \mathcal{H}_2$ (with factor dimensions d_1 and d_2) can always be expressed

in the form

$$|\psi\rangle = \sum_{k=1}^{\min\{d_1,d_2\}} \lambda_k \, |\tilde{e}_k^{(1)}\rangle \otimes |\tilde{e}_k^{(2)}\rangle. \tag{2.16}$$

Here, $\lambda_k \geq 0$, $\sum_k \lambda_k^2 = 1$, the $|\tilde{e}_k^{(1)}\rangle$'s and $|\tilde{e}_k^{(2)}\rangle$'s are orthonormal, respectively, in $\mathcal{H}_1$ and $\mathcal{H}_2$. Moreover, the new (tilde) bases, as well as the λ_k's, follow as the solution of the eigenproblems of the reduced density matrix that one obtains by tracing $|\psi\rangle\langle\psi|$ over party 1 or 2:

$$\mathrm{Tr}_2\big(|\psi\rangle\langle\psi|\big)|\tilde{e}_k^{(1)}\rangle = \lambda_k^2 |\tilde{e}_k^{(1)}\rangle, \tag{2.17a}$$

$$\mathrm{Tr}_1\big(|\psi\rangle\langle\psi|\big)|\tilde{e}_k^{(2)}\rangle = \lambda_k^2 |\tilde{e}_k^{(2)}\rangle. \tag{2.17b}$$

These are Eqs. (2.14); thus we see that determining entanglement for bi-partite pure states is equivalent to finding their Schmidt decomposition, except that one only needs the *largest* Schmidt coefficient $\Lambda_{\max} = \lambda_{\max}$.

By contrast, for the case of three or more parts, the eigenproblem is a *nonlinear* one. For example, in the setting of tri-partite systems, the stationarity conditions (2.8) associated with the pure state $|\psi\rangle = \sum_{p_1p_2p_3} \chi_{p_1p_2p_3} |e_{p_1}^{(1)} e_{p_2}^{(2)} e_{p_3}^{(3)}\rangle$ become

$$\sum_{p_2p_3} \chi^*_{p_1p_2p_3} c_{p_2}^{(2)} c_{p_3}^{(3)} = \Lambda \, c_{p_1}^{(1)*}, \tag{2.18a}$$

$$\sum_{p_1p_3} \chi^*_{p_1p_2p_3} c_{p_1}^{(1)} c_{p_3}^{(3)} = \Lambda \, c_{p_2}^{(2)*}, \tag{2.18b}$$

$$\sum_{p_1p_2} \chi^*_{p_1p_2p_3} c_{p_1}^{(1)} c_{p_2}^{(2)} = \Lambda \, c_{p_3}^{(3)*}. \tag{2.18c}$$

Note the nonlinear structure of this tri-partite (and, in general, any $n \geq 3$-partite) eigenproblem. As far as we are aware, for nonlinear eigenproblems such as these, one cannot take advantage of the simplicity of linear eigenproblems, for which one can address the task of determining the eigenvalues directly (via the characteristic polynomial), without having to address the eigenvectors. Hence, even for systems comprising qubits, one is forced to proceed numerically. This is consistent with the notion that no Schmidt decomposition exists beyond bi-partite systems. Yet, as we shall illustrate shortly, there do exist certain families of pure states whose entanglement eigenvalues can be determined analytically.

For $C^d \otimes C^d$ bi-partite systems, the equivalence between the geometric approach and Schmidt decomposition immediately indicates why the maximally entangled pure states have (up to local unitary transformations) the well-known form $|\Phi^+\rangle \equiv \frac{1}{\sqrt{d}} \sum_{i=1}^{d} |ii\rangle$. As the Schmidt coefficients are non-negative and sum (when squared) to unity, any less symmetric state must have a larger $\Lambda_{\max}$, i.e., a smaller entanglement.

2.2.1 Illustrative examples

Suppose we are already in possession of the Schmidt decomposition of some two-qubit pure state:

$$|\psi\rangle = \sqrt{p}\,|00\rangle + \sqrt{1-p}\,|11\rangle. \tag{2.19}$$

Then we can read off the entanglement eigenvalue:

$$\Lambda_{\max} = \max\{\sqrt{p}, \sqrt{1-p}\}. \tag{2.20}$$

Another approach to obtain $\Lambda_{\max}$ is to solve, e.g., Eqs. (2.14), which lead to solving the maximal eigenvalue of

$$\begin{pmatrix} p & 0 \\ 0 & 1-p \end{pmatrix} \vec{v} = \Lambda^2\, \vec{v}, \tag{2.21}$$

resulting in the solution (2.20).

Now, recall [22] that the concurrence C for this state is $2\sqrt{p(1-p)}$ [see Appendix C]. Hence, one has

$$\Lambda_{\max}^2 = \frac{1}{2}\left(1 + \sqrt{1-C^2}\right), \tag{2.22}$$

a connection between the entanglement eigenvalue and the concurrence that holds for arbitrary two-qubit pure states.

The possession of symmetry by a state can alleviate the difficulty associated with solving the

nonlinear eigenproblem. To see this, consider a state

$$|\psi\rangle = \sum_{p_1 \cdots p_n} \chi_{p_1 p_2 \cdots p_n} |e_{p_1}^{(1)} e_{p_2}^{(2)} \cdots e_{p_n}^{(n)}\rangle \tag{2.23}$$

that possesses the symmetry that the (nonzero) amplitudes χ are invariant under permutations. What we mean by this is that, regardless of the dimensions of the factor Hilbert spaces, the amplitudes are only nonzero when the indices take on the first ν values (or can be arranged to do so by appropriate relabeling of the basis in each factor) and, moreover, that these amplitudes are invariant under permutations of the parties, i.e., $\chi_{\sigma_1 \sigma_2 \cdots \sigma_n} = \chi_{p_1 p_2 \cdots p_n}$, where the σ's are any permutation of the p's. (This symmetry may be obscured by arbitrary local unitary transformations.) For such states, it seems reasonable to anticipate that the closest Hartree approximant retains this permutation symmetry. Assuming this to be the case—and numerical experiments of ours support this assumption—in the task of determining the entanglement eigenvalue one can start with the Ansatz that the closest separable state has the form

$$|\phi\rangle \equiv \otimes_{i=1}^{n} \left(\sum\nolimits_j c_j |e_j^{(i)}\rangle \right), \tag{2.24}$$

i.e., is expressed in terms of copies of a single factor state, for which $c_j^{(i)} = c_j$. To obtain the entanglement eigenvalue it is thus only necessary to maximize $\mathrm{Re}\,\langle\phi|\psi\rangle$ with respect to the ν amplitudes $\{c_j\}_{j=1}^{\nu}$, a simpler task than maximization over the $\sum_{i=1}^{n} d_i$ amplitudes of a generic product state.

To illustrate this symmetry-induced simplification, we consider several examples involving permutation-invariant states, first restricting our attention to the case $\nu = 2$ (i.e., two-state parties). The most natural realizations are n-qubit systems. One can label these symmetric states according to the number of 0's, as follows [39]:

$$|S(n,k)\rangle \equiv \sqrt{\frac{k!(n-k)!}{n!}} \sum_{\text{permutations}} |\underbrace{0 \cdots 0}_{k} \underbrace{1 \cdots 1}_{n-k}\rangle. \tag{2.25}$$

As the amplitudes in this state are all positive and the state is permutationally invariant, one can assume that the closest Hartree state also has the symmetry and has non-negative amplitudes, and

is of the form

$$|\phi\rangle = \Big(\sqrt{p}\,|0\rangle + \sqrt{1-p}\,|1\rangle\Big)^{\otimes n}. \tag{2.26}$$

Maximizing the overlap with respect to p, one obtains the entanglement eigenvalue for $|\mathrm{S}(n,k)\rangle$:

$$\Lambda_{\max}(n,k) = \sqrt{\frac{n!}{k!(n-k)!}}\left(\frac{k}{n}\right)^{\frac{k}{2}}\left(\frac{n-k}{n}\right)^{\frac{n-k}{2}}. \tag{2.27}$$

For fixed n, the minimum $\Lambda_{\max}$ (and hence the maximum entanglement) among the $|\mathrm{S}(n,k)\rangle$'s occurs for $k = n/2$ (for n even) and $k = (n \pm 1)/2$ (for n odd). In fact, for fixed n the general permutation-invariant state can be expressed as $\sum_k \alpha_k |\mathrm{S}(n,k)\rangle$ with $\sum_k |\alpha_k|^2 = 1$. The entanglement of such states can be addressed via the strategy that we have been discussing, i.e., via the maximization of a function of (at most) three real parameters. The simplest example is provided by the nGHZ state:

$$|n\mathrm{GHZ}\rangle \equiv \frac{1}{\sqrt{2}}\big(|\mathrm{S}(n,0)\rangle + |\mathrm{S}(n,n)\rangle\big). \tag{2.28}$$

It is easy to show that (for all n) $\Lambda_{\max}(n\mathrm{GHZ}) = 1/\sqrt{2}$ and, equivalently, $E_{\sin^2} = 1/2$. Note that one could have rescale the definion of the GME by a factor of two such that Bell and N-GHZ states have entanglement of unity. However, we do not make this rescaling.

We now focus our attention on three-qubit settings. Of these, the states $|S(3,0)\rangle = |000\rangle$ and $|S(3,3)\rangle = |111\rangle$ are not entangled and are, respectively, the components of the 3-GHZ state: $|\mathrm{GHZ}\rangle \equiv \big(|000\rangle + |111\rangle\big)/\sqrt{2}$. The states $|\mathrm{S}(3,2)\rangle$ and $|\mathrm{S}(3,1)\rangle$, are the W state and the "inverted W" state, respectively,

$$|\mathrm{W}\rangle \equiv |\mathrm{S}(3,2)\rangle = \frac{1}{\sqrt{3}}\big(|001\rangle + |010\rangle + |100\rangle\big), \tag{2.29a}$$

$$|\widetilde{\mathrm{W}}\rangle \equiv |\mathrm{S}(3,1)\rangle = \frac{1}{\sqrt{3}}\big(|110\rangle + |101\rangle + |011\rangle\big), \tag{2.29b}$$

are equally entangled, having $\Lambda_{\max} = 2/3$ and $E_{\sin^2} = 1 - \Lambda_{\max}^2 = 5/9$.

Next, consider a superposition of the W and $\widetilde{\mathrm{W}}$ states:

$$|\mathrm{W}\widetilde{\mathrm{W}}(s,\phi)\rangle \equiv \sqrt{s}\,|\mathrm{W}\rangle + \sqrt{1-s}\,\mathrm{e}^{i\phi}|\widetilde{\mathrm{W}}\rangle. \tag{2.30}$$

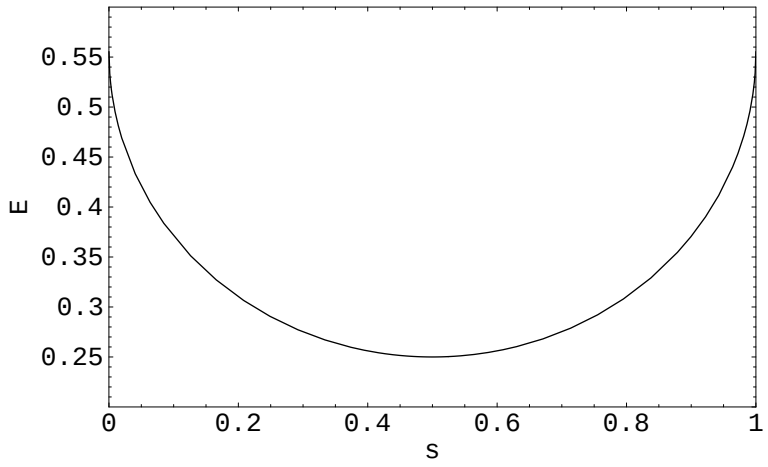

Figure 2.2: Entanglement of the pure state $\sqrt{s}\,|\mathrm{W}\rangle + \sqrt{1-s}\,|\widetilde{\mathrm{W}}\rangle$ vs. s. This also turns out to be the entanglement curve for the mixed state $s\,|\mathrm{W}\rangle\langle\mathrm{W}| + (1-\mathrm{s})|\widetilde{\mathrm{W}}\rangle\langle\widetilde{\mathrm{W}}|$.

It is straightforward to see that its entanglement is independent of ϕ: the transformation $\{|0\rangle, |1\rangle\} \to \{|0\rangle, \mathrm{e}^{-i\phi}|1\rangle\}$ induces $|\mathrm{W}\widetilde{\mathrm{W}}(s,\phi)\rangle \to \mathrm{e}^{-i\phi}|\mathrm{W}\widetilde{\mathrm{W}}(s,0)\rangle$, and the entanglement is independent of the overall phase of a state. To calculate $\Lambda_{\max}$, we assume that the separable state is of the form $(\cos\theta|0\rangle + \sin\theta|1\rangle)^{\otimes 3}$, and maximize its overlap with $|\mathrm{W}\widetilde{\mathrm{W}}(s,0)\rangle$ with respect to θ. Thus we find that $\theta(s)$ is determined via its tangent $t \equiv \tan\theta$, which is the particular root of the polynomial equation

$$\sqrt{1-s}\,t^3 + 2\sqrt{s}\,t^2 - 2\sqrt{1-s}\,t - \sqrt{s} = 0 \tag{2.31}$$

that lies in the range $t \in [\sqrt{1/2}, \sqrt{2}]$. Via $\theta(s)$, $\Lambda_{\max}$ (and thus $E_{\sin^2} = 1 - \Lambda_{\max}^2$) can be expressed as

$$\Lambda_{\max}(s) = \frac{\sqrt{3}}{2}\big[\sqrt{s}\cos\theta(s) + \sqrt{1-s}\sin\theta(s)\big]\sin 2\theta(s). \tag{2.32}$$

In Fig. 2.2, we show $E_{\sin^2}\big(|\mathrm{W}\widetilde{\mathrm{W}}(s,\phi)\rangle\big)$ vs. s.

In fact, for the more general superposition

$$|\mathrm{SS}_{n;k_1k_2}(r,\phi)\rangle \equiv \sqrt{r}\,|\mathrm{S}(n,k_1)\rangle + \sqrt{1-r}\,\mathrm{e}^{i\phi}\,|\mathrm{S}(n,k_2)\rangle \tag{2.33}$$

(with $k_1 \neq k_2$) $\Lambda_{\max}$ also turns out to be independent of ϕ, and can be computed in the same way as was used for $|\mathrm{W}\widetilde{\mathrm{W}}(s,\phi)\rangle$. We note that although the curve in Fig. 2.2 is convex, convexity

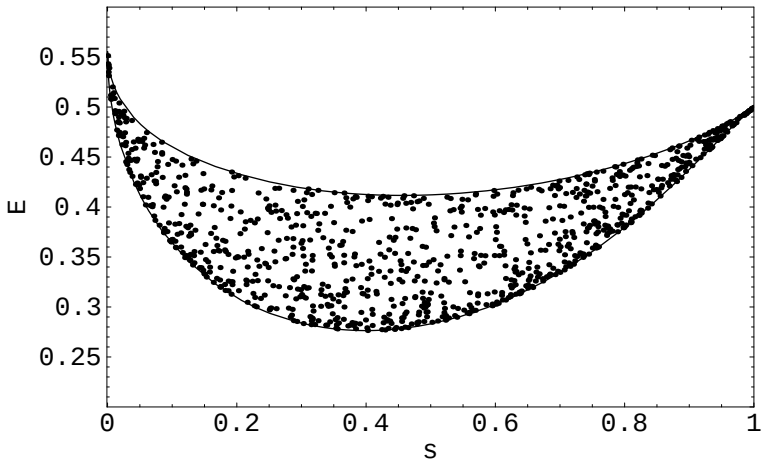

Figure 2.3: Entanglement of $|\Psi_{\rm GHZ+W}(s,\phi)\rangle$ vs. s. The upper curve is for $\phi=\pi$ whereas the lower one is for $\phi=0$. Dots represent states with randomly generated s and ϕ.

does not hold uniformly over k_1 and k_2. This adds some complexity to calculation of mixed-state entanglement, as we shall see later.

As our last pure-state example in the qubit setting, we consider superpositions of W and GHZ states:

$$|\Psi_{\rm GHZ+W}(s,\phi)\rangle \equiv \sqrt{s}\,|{\rm GHZ}\rangle + \sqrt{1-s}\;{\rm e}^{i\phi}|{\rm W}\rangle. \tag{2.34}$$

For these, the phase ϕ cannot be "gauged" away and, hence, $E_{\sin^2}$ depends on ϕ. In Fig. 2.3 we show $E_{\sin^2}$ vs. s at $\phi=0$ and $\phi=\pi$ (i.e., the bounding curves), as well as $E_{\sin^2}$ for randomly generated values of $s\in[0,1]$ and $\phi\in[0,2\pi]$ (dots). We observe that the 'π' state has higher entanglement than the '0' does. As the numerical results suggest, the (ϕ-parametrized) $E_{\sin^2}$ vs. s curves of the states $|\Psi_{\rm GHZ+W}(s,\phi)\rangle$ lie between the 'π' and '0' curves.

We remark that, more generally, for systems comprising n parts, each being a d-level system, the symmetric state

$$|S(n;\{k\})\rangle \equiv \sqrt{\frac{\prod_i k_i!}{n!}}\sum_{\rm P}|\underbrace{0\ldots0}_{k_0}\underbrace{1\ldots1}_{k_1}\ldots\underbrace{(d-1)\ldots(d-1)}_{k_{d-1}}\rangle \tag{2.35}$$

(with $\sum_i k_i = n$) has entanglement eigenvalue

$$\Lambda_{\max}(n;\{k\}) = \sqrt{\frac{n!}{\prod_i (k_i!)}}\;\prod_{i=0}^{d-1}\left(\frac{k_i}{n}\right)^{\frac{k_i}{2}}. \tag{2.36}$$

One can also consider other symmetries. Consider the totally *anti*-symmetric (viz. determinant) state of n parts, each with n levels,

$$|\mathrm{Det}_n\rangle \equiv \frac{1}{\sqrt{n!}} \sum_{i_1,\ldots,i_n=1}^{n} \epsilon_{i_1,\ldots,i_n} |i_1,\ldots,i_n\rangle. \tag{2.37}$$

It has been shown by Bravyi [40] that the maximal squared overlap of this state $\Lambda^2_{\max}$ is $1/n!$. Bravyi has also generalized the anti-symmetric state to the $n = p\,d^p$-partite determinant state, via the construction

$$\begin{aligned}
\phi(1) &= (0,0,\ldots,0,0),\\
\phi(2) &= (0,0,\ldots,0,1),\\
&\vdots\\
\phi(d^p-1) &= (d-1,d-1,\ldots,d-1,d-2),\\
\phi(d^p) &= (d-1,d-1,\ldots,d-1,d-1),
\end{aligned}$$

and

$$|\mathrm{Det}_{n,d}\rangle \equiv \frac{1}{\sqrt{(d^p!)}} \sum_{i_1,\ldots,i_{d^p}} \epsilon_{i_1,\ldots,i_{d^p}} |\phi(i_1),\ldots,\phi(i_{d^p})\rangle. \tag{2.38}$$

In this case, we can show that $\Lambda^2_{\max} = [(d^p)!]^{-1}$.

2.2.2 Connection with the Hartree approximation

Recall from Eq. (2.11) that the maximal overlap or the entanglement eigenvalue of a pure state $|\psi\rangle$ is defined as $\Lambda_{\max}(\psi) = \max_\phi ||\langle\phi|\psi\rangle||$, where the maximization is taken over arbitrary product state $|\phi\rangle$. On the other hand, consider the Hamiltonian constructed from the entangled state $|\psi\rangle$

$$\mathcal{H}_\psi = -|\psi\rangle\langle\psi|, \tag{2.39}$$

which has the form of a projector on to the state $|\psi\rangle$ and which has the minimum eigen-energy -1. The Hartree approximation is to take some product state $|\psi\rangle$ such that it minimzes the expectation

value of the Hamiltonian

$$\min_{\phi} \langle \phi | \mathcal{H}_{\psi} | \phi \rangle = - \max_{\phi} |\langle \phi | \psi \rangle|^2 = -\Lambda^2_{\max}(\psi). \tag{2.40}$$

It thus arises that the difference between the true ground-state energy of $\mathcal{H}_{\psi}$ and the one given by the best Hartree approximation (2.40) is

$$1 - \Lambda^2_{\max}(\psi), \tag{2.41}$$

i.e., the GME of $|\psi\rangle$ and that that the best Hartree approximant $|\phi^*\rangle$ is the closest separable state to $|\psi\rangle$.

This connection, although elementary, can be generalized to the Hartree-Fock approximation when we wish to extend the idea of entanglement to fermionic systems.

If we are interested in the entanglement of a nondegenerate ground state (with energy E_0) of a Hamiltonian, in principle, we can express the maximal overlap as

$$\Lambda^2_{\max}(|E_0\rangle) = \lim_{\beta \to \infty} \min_{\phi} \langle \phi | e^{-\beta(\mathcal{H} - E_0)} | \phi \rangle. \tag{2.42}$$

2.2.3 Connection with entanglement witnesses

We now digress to discuss a relationship between the geometric measure of entanglement and another entanglement property—entanglement witnesses. The entanglement witness $\mathcal{W}$ for an entangled state ρ is defined to be an operator that is (a) Hermitian and (b) obeys the following conditions [13]:

(i) $\mathrm{Tr}(\mathcal{W}\sigma) \geq 0$ for all separable states σ, and

(ii) $\mathrm{Tr}(\mathcal{W}\rho) < 0$.

Here, we wish to establish a correspondence between $\Lambda_{\max}$ for the entangled pure state $|\psi\rangle$ and the optimal element of the set of entanglement witnesses $\mathcal{W}$ for $|\psi\rangle$ that have the specific form

$$\mathcal{W} = \lambda^2 \mathbb{1} - |\psi\rangle\langle\psi|, \tag{2.43}$$

where $\mathbb{1}$ is the identity operator. This set is parametrized by the real, non-negative number λ^2. By *optimal* we mean that, for this specific form of witnesses, the value of the expression $\mathrm{Tr}\big(\mathcal{W}|\psi\rangle\langle\psi|\big)$ is as negative as can be.

In order to satisfy condition (i) we must ensure that, for any *separable* state σ, we have $\mathrm{Tr}\big(\mathcal{W}\sigma\big) \geq 0$. As the density matrix for any separable state can be decomposed into a mixture of *separable pure* states [i.e., $\sigma = \sum_i |\phi_i\rangle\langle\phi_i|$ where $\{|\phi_i\rangle\}$ are separable pure states], condition (i) will be satisfied as long as $\mathrm{Tr}\big(\mathcal{W}|\phi\rangle\langle\phi|\big) \geq 0$ for all separable *pure* states $|\phi\rangle$. This condition is equivalent to

$$\lambda^2 - ||\langle\psi|\phi\rangle||^2 \geq 0 \text{ (for all separable } |\phi\rangle), \tag{2.44}$$

which leads to

$$\lambda^2 \geq \max_{|\phi\rangle} ||\langle\psi|\phi\rangle||^2 = \Lambda^2_{\max}(|\psi\rangle). \tag{2.45}$$

Condition (ii) requires that $\mathrm{Tr}\big(\mathcal{W}|\psi\rangle\langle\psi|\big) < 0$, in order for $\mathcal{W}$ to be a valid entanglement witness for $|\psi\rangle$; this gives $\lambda^2 - 1 < 0$. Thus, we have established the range of λ for which $\lambda^2\mathbb{1} - |\psi\rangle\langle\psi|$ is a valid entanglement witness for $|\psi\rangle$:

$$\Lambda^2_{\max}(|\psi\rangle) \leq \lambda^2 < 1. \tag{2.46}$$

With these preliminaries in place, we can now establish the connection we are seeking. Of the specific family (2.43) of entanglement witnesses for $|\psi\rangle$, the one of the form $\mathcal{W}_{\text{opt}} = \Lambda^2_{\max}(|\psi\rangle)\mathbb{1} - |\psi\rangle\langle\psi|$ is optimal, in the sense that it achieves the most negative value for the detector $\mathrm{Tr}\big(\mathcal{W}_{\text{opt}}|\psi\rangle\langle\psi|\big)$:

$$\min_{\mathcal{W}} \mathrm{Tr}\big(\mathcal{W}|\psi\rangle\langle\psi|\big) = \mathrm{Tr}\big(\mathcal{W}_{\text{opt}}|\psi\rangle\langle\psi|\big) = -E_{\sin^2}(|\psi\rangle), \tag{2.47}$$

where $\mathcal{W}$ runs over the class (2.43) of witnesses.

We now look at some examples. For the GHZ state the optimal witness is

$$\mathcal{W}_{\text{GHZ}} = \frac{1}{2}\mathbb{1} - |\text{GHZ}\rangle\langle\text{GHZ}| \tag{2.48}$$

and $\mathrm{Tr}\big(\mathcal{W}_{\text{GHZ}}|\text{GHZ}\rangle\langle\text{GHZ}|\big) = -E_{\sin^2}(|\text{GHZ}\rangle) = -1/2$. Similarly, for the W and inverted-W states

we have

$$\mathcal{W}_{\mathrm{W}} = \frac{4}{9}\mathbb{1} - |\mathrm{W}\rangle\langle\mathrm{W}| \quad \text{and} \quad \mathcal{W}_{\widetilde{\mathrm{W}}} = \frac{4}{9}\mathbb{1} - |\widetilde{\mathrm{W}}\rangle\langle\widetilde{\mathrm{W}}| \tag{2.49}$$

and $\mathrm{Tr}\big(\mathcal{W}_{\mathrm{W}}|\mathrm{W}\rangle\langle\mathrm{W}|\big) = -E_{\sin^2}(|\mathrm{W}\rangle) = -5/9$, and similarly for $|\widetilde{\mathrm{W}}\rangle$. For the four-qubit state

$$|\Psi\rangle \equiv (|0011\rangle + |0101\rangle + |0110\rangle + |1001\rangle + |1010\rangle + |1100\rangle)/\sqrt{6} \tag{2.50}$$

the optimal witness is

$$\mathcal{W}_{\Psi} = \frac{3}{8}\mathbb{1} - |\Psi\rangle\langle\Psi| \tag{2.51}$$

and $\mathrm{Tr}\big(\mathcal{W}_{\Psi}|\Psi\rangle\langle\Psi|\big) = -E_{\sin^2}(|\Psi\rangle) = -5/8$.

Although the observations we have made in this section are, from a technical standpoint, elementary, we nevertheless find it intriguing that two distinct aspects of entanglement—the geometric measure of entanglement and entanglement witnesses—are so closely related. Furthermore, this connection sheds new light on the content of the geometric measure of entanglement. In particular, as entanglement witnesses are Hermitian operators, they can, at least in principle, be realized and measured locally [41]. Their connection with the geometric measure of entanglement ensures that the geometric measure of entanglement can, at least in principle, be verified experimentally.

2.2.4 Connection with correlation functions

In this section we explore the connection of the entanglement eigenvalue to the correlation functions. To illustrate the connection, we shall mainly focus on N-qubit systems. Recall that a single pure qubit state, when written in the form of a density matrix, can be expressed in terms of Pauli matrices plus the identity:

$$\frac{1}{2}(\mathbb{1} + \vec{r}\cdot\vec{\sigma}), \tag{2.52}$$

with the constraint on the real vector parameter $\vec{r}$ that $|\vec{r}| = 1$. The density matrix for an N-qubit separable pure state $|\phi\rangle$ (2.5) is hence a direct product of N such terms:

$$|\phi\rangle\langle\phi| = \frac{1}{2}(\mathbb{1} + \vec{r}_1\cdot\vec{\sigma}^{(1)}) \otimes \frac{1}{2}(\mathbb{1} + \vec{r}_2\cdot\vec{\sigma}^{(2)}) \otimes \cdots \otimes \frac{1}{2}(\mathbb{1} + \vec{r}_N\cdot\vec{\sigma}^{(N)}), \tag{2.53}$$

and expanding out the products gives the decomposition of $|\phi\rangle\langle\phi|$

$$\frac{1}{2^N}\left\{\mathbb{1}+\sum_{j=1}^{N}\vec{r}_j\cdot\vec{\sigma}^{(j)}+\sum_{j<k}\vec{r}_j\cdot\vec{\sigma}^{(j)}\otimes\vec{r}_k\cdot\vec{\sigma}^{(k)}+\sum_{j<k<l}\vec{r}_j\cdot\vec{\sigma}^{(j)}\otimes\vec{r}_k\cdot\vec{\sigma}^{(k)}\otimes\vec{r}_l\cdot\vec{\sigma}^{(l)}+\cdots\right\}. \quad (2.54)$$

The overlap squared of any N-qubit state $|\psi\rangle$ with the separable state $|\phi\rangle$ is

$$\Lambda^2=\langle\psi|\big(|\phi\rangle\langle\phi|\big)|\psi\rangle, \quad (2.55)$$

which can in turn be expressed in terms of the correlations of the operators of the form $\sigma\otimes\cdots\otimes\sigma\otimes\cdots$. Therefore, the maximal overlap is a maximization over all combinations of M-point (with $M\leq N$) correlation functions:

$$\begin{aligned}\Lambda^2_{\max} &= \max_{|\vec{r}|=1}\frac{1}{2^N}\left\{1+\sum_{j=1}^{N}\langle\vec{r}_j\cdot\vec{\sigma}^{(j)}\rangle+\sum_{j<k}\langle\vec{r}_j\cdot\vec{\sigma}^{(j)}\otimes\vec{r}_k\cdot\vec{\sigma}^{(k)}\rangle\right.\\ &\left.+\sum_{j<k<l}\langle\vec{r}_j\cdot\vec{\sigma}^{(j)}\otimes\vec{r}_k\cdot\vec{\sigma}^{(k)}\otimes\vec{r}_l\cdot\vec{\sigma}^{(l)}\rangle+\cdots+\langle\cdots\rangle+\cdots\right\}. \quad (2.56)\end{aligned}$$

The average is taken with respect to the N-qubit pure state $|\psi\rangle$ whose entanglement we are to quantify. This result echos the fact mentioned in the previous section that the geometric measure (or here the maximal overlap) can be measured, via the correlations, which are physical quantities.

2.3 Extension to mixed states

The extension of the geometric measure to mixed states ρ can be made via the use of the *convex roof* (or *hull*) construction [indicated by "co"], as was done for the entanglement of formation [c.f. Eq. (1.30)] [22]. The essence is a minimization over all decompositions $\rho=\sum_i p_i\,|\psi_i\rangle\langle\psi_i|$ into pure states, i.e.,

$$E(\rho)\equiv(\mathrm{co}\,E_{\mathrm{pure}})(\rho)\equiv\min_{\{p_i,\psi_i\}}\sum\nolimits_i p_i\,E_{\mathrm{pure}}(|\psi_i\rangle). \quad (2.57)$$

This convex hull construction ensures that the measure gives zero for separable states; however, in general it also complicates the task of determining mixed-state entanglement.

Now, any good entanglement measure E should, at least, satisfy the following criteria (c.f. Refs. [26, 28, 42])

C1. (a) $E(\rho) \geq 0$; (b) $E(\rho) = 0$ if ρ is not entangled.

C2. Local unitary transformations do not change E.

C3. Local operations and classical communication (LOCC) (as well as post-selection) do not increase the expectation value of E [1].

C4. Entanglement is convex under the discarding of information, i.e., $\sum_i p_i E(\rho_i) \geq E(\sum_i p_i \rho_i)$.

The first requirement simply states that the entanglement is a non-negative quantity, and it vanishes for unentangled states. Local unitary transformations are simply a change of local basis, and entanglement should be invariant under such a change. The third criterion simply requires that the average entanglement cannot be increased during manipulations that are local, which reflects the fact that entanglement is a nonlocal resource. The last criterion states the fact that, for a set of states, entanglement can never be increased if the information about which state is which is lost. The issue of the desirability of additional features, such as continuity and additivity, requires further investigation, but C1-C4 are regarded as the minimal set. If a measure satisfies C1-C4, it is called an *entanglement monotone* [42].

Does the geometric measure of entanglement obey C1-4? The answer is affirmative but we shall relegate the proof to Appendix D. We remark that from the definition (2.57) it is evident that C1 and C2 are satisfied, provided that $E_{\rm pure}$ satisfies them. Furthermore, the convex-hull construction automatically fulfills C4. The consideration of C3 seems to be more delicate and whether or not it holds depends on the explicit form of $E_{\rm pure}$. In Appendix D we show that the choice of taking $E_{\sin^2}$ as the entanglement measure *does* satisfy C3.

2.4 Analytic results for mixed states

Before moving on to the *terra incognita* of mixed *multi-partite* entanglement, we test the geometric approach in the setting of mixed *bi-partite* states, by computing $E_{\sin^2}$ for three classes of states for which $E_{\rm F}$ is known.

[1] This requirement does not contradict with distillation, as it takes into account the cases when distillation fails.

2.4.1 Arbitrary two-qubit mixed states

For arbitrary two-qubit states we can show that

$$E_{\sin^2}(\rho) = \frac{1}{2}\big(1 - \sqrt{1 - C(\rho)^2}\,\big), \tag{2.58}$$

where $C(\rho)$ is the Wootters concurrence of the state ρ. The essential point is that, in his derivation of the formula for $E_{\rm F}$, Wootters showed that there exists an optimal decomposition $\rho = \sum_i p_i \, |\psi_i\rangle\langle\psi_i|$ in which every $|\psi_i\rangle$ has the concurrence of ρ itself. (More explicitly, every $|\psi_i\rangle$ has the identical concurrence, that concurrence being the infimum over all decompositions.) By using Eq. (2.22) we see that Eq. (2.58)holds for any two-qubit *pure* state. As $E_{\sin^2}$ is a monotonically increasing convex function of $C \in [0, 1]$, the optimal decomposition for $E_{\sin^2}$ is identical to that for the entanglement of formation $E_{\rm F}$. Thus, we see that Eq. (2.58) holds for *any two-qubit mixed state*.

The fact that $E_{\sin^2}$ is related to $E_{\rm F}$ via the concurrence C is inevitable for two-qubit systems, as both are fully determined by the one independent Schmidt coefficient. We note that Vidal [44] has derived this expression when he considered the probability of success for converting a single copy of some pure state $|\psi\rangle$ into the desired mixed state ρ. The probability of the conversion is

$$P(\psi \to \rho) = \min\left\{1, \frac{E_{\sin^2}(\psi)}{E_{\sin^2}(\rho)}\right\}, \tag{2.59}$$

which gives a physical interpretation of the geometric measure of entanglement. Unfortunately, this connection only holds for two-qubit states.

2.4.2 Generalized Werner states

Any state $\rho_{\rm W}$ of a $C^d \otimes C^d$ system is called a generalized Werner state if it is invariant under

$$\mathbf{P}_1 : \rho \to \int dU (U \otimes U)\rho\,(U^\dagger \otimes U^\dagger), \tag{2.60}$$

where U is any element of the unitary group $\mathcal{U}(d)$ and dU is the corresponding normalized Haar measure. Both parties perform the same unitary transformation U on their own system but they choose U randomly according to the measure dU.

Generalized Werner states can be expressed as a linear combination of two operators: the *identity* $\hat{\mathbb{1}}$, and the *swap* $\hat{\mathrm{F}} \equiv \sum_{ij} |ij\rangle\langle ji|$, i.e., $\rho_{\mathrm{W}} \equiv a\hat{\mathbb{1}} + b\hat{\mathrm{F}}$, where a and b are real parameters related via the constraint $\mathrm{Tr}\rho_{\mathrm{W}} = 1$. This one-parameter family of states can be neatly expressed in terms of the single parameter $f \equiv \mathrm{Tr}(\rho_{\mathrm{W}}\hat{\mathrm{F}})$:

$$\rho_{\mathrm{W}}(f) = \frac{d^2 - fd}{d^4 - d^2}\mathbb{1} \otimes \mathbb{1} + \frac{fd^2 - d}{d^4 - d^2}\hat{\mathrm{F}}. \tag{2.61}$$

By applying to $E_{\sin^2}$ the technique by developed by Vollbrecht and Werner for $E_{\mathrm{F}}(\rho_{\mathrm{W}})$ [to be briefly reviewed shortly; or see Ref. [24]], one arrives at the geometric entanglement function for Werner states:

$$E_{\sin^2}\big(\rho_{\mathrm{W}}(f)\big) = \frac{1}{2}\big(1 - \sqrt{1 - f^2}\,\big) \quad \text{for } f \leq 0, \tag{2.62}$$

and zero otherwise.

In order to prepare for this, we now briefly review the technique developed by Vollbrecht and Werner [24] for computing the entanglement of formationfor ρ_{W}; this turns out to be applicable to the computation of the sought quantity $E_{\sin^2}$. We start by fixing some notation. Let

K be a compact convex set (e.g., a set of states that includes both pure and mixed ones);

M be a convex subset of K (e.g., set of pure states);

$E : M \to R \cup \{+\infty\}$ be function that maps elements of M to the real numbers (e.g., $E = E_{\sin^2}$); and

G be a compact group of symmetries, acting on K (e.g., the group $U \times U^{\dagger}$) as $\alpha_g : K \to K$ (where α_g is the representation of the element $g \in G$) that preserve convex combinations.

We assume that $\alpha_g M \subset M$ (e.g., pures states are mapped into pure states), and that $E(\alpha_g m) = E(m)$ for all $m \in M$ and $g \in G$ (e.g., that the entanglement of a pure state is preserved under α_g). We denote by $\mathbf{P}$ the invariant projection operator defined via

$$\mathbf{P}k = \int dg \alpha_g(k), \tag{2.63}$$

where $k \in K$. One example of $\mathbf{P}_1$ is the operation in Eq. (2.60). Vollbrecht and Werner also defined

the following real-valued function ϵ on the invariant subset $\mathbf{P}K$:

$$\epsilon(x) = \inf\{E(m)|m \in M, \mathbf{P}m = x\}. \tag{2.64}$$

They then showed that, for $x \in \mathbf{P}K$,

$$\operatorname{co} E(x) = \operatorname{co} \epsilon(x), \tag{2.65}$$

and provided the following recipe for computing the function $\operatorname{co} E$ for G-invariant states:

1. For every invarinat state ρ (i.e., obeying $\rho = \mathbf{P}\rho$), find the set M_ρ of pure states σ such that $\mathbf{P}\sigma = \rho$.

2. Compute $\epsilon(\rho) \equiv \inf\{E(\sigma)|\sigma \in M_\rho\}$.

3. Then $\operatorname{co} E$ is the convex hull of this function ϵ.

Having reviewed the Vollbrecht-Werner technique, we now apply it to the geometric measure of entanglement $E_{\sin^2}$ by applying their recipe.

The essential points of the derivation are as follows:

(i) In order to find the set $M_{\rho_{\mathrm{W}}}$ it is sufficient, due to the invariance of ρ_{W} under $\mathbf{P_1}$, to consider any pure state $|\Phi\rangle = \sum_{jk} \Phi_{jk}|e_j^{(1)}\rangle \otimes |e_k^{(2)}\rangle$ that has a diagonal reduced density matrix $\mathrm{Tr}_2|\Phi\rangle\langle\Phi|$ and the value $\mathrm{Tr}(|\Phi\rangle\langle\Phi|\hat{F})$ equal to the parameter f associated with the Werner state $\rho_{\mathrm{W}}(f)$. It can be shown that

$$E_{\sin^2}(|\Phi\rangle\langle\Phi|) \geq \frac{1}{2}\left(1 - \sqrt{1 - (f - \sum\nolimits_i \lambda_{ii})^2}\right), \tag{2.66}$$

where $\lambda_{ii} \equiv |\Phi_{ii}|^2$.

(ii) If $f > 0$, we can set the only nonzero elements of $|\Phi\rangle$ to be Φ_{i1}, $\Phi_{i2}, \ldots, \Phi_{ii}, \ldots, \Phi_{id}$ such that $|\Phi_{ii}|^2 = f$, this state obviously being separable. Hence, for $f > 0$ we have $E_{\sin^2}(\rho_{\mathrm{W}}(f)) = 0$. On the other hand, if $f < 0$ then any nonzero λ_{ii} would increase $(f - \sum_i \lambda_{ii})^2$ and, hence, increase the value of $E(|\Phi\rangle\langle\Phi|)$, not conforming with the convex hull. Thus, for a fixed value of f, the lowest possible value of the entanglement $E(|\Phi\rangle\langle\Phi|)$ that can be achieved occurs when $\lambda_{ii} = 0$ and there

are only two nonzero elements Φ_{ij} and Φ_{ji} $(i \neq j)$. This leads to

$$\min_{|\Phi\rangle \text{ at fixed } f} E(|\Phi\rangle\langle\Phi|) = \frac{1}{2}\left(1 - \sqrt{1-f^2}\right). \tag{2.67}$$

Thus, as a function of f, $\epsilon(f)$ is given by

$$\epsilon(f) = \begin{cases} \frac{1}{2}\left(1 - \sqrt{1-f^2}\right) & \text{for } f \leq 0, \\ 0 & \text{for } f \geq 0, \end{cases} \tag{2.68}$$

which, being convex for $f \in [-1, 1]$, gives the entanglement function (2.62) for Werner states.

2.4.3 Isotropic states

Instead of both performing U on their system, one of the two parties performs U whereas the other performs U^*. The isotropic states are are invariant under

$$\mathbf{P}_2 : \rho \to \int dU\, (U \otimes U^*)\rho\, (U^\dagger \otimes U^{*\dagger}), \tag{2.69}$$

and can be expressed as

$$\rho_{\text{iso}}(F) \equiv \frac{1-F}{d^2-1}\left(\hat{\mathbb{1}} - |\Phi^+\rangle\langle\Phi^+|\right) + F|\Phi^+\rangle\langle\Phi^+|, \tag{2.70}$$

where $|\Phi^+\rangle \equiv \frac{1}{\sqrt{d}}\sum_{i=1}^{d}|ii\rangle$ and $F \in [0, 1]$. For $F \in [0, 1/d]$ this state is known to be separable [43]. By following arguments similar to those applied by Terhal and Vollbrecht [23] for $E_{\text{F}}(\rho_{\text{iso}})$ one arrives at

$$E_{\sin^2}\left(\rho_{\text{iso}}(F)\right) = 1 - \frac{1}{d}\left(\sqrt{F} + \sqrt{(1-F)(d-1)}\,\right)^2, \tag{2.71}$$

for $F \geq 1/d$. The essential point of the derivation is the following Lemma (c.f. Ref. [23]):

Lemma 1. The entanglement $E_{\sin^2}$ for isotropic states in $C^d \otimes C^d$ for $F \in [1/d, 1]$ is given by

$$E_{\sin^2}(\rho_{\text{iso}}(F)) = \text{co}(R(F)), \tag{2.72}$$

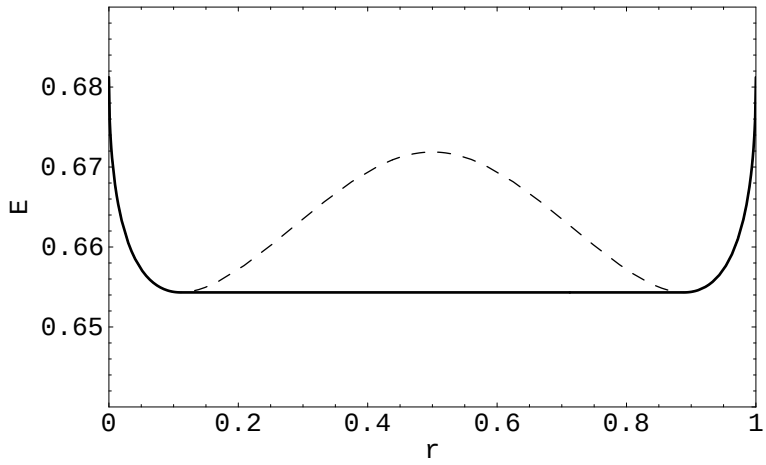

Figure 2.4: Entanglement curve for the mixed state $\rho_{7;2,5}(r)$ (full line) constructed as the convex hull of the curve for the pure state $|\mathrm{SS}_{7;2,5}(r,\phi)\rangle$ (dashed in the middle; full at the edges).

where $\mathrm{co}(R(F))$ is the convex hull of the function R and

$$R(F) = 1 - \max_{\{\mu_i\}} \big\{ \mu_i \,|F = \Big(\sum_{i=1}^{d} \sqrt{\mu_i} \Big)^2 / d;\ \sum_{i=1}^{d} \mu_i = 1 \big\}. \tag{2.73}$$

Straightforward extremization shows that

$$R(F) = 1 - \left(\sqrt{\frac{F}{d}} + \sqrt{\frac{F+d-1}{d} - F} \right)^2, \tag{2.74}$$

which is convex, and hence $\mathrm{co}(R(F)) = R(F)$. Thus we arrive at the entanglement result for isotropic states given in Eq. (2.71).

2.4.4 Mixtures of multi-partite symmetric states

Before exploring more general mixed states, it is useful to first examine states with high symmetry. With this in mind, we consider states formed by mixing two distinct symmetric states (i.e., $k_1 \neq k_2$):

$$\rho_{n;k_1k_2}(r) \equiv r\,|\mathrm{S}(n,k_1)\rangle\langle \mathrm{S}(n,k_1)| + (1-r)|\mathrm{S}(n,k_2)\rangle\langle \mathrm{S}(n,k_2)|. \tag{2.75}$$

From the independence of $E_{\sin^2}\left(|\mathrm{SS}_{n;k_1k_2}(r,\phi)\rangle\right)$ on ϕ and the fact that the mixed state $\rho_{n;k_1k_2}(r)$ is invariant under the projection

$$\mathrm{P}_3 : \rho \to \int \frac{d\phi}{2\pi}\, U^{\otimes n} \rho\, U^{\dagger\otimes n} \tag{2.76}$$

with $U : \{|0\rangle, |1\rangle\} \to \{|0\rangle, \mathrm{e}^{-i\phi}|1\rangle\}$, we have that $E_{\sin^2}\left(\rho_{n;k_1k_2}(r)\right)$ vs. r can be constructed from the convex hull of the entanglement function of $|\mathrm{SS}_{n;k_1k_2}(r,0)\rangle$ vs. r. An example, $(n,k_1,k_2) = (7,2,5)$, is shown in Fig. 2.4. If the dependence of $E_{\sin^2}$ on r is already convex for the pure state, its mixed-state counterpart has precisely the same dependence. Figure 2.2, for which $(n,k_1,k_2) = (3,1,2)$, exemplifies such behavior. More generally, one can consider mixed states of the form

$$\rho(\{p\}) = \sum_k p_k |S(n,k)\rangle\langle S(n,k)|. \tag{2.77}$$

The entanglement $E_{\mathrm{mixed}}(\{p\})$ can then be obtained as a function of the mixture $\{p\}$ from the convex hull of the entanglement function $E_{\mathrm{pure}}(\{q\})$ for the *pure* state $\sum_k \sqrt{q_k}|S(n,k)\rangle$. That is, $E_{\mathrm{mix}}(\{p\}) = \mathrm{co}\, E_{\mathrm{pure}}(\{q\})|_{\{q=p\}}$. Therefore, the entanglement for a mixture of symmetric states $|S(n,k)\rangle$ is known from $E_{\mathrm{pure}}(\{q\})$, up to some convexification.

2.5 Application to arbitrary mixture of GHZ, W and inverted-W states

Having warmed up in Sec. 2.4.4 by analyzing mixtures of multi-partite symmetric states, we now turn our attention to mixtures of three-qubit GHZ, W and inverted-W states.

2.5.1 Symmetry and entanglement preliminaries

These states—GHZ, W and inverted-W states—are important, in the sense that all pure three-qubit entangled states can, under probabilistic LOCC, be transformed either to GHZ or W (equivalently inverted-W) states. It is thus interesting to determine the entanglement content (using any measure

of entanglement) for mixed states of the form:

$$\rho(x,y) \equiv x|\mathrm{GHZ}\rangle\langle\mathrm{GHZ}| + y|\mathrm{W}\rangle\langle\mathrm{W}| + (1-x-y)|\widetilde{\mathrm{W}}\rangle\langle\widetilde{\mathrm{W}}|, \tag{2.78}$$

where $x, y \geq 0$ and $x + y \leq 1$. This family of mixed states is not contained in the family (2.77), as $|\mathrm{GHZ}\rangle = \big(|\mathrm{S}(3,0)\rangle + |\mathrm{S}(3,3)\rangle\big)/\sqrt{2}$. The property of $\rho(x,y)$ that facilitates the computation of its entanglement is a certain invariance, which we now describe. Consider the local unitary transformation on a single qubit:

$$|0\rangle \;\rightarrow\; |0\rangle, \tag{2.79a}$$

$$|1\rangle \;\rightarrow\; g^k|1\rangle, \tag{2.79b}$$

where $g = \exp(2\pi i/3)$, i.e., a relative phase shift. This transformation, when applied simultaneously to all three qubits, is denoted by U_k. It is straightforward to see that $\rho(x,y)$ is invariant under the mapping

$$\mathbf{P}_4 : \rho \rightarrow \frac{1}{3}\sum_{k=1}^{3} U_k\,\rho\,U_k^\dagger\,. \tag{2.80}$$

Thus, we can apply Vollbrecht-Werner technique [24] to the compution of the entanglement of $\rho(x,y)$.

Now, the Vollbrecht-Werner procedure requires one to characterize the set S_{inv} of all pure states that are invariant under the projection $\mathbf{P}_4$. Then, the convex hull of $E_{\sin^2}(\rho)$ need only be taken over S_{inv}, instead of the set of *all* pure states. However, as the state $\rho(x,y)$ is a mixture of three orthogonal pure states (viz. $|\mathrm{GHZ}\rangle$, $|\mathrm{W}\rangle$ and $|\widetilde{\mathrm{W}}\rangle$) that are themselves invariant under $\mathbf{P}_4$, the pure states that can enter any possible decomposition of ρ must be of the restricted form:

$$\alpha|\mathrm{GHZ}\rangle + \beta|\mathrm{W}\rangle + \gamma|\widetilde{\mathrm{W}}\rangle, \tag{2.81}$$

with $|\alpha|^2 + |\beta|^2 + |\gamma|^2 = 1$. Thus, there is no need to characterize S_{inv}, but only to characterize the pure states that, under $\mathbf{P}_4$, are projected to $\rho(x,y)$. These states are readily seen to be of the form:

$$\sqrt{x}\,e^{i\phi_1}|\mathrm{GHZ}\rangle + \sqrt{y}\,e^{i\phi_2}|\mathrm{W}\rangle + \sqrt{1-x-y}\,e^{i\phi_3}|\widetilde{\mathrm{W}}\rangle. \tag{2.82}$$

Of these, the least entangled state, for given (x, y), has all coefficients non-negative (up to a global phase), i.e.,

$$|\psi(x,y)\rangle \equiv \sqrt{x}|\mathrm{GHZ}\rangle + \sqrt{y}|\mathrm{W}\rangle + \sqrt{1-x-y}|\widetilde{\mathrm{W}}\rangle. \tag{2.83}$$

The entanglement eigenvalue of $|\psi(x,y)\rangle$ can then be readily calculated, and one obtains

$$\Lambda(x,y) = \frac{1}{(1+t^2)^{\frac{3}{2}}}\left\{\sqrt{\frac{x}{2}}(1+t^3) + \sqrt{3y}\,t + \sqrt{3(1-x-y)}\,t^2\right\}, \tag{2.84}$$

where t is the (unique) non-negative real root of the following third-order polynomial equation:

$$3\sqrt{\frac{x}{2}}(-t+t^2) + \sqrt{3y}(-2t^2+1) + \sqrt{3(1-x-y)}(-t^3+2t) = 0. \tag{2.85}$$

Hence, the entanglement function for $|\psi(x,y)\rangle$, i.e., $E_\psi(x,y) \equiv 1 - \Lambda(x,y)^2$, is determined (up to the numerically straightforward task of root-finding).

2.5.2 Finding the convex hull

Recall that our aim is to determine the entanglement of the mixed state $\rho(x,y)$. As we already know the entanglement of the corresponding pure state $|\psi(x,y)\rangle$, we may accomplish our aim via the Vollbrecht-Werner technique [24], which gives the entanglement of $\rho(x,y)$ in terms of that of $|\psi(x,y)\rangle$ via the convex hull construction: $E_\rho(x,y) = (\mathrm{co}\, E_\psi)(x,y)$. Said in words, the entanglement surface $z = E_\rho(x,y)$ is the convex surface constructed from the surface $z = E_\psi(x,y)$.

The idea underlying the use of the convex hull is this. Due to its linearity in x and y, the state $\rho(x,y)$ (2.78) can [except when (x,y) lies on the boundary] be decomposed into two parts:

$$\rho(x,y) = p\,\rho(x_1,y_1) + (1-p)\rho(x_2,y_2), \tag{2.86}$$

with the (real, non-negative) weight p and end-points (x_1,y_1) and (x_2,y_2) related by

$$p\,x_1 + (1-p)x_2 = x, \tag{2.87a}$$

$$p\,y_1 + (1-p)y_2 = y. \tag{2.87b}$$

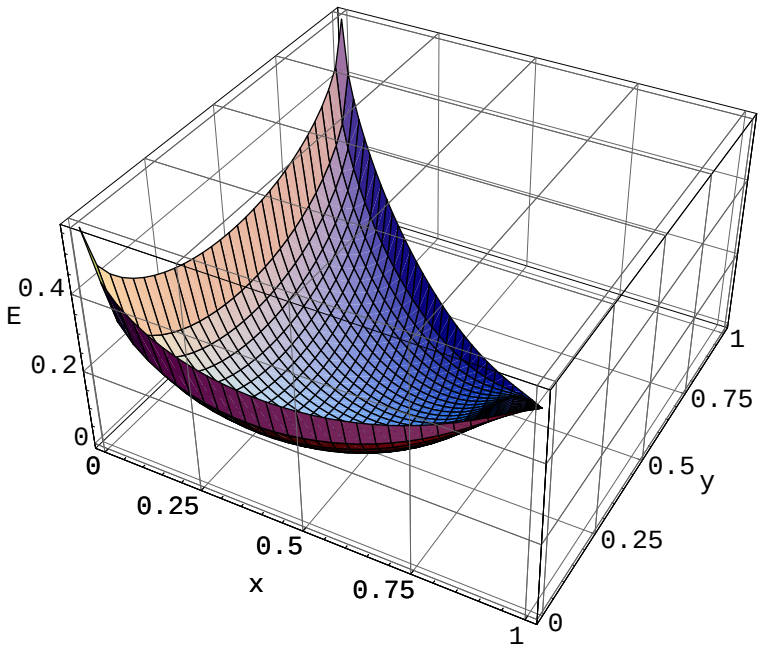

Figure 2.5: Entanglement vs. the composition of the pure state $|\psi(x,y)\rangle$. Although not obvious from the plot, this entanglement surface is not convex near $(x,y)=(1,0)$,

Now, if it should happen that

$$pE_\psi(x_1,y_1)+(1-p)E_\psi(x_2,y_2)<E_\psi(x,y) \tag{2.88}$$

then the entanglement, averaged over the end-points, would give a value lower than that at the interior point (x,y); this conforms with the convex-hull construction.

It should be pointed out that the convex hull should be taken with respect to parameters on which the density matrix depends *linearly*, such as x and y in the example of $\rho(x,y)$. Furthermore, in order to obtain the convex hull of a function, one needs to know the *global* structure of the function—in the present case $E_\psi(x,y)$. We note that efficient numerical algorithms have been developed for constructing convex hulls [45].

As we have discussed, our route to establishing the entanglement of $\rho(x,y)$ involves the analysis of the entanglement of $|\psi(x,y)\rangle$, which we show in Fig. 2.5. Although it is not obvious from the figure, the corresponding surface fails to be convex near the point $(x,y)=(1,0)$, and therefore in this region we must suitably convexify in order to obtain the entanglement of $\rho(x,y)$. As previously

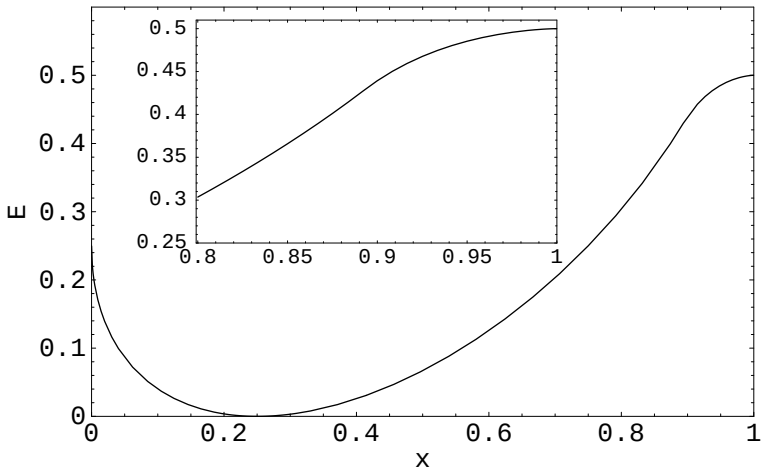

Figure 2.6: Entanglement of the pure state $|\psi\big(x, y = (1-x)/2\big)\rangle = \sqrt{x}\,|\mathrm{GHZ}\rangle + \sqrt{(1-x)/2}\,|\mathrm{W}\rangle + \sqrt{(1-x)/2}\,|\widetilde{\mathrm{W}}\rangle$ vs. x. This shows the entanglement along the diagonal boundary $x+2y=1$. Note the absence of convexity near $x=1$; this region is repeated in the inset.

shown in Fig. 2.2, where the entanglement of $|\psi(x,y)\rangle$ is plotted along the line $(x,y)=(0,s)$, the behavior of the entanglement curve is convex. By contrast, along the line $x+2y=1$ there is a region in which the entanglement is not convex, as Fig. 2.6 shows. The nonconvexity of the entanglement of $|\psi(x,y)\rangle$ complicates the calculation of the entanglement of $\rho(x,y)$, as it necessitates a procedure for constructing the convex hull in the (as it happens, small) nonconvex region. Elsewhere in the xy plane the entanglement of $\rho(x,y)$ is given directly by the entanglement of $|\psi(x,y)\rangle$.

At worst, convexification would have to be undertaken numerically. However, in the present setting it turns out that one can determine the convex surface essentially analytically, by performing the necessary convexifying surgery on surface $z = E_\psi(x,y)$. To do this, we make use of the fact that if we parametrize y via $(1-x)r$, i.e., we consider

$$\rho\big(x,(1-x)r\big) = x\,|\mathrm{GHZ}\rangle\langle\mathrm{GHZ}| + (1-x)r\,|\mathrm{W}\rangle\langle\mathrm{W}| + (1-x)(1-r)|\widetilde{\mathrm{W}}\rangle\langle\widetilde{\mathrm{W}}|, \tag{2.89}$$

where $0 \le r \le 1$ [and similarly for $|\psi(x,y)\rangle$] then, as a function of (x,r), the entanglement would be symmetric with respect to $r = 1/2$, as Fig. 2.7 makes evident. With this parametrization, the nonconvex region of the entanglement of $|\psi\rangle$ can more clearly be identified. To convexify this surface we adopt the following convenient strategy. First, we reparametrize the coordinates, exchanging y by $(1-x)r$. Now, owing to the linearity, in r at fixed x and *vice versa*, of the

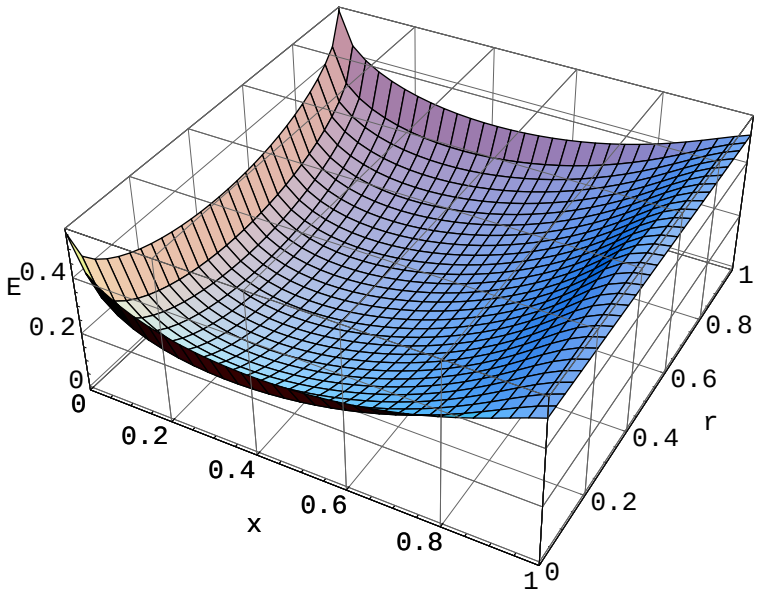

Figure 2.7: Entanglement of the pure state $|\psi\big(x,(1-x)r\big)\rangle = \sqrt{x}\,|\mathrm{GHZ}\rangle + \sqrt{(1-x)r}\,|\mathrm{W}\rangle + \sqrt{(1-x)(1-r)}|\widetilde{\mathrm{W}}\rangle$ vs. x and r. Note the symmetry of the surface with respect with $r = 1/2$.

coefficients x, $(1-x)r$ and $(1-x)(1-r)$ in Eq. (2.89), it is certainly necessary for the entanglement of ρ to be a convex function of r at fixed x and *vice versa*. Convexity is, however, not necessary in other directions in the (x,r) plane, owing to the nonlinearity of the coefficients under simultaneous variations of x and r. Put more simply: convexity is not necessary throughout the (x,r) plane because straight lines in the (x,r) plane do not correspond to straight lines in the (x,y) plane (except along lines parallel either to the r or the x axis). Thus, our strategy will be to convexify in a restricted sense: first along lines parallel to the r axis and then along lines parallel to the x axis. Having done this, we shall check to see that no further convexification is necessary.

For each x, we convexify the curve $z = E_\psi\big(x,(1-x)r\big)$ as a function of r, and then generate a new surface by allowing x to vary. More specifically, the nonconvexity in this direction has the form of a symmetric pair of minima located on either side of a cusp, as shown in Fig. 2.8. Thus, to correct for it, we simply locate the minima and connect them by a straight horizontal line.

What remains is to consider the issue of convexity along the x (i.e., fixed r) direction for the surface just constructed. In this direction, nonconvexity occurs when x is, roughly speaking, greater than 0.8, as Fig. 2.9 suggests. In contrast with the case of nonconvexity at fixed r, this nonconvexity is due to an inflection point, at which the second derivative vanishes. To correct for it, we locate

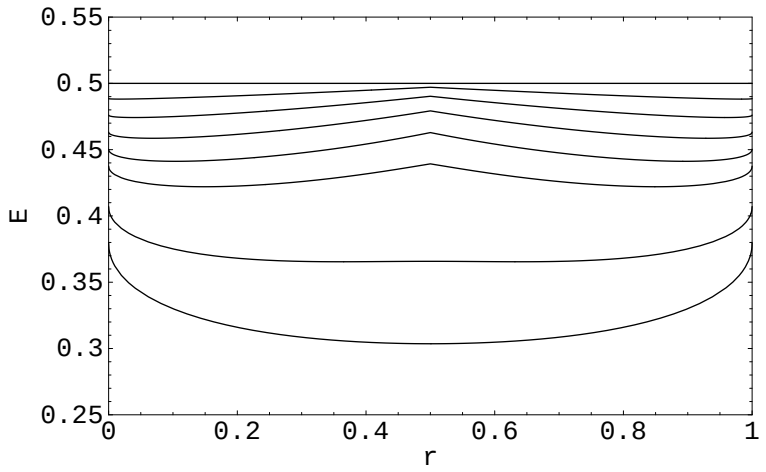

Figure 2.8: Entanglement of the pure states $|\psi\big(x,(1-x)r\big)\rangle = \sqrt{x}\,|\mathrm{GHZ}\rangle + \sqrt{(1-x)r}\,|\mathrm{W}\rangle + \sqrt{(1-x)(1-r)}|\widetilde{\mathrm{W}}\rangle$ vs. r for various values of x (from the bottom: 0.8, 0.85, 0.9, 0.92, 0.94, 0.96, 0.98, 1). This reveals the nonconvexity in r for intermediate values of x.

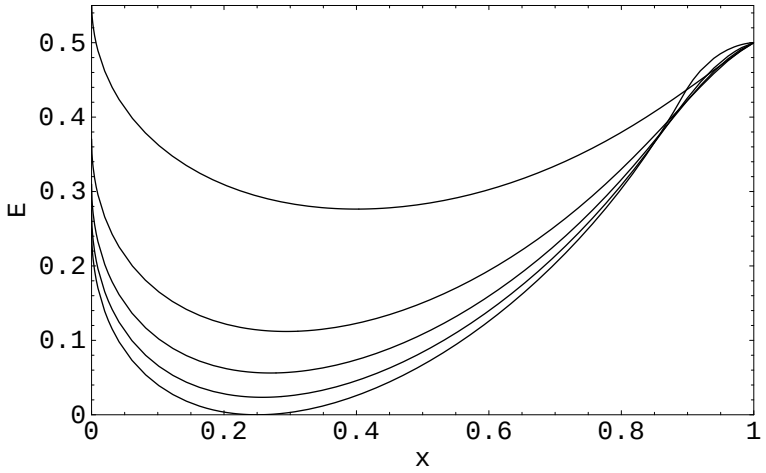

Figure 2.9: Entanglement of the pure states $|\psi\big(x,(1-x)r\big)\rangle = \sqrt{x}\,|\mathrm{GHZ}\rangle + \sqrt{(1-x)r}\,|\mathrm{W}\rangle + \sqrt{(1-x)(1-r)}|\widetilde{\mathrm{W}}\rangle$ vs. x for various values of r (from the top: 0, 0.1, 0.2, 0.3, 0.5). This reveals the nonconvexity in x in the (approximate) interval $[0.85, 1]$.

the point $x = x_0$ such that the tangent at $x = x_0$ is equal to that of the line between the point on the curve at x_0 and the end-point at $x = 1$, and connect them with a straight line. This furnishes us with a surface convexified with respect to x (at fixed r) and *vice versa*.

Armed with this surface, we return to the (x, y) parametrization, and ask whether it is fully convex (i.e., convex along straight lines connecting *any* pair of points). Said equivalently, we ask whether or not any further convexification is required. Although we have not proven it, on the basis of extensive numerical exploration we are confident that the resulting surface is, indeed, convex.

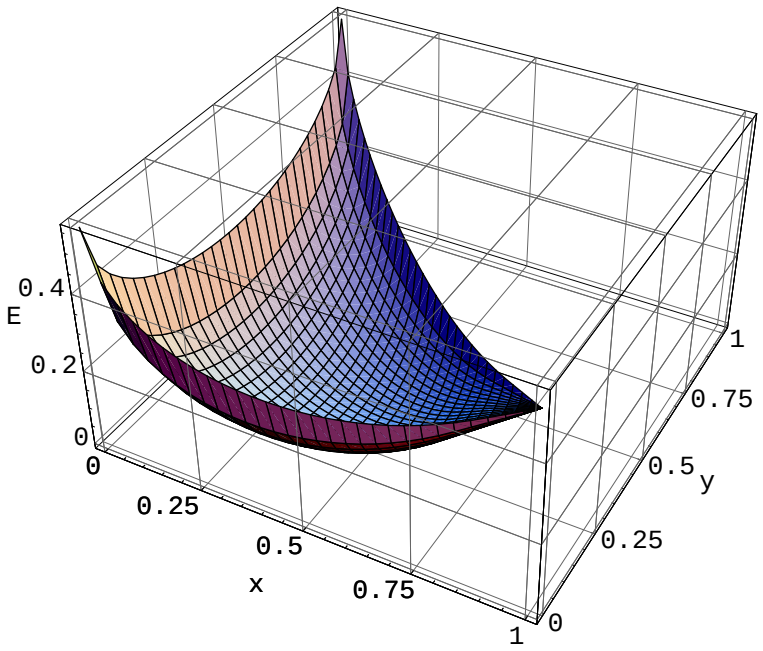

Figure 2.10: Entanglement of the mixed state $\rho(x, y)$.

The resulting convex entanglement surface for $\rho(x, y)$ is shown in Fig. 2.10. Figure 2.11 exemplifies this convexity along the line $2y + x = 1$. We have observed that, for the case at hand, it is adequate to correct for nonconvexity only in the x direction at fixed r.

2.5.3 Comparison with the negativity

As introduced in Sec. 1.1 the negativity measure of entanglement is defined to be twice the absolute value of the sum of the negative eigenvalues of the partial transpose of the density matrix [14, 15, 46]. In the present setting, viz., the family $\rho(x, y)$ of three-qubit states, the partial transpose may equivalently be taken with respect to any one of the three parties, owing to the invariance of $\rho(x, y)$ under all permutations of the parties. Transposing with respect to the third party, one has

$$\mathcal{N}(\rho) \equiv -2 \sum_{\lambda_i < 0} \lambda_i, \tag{2.90}$$

where the λ's are the eigenvalues of the matrix ρ^{T_3},

It is straightforward to calculate the negativity of $\rho(x, y)$; the results are shown in Fig. 2.12. Interestingly, for all allowed values of (x, y), the state $\rho(x, y)$ has nonzero negativity, except at

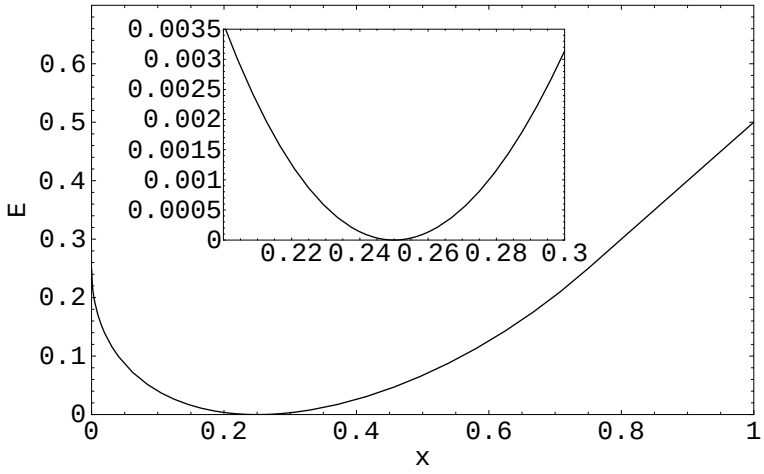

Figure 2.11: Entanglement of the mixed state $\rho\big(x, y = (1-x)/2\big) = x\,|\mathrm{GHZ}\rangle\langle\mathrm{GHZ}| + \frac{1-x}{2}\big(|\mathrm{W}\rangle\langle\mathrm{W}| + |\widetilde{\mathrm{W}}\rangle\langle\widetilde{\mathrm{W}}|\big)$ vs. x. Inset: enlargement of the region $x \in [0.2, 0.3]$. This contains the only point, $(x, y) = (1/4, 3/8)$, at which $E_\rho(x, y)$ vanishes.

$(x, y) = (1/4, 3/8)$, at which the calculation of the GME shows that the density matrix is indeed separable. One also sees from that fact that it can be obtained by applying the projection $\mathbf{P}_4$ to the (un-normalized) separable pure state $\big(|0\rangle + |1\rangle\big)^{\otimes 3}$ that $\rho(1/4, 3/8)$ is a separable state. The fact that the only positve-partial-transpose (PPT) state is separable is the statement that there are no entangled PPT states (i.e., no PPT bound entangled states) within this family of three-qubit mixed states. The negativity surface, Fig. 2.12, is qualitatively—but not quantitatively—the same as that of GME. By inspecting the negativity and GME surfaces one can see that they present ordering difficulties. This means that one can find pairs of states $\rho(x_1, y_1)$ and $\rho(x_2, y_2)$ that have respective negativities $\mathcal{N}_1$ and $\mathcal{N}_2$ and GMEs E_1 and E_2 such that, say, $\mathcal{N}_1 < \mathcal{N}_2$ but $E_1 > E_2$. Said equivalently, the negativity and the GME do not necessarily agree on which of a pair of states is the more entangled. For two-qubit settings, such ordering difficulties do not show up for pure states, but can for mixed states [46, 47]. On the other hand, for three qubits, such ordering difficulties already show up for pure states, as the following example shows: $\mathcal{N}(\mathrm{GHZ}) = 1 > \mathcal{N}(\mathrm{W}) = 2\sqrt{2}/3$ whereas for the GME the order is reversed. We note, however, that for the relative entropy of entanglement E_R, one has $E_R(\mathrm{GHZ}) = \log_2 2 < E_R(\mathrm{W}) = \log_2(9/4)$ [48], which for this particular case is in accord with the GME.

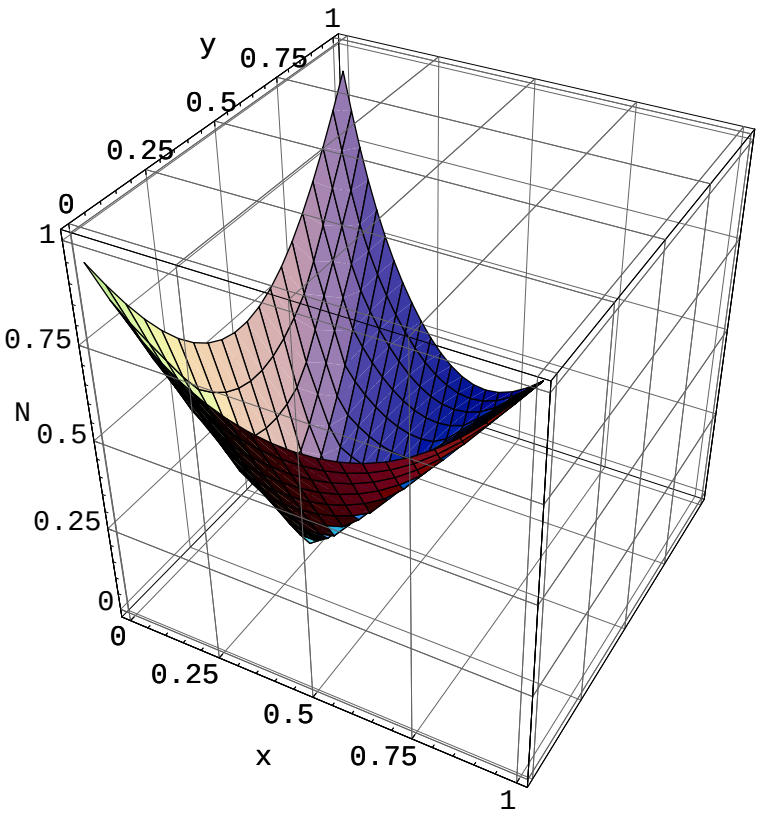

Figure 2.12: Negativity of the mixed state $\rho(x, y)$.

2.6 Concluding remarks

We have considered a rather general, geometrically motivated, measure of entanglement, applicable to pure and mixed quantum states involving arbitrary numbers and structures of parties. In bi-partite settings, this approach provides an alternative—and generally inequivalent—measure to the entanglement of formation. For multi-partite settings, there is, to date, no explicit generalization of entanglement of formation. However, if such a generalization should emerge, and if it should be based on the convex hull construction (as it is in the bi-partite case), then one may be able to calculate the entanglement of formation for the families of multi-partite mixed states considered in the present chapter.

As for explicit implementations, the geometric measure of entanglement yields analytic results in several bi-partite cases for which the entanglement of formation is already known. These cases include: (i) arbitrary two-qubit mixed, (ii) generalized Werner, and (iii) isotropic states. Furthermore, we have obtained the geometric measure of entanglement for certain multi-partite mixed

states, such as mixtures of symmetric states. In addition, by making use of the geometric measure, we have addressed the entanglement of a rather general family of three-qubit mixed states analytically (up to root-finding). This family consists of arbitrary mixtures of GHZ, W, and inverted-W states. To the best of our knowledge, corresponding results have not, to date, been obtained for other measures of entanglement, such as entanglement of formation and relative entropy of entanglement. We have also obtained corresponding results for the negativity measure of entanglement. Among other things, we have found that there are no PPT bound entangled states within this general family.

A significant issue that we have not discussed is how to use the geometric measure to provide a classification of entanglement of various multi-partite entangled states, even in the pure-state setting. For example, given a tri-partite state, is all the entanglement associated with pairs of parts, or is some attributable only to the system as a whole? More generally, one can envisage all possible partitionings of the parties, and for each, compute the geometric measure of entanglement. This would provide a hierarchical characterization of the entanglement of states, more refined than the *global* characterization discussed here. Another extension would involve augmenting the set of separable pure states with certain classes of entangled pure states, such as bi-separable entangled, W-type and GHZ-type states [49].

Although there is no generally valid analytic procedure for computing the entanglement eigenvalue $\Lambda_{\max}$, one can give—and indeed we have given—analytical results for several elementary cases. Harder examples require computation, but often this is (by today's computational standards) trivial. We note that in order to find $\Lambda_{\max}$ for the state $|\psi\rangle$ it is not necessary to solve the nonlinear eigenproblem (2.8); one can instead appropriately parametrize the family of separable states $|\phi\rangle$ and then directly maximize their overlap with the entangled state $|\psi\rangle$, i.e., $\Lambda_{\max} = \max_{\phi} ||\langle\phi|\psi\rangle||$. Recently, Eisert and co-workers [50] have reformulated the problem of finding the entanglement eigenvalue as an efficient convex optimization. Furthermore, there already exist numerical techniques for determing E_{F} (see, e.g., Ref. [51]), the construction of this measure being also via the convex-hull construction. We believe that numerical techniques for solving the geometric measure of entanglement for general multi-partite mixed states can readily be developed.

The motivation for constructing the measure discussed in the present chapter is that we wish

to address the degree of entanglement from a geometric viewpoint, regardless of the number of parties. Although the construction is purely geometric, we have related this measure to entanglement witnesses, which can in principle be measured locally [41]. Moreover, the geometric measure of entanglement is related to the probability of preparing a single copy of a two-qubit mixed state from a certain pure state [44]. Yet it is still desirable to see whether, in general, this measure can be associated with any physical process in quantum information, as are the entanglement of formation and distillation.

There are further issues that remain to be explored, such as additivity and ordering. The present form of entanglement for pure states, $E_{\sin^2} \equiv 1 - \Lambda^2$, is not additive. However, one can consider a related form, $E_{\log_2} \equiv -\log_2 \Lambda^2$, which, e.g., is additive for $|\psi\rangle_{AB} \otimes |\psi\rangle_{CD}$, i.e.,

$$E_{\log_2}\big(|\psi_1\rangle_{AB} \otimes |\psi_2\rangle_{CD}\big) = E_{\log_2}\big(|\psi_1\rangle_{AB}\big) + E_{\log_2}\big(|\psi_2\rangle_{CD}\big). \tag{2.91}$$

This suggests that it is more appropriate to use this logarithmic form of entanglement to discuss additivity issues. However, $E_{\log_2}$ is not an entanglement monotone when extended to mixed states by convex hull, as we shall show later.

As regards the ordering issue, we first mention a result of bi-partite entanglement measures, due to Virmani and Plenio [47], which states that any two measures with continuity that give the same value as the entanglement of formation for *pure* states are either "identical or induce different orderings in general." This result points out that different entanglement measures will inevitably induce different orderings if they are inequivalent. This result might still hold for multi-partite settings, despite their discussion being based on the existence of entanglement of formation and distillation, which have not been generalized to multi-partite settings. Although the geometric measure gives the same ordering as the entanglement of formation for two-qubit mixed states [see Eq. (2.58)], the geometric measure will, in general, give a different ordering. It is interesting to note that for bi-partite systems, even though the relative entropy of entanglement coincides with entanglement of formation for pure states, they can give different orderings for mixed states, as pointed out by Verstraete and co-workers [47].

We conclude by remarking that the measure discussed in the present chapter is not the same as the Bures measure [27] (see also Sec. 1.4). The Bures measure of entanglement is based on the

minimal distance between the entangled state and the set of separable *mixed* states. By contrast, the measure considered here is based upon the minimal distance between the entangled pure state and the set of separable pure states, and is extended to mixed states by a convex hull construction.

Chapter 3

Connections between relative entropy of entanglement and geometric measure of entanglement

3.1 Introduction

In Sec. 2.1 we saw some difficulties with generalization to multi-partite settings of entanglement measures such as entanglement of formation and of distillation. These difficulties necessitate the study of other measures, e.g., the relative entropy of entanglement (REE) [27, 48]. One of the reasons that the REE is interesting in the bi-partite setting is that it provides a lower bound on the distillable entanglement, the latter being very difficult to calculate generally. However, it is still non-trivial to calculate the REE for generic states, and can be more challenging for multi-partite states. One reason is the absence, in general, of Schmidt decompositions for multi-partite pure states [52]. This implies that for multi-partite pure states the entropies of the reduced density matrices can differ, in contrast to bi-partite pure states, as the following example shows.

Consider a three-qubit pure state $|\psi\rangle_{ABC} \equiv \alpha|001\rangle + \beta|010\rangle + \gamma|100\rangle$, where $|\alpha|^2 + |\beta|^2 + |\gamma|^2 = 1$. The reduced density matrices for parties A, B, and C are, respectively,

$$\rho_A = (|\alpha|^2 + |\beta|^2)|0\rangle\langle 0| + |\gamma|^2|1\rangle\langle 1|, \tag{3.1a}$$

$$\rho_B = (|\alpha|^2 + |\gamma|^2)|0\rangle\langle 0| + |\beta|^2|1\rangle\langle 1|, \tag{3.1b}$$

$$\rho_C = (|\gamma|^2 + |\beta|^2)|0\rangle\langle 0| + |\alpha|^2|1\rangle\langle 1|, \tag{3.1c}$$

which, in general, have different entropies. Thus, for a multi-partite pure state the entropy of the reduced density matrix does not give a consistent entanglement measure. However, even in the case in which all parties have the identical entropy, e.g., $\alpha = \beta = \gamma = 1/\sqrt{3}$ [53], it is in general nontrivial to obtain the relative entropy of entanglement for the state. More generally, for pure multi-partite states, it is not yet known how to obtain their relative entropy of entanglement analytically. The situation is even worse for *mixed* multi-partite states.

In Chapter 2 we have developed a multi-partite measure based on a simple geometric picture. For pure states, this geometric measure of entanglement depends on the maximal overlap between the entangled state and unentangled states, and is easy to compute numerically. We have examined this measure for several bi-partite and multi-partite pure and mixed states [37, 38]. We shall see in the next chapter the application to two distinct multi-partite bound entangled states [54]. In the present chapter, we explore connections between this measure and the relative entropy of entanglement. For certain pure states, some bi-partite and some multi-partite, we find that this lower bound is saturated, and thus their relative entropy of entanglement can be found analytically, in terms of their known geometric measure of entanglement. For certain mixed states, upper bounds on the relative entropy of entanglement are also established. Numerical evidence strongly suggests that these upper bounds are tight, i.e., they are actually the relative entropy of entanglement. These results, although not general enough to solve the problem of calculating the relative entropy of entanglement for arbitrary multi-partite states, may offer some insight into, and serve as a testbed for, future analytic progress related to the relative entropy of entanglement.

The structure of the present chapter is as follows. In Sec. 3.2 we review the two entanglement measures considered in the paper: the relative entropy of entanglement and the geometric measure of entanglement. In Sec. 3.3 we explore connections between the two, in both pure- and mixed-state settings. Examples are provided in which bounds and exact values of the relative entropy of entanglement are obtained. In Sec. 3.4 we give some concluding remarks. The discussion in the present chapter is based on Ref. [55].

3.2 Entanglement measures

In this section we briefly review the two measures considered in the present paper: the relative entropy of entanglement and the geometric measure of entanglement.

3.2.1 Relative entropy of entanglement

The relative entropy $S(\rho||\sigma)$ between two states ρ and σ is defined via

$$S(\rho||\sigma) \equiv \mathrm{Tr}\left(\rho \log_2 \rho - \rho \log_2 \sigma\right), \tag{3.2}$$

which is evidently not symmetric under exchange of ρ and σ, and is non-negative, i.e., $S(\rho||\sigma) \geq 0$. The relative REE for a mixed state ρ is defined to be the minimal relative entropy of ρ over the set of separable mixed states [27, 26]:

$$E_{\mathrm{R}}(\rho) \equiv \min_{\sigma \in \mathcal{D}} S(\rho||\sigma) = \min_{\sigma \in \mathcal{D}} \mathrm{Tr}\left(\rho \log_2 \rho - \rho \log_2 \sigma\right), \tag{3.3}$$

where $\mathcal{D}$ denotes the set of all separable states.

In general, the task of finding the REE for arbitrary states ρ involves a minimization over all separable states, and this renders its computation very difficult. For bi-partite pure states, the REE is equal to entanglements of formation and of distillation. But, despite recent progress [56], for mixed states—even in the simplest setting of two qubits—no analog of Wootters' formula [22] for the entanglement of formation has been found. Things are even worse in multi-partite settings. Even for pure states, there has not been a systematic method for computing REE's. It is thus worthwhile to seek cases in which one can explicitly obtain an expression for the REE. A trivial case arises when there exists a Schmidt decomposition for a multi-partite pure state: in this case, the REE is the usual expression

$$-\sum_i \alpha_i^2 \log_2 \alpha_i^2, \tag{3.4}$$

where the α_i's are Schmidt coefficients (with $\sum_i \alpha_i^2 = 1$). We shall see that there exist other cases in which the REE can be determined analytically, even though no Schmidt decomposition exists.

We remark that an alternative definition of the REE is to replace the set of separable states by

the set of postive partial transpose (PPT) states. The REE thus defined, as well as its regularized version, gives a tighter bound on distillable entanglement. There has been important progress in calculating the REE [and its regularized version, see Eq. (3.61)] with respect to PPT states for certain bi-partite mixed states; see Refs. [57] for more detailed discussions. For multi-partite settings one could define the set of states to optimize over to be the set of states that are PPT with respect to all bi-partite partitionings. However, throughout the discussion of the present chapter, we shall use the first definition, i.e., optimization over the set of completely separable states.

3.2.2 Geometric measure of entanglement

We have introduced the geometric measure of entanglement (GME) in Sec. 2.2 in the pure-state settings, and generalized it to mixed-state settings via the convex-hull construction in Sec. 2.3. The essential point is to find the maximal overlap (a.k.a. entanglement eigenvalue) of the entangled state $|\psi\rangle$ with unentangled states:

$$\Lambda_{\max}(|\psi\rangle) = \max_{\phi} |\langle\phi|\psi\rangle|, \tag{3.5}$$

where $|\phi\rangle$ is an arbitrary unentangled pure state. The explicit form of the measure we shall be concerned with in the present chapter is $E_{\log_2}(\psi) \equiv -2\log_2 \Lambda_{\max}(|\psi\rangle)$. We shall later show that it is a lower bound of the REE.

Some of the examples we considered in previous chapter are relevant to the discussion in the present chapter. We now briefly recap them here. The first class contains the permutation-invariant pure states

$$|S(n,k)\rangle \equiv \sqrt{\frac{k!(n-k)!}{n!}} \sum_{\text{Permutations}} \mathrm{P}|\underbrace{0\cdots0}_{k}\underbrace{1\cdots1}_{n-k}\rangle, \tag{3.6}$$

which has the entanglement eigenvalue

$$\Lambda_{\max}(n,k) = \sqrt{\frac{n!}{k!(n-k)!}} \left(\frac{k}{n}\right)^{\frac{k}{2}} \left(\frac{n-k}{n}\right)^{\frac{n-k}{2}}. \tag{3.7}$$

More generally, for n parties each a $(d+1)$-level system, the state

$$|S(n;\{k\})\rangle \equiv \sqrt{\frac{k_0!k_1!\cdots k_d!}{n!}} \sum_{\text{Permutations}} \mathrm{P}\,|\underbrace{0\ldots0}_{k_0}\,\underbrace{1\ldots1}_{k_1}\ldots\underbrace{d\ldots d}_{k_d}\rangle \tag{3.8}$$

has the entanglement eigenvalue

$$\Lambda_{\max}(n;\{k\}) = \sqrt{\frac{n!}{\prod_i (k_i!)}} \prod_{i=0}^{d} \left(\frac{k_i}{n}\right)^{\frac{k_i}{2}}. \tag{3.9}$$

The next is the totally antisymmetric state $|\mathrm{Det}_n\rangle$, defined via

$$|\mathrm{Det}_n\rangle \equiv \frac{1}{\sqrt{n!}} \sum_{i_1,\ldots,i_n=1}^{n} \epsilon_{i_1,\ldots,i_n} |i_1,\ldots,i_n\rangle, \tag{3.10}$$

which has $\Lambda^2_{\max} = 1/n!$. The generalization of the antisymmetric state to the $n = p\,d^p$-partite determinant state is

$$|\mathrm{Det}_{n,d}\rangle \equiv \frac{1}{\sqrt{(d^p!)}} \sum_{i_1,\ldots,i_{d^p}} \epsilon_{i_1,\ldots,i_{d^p}} |\phi(i_1),\ldots,\phi(i_{d^p})\rangle, \tag{3.11}$$

with the ϕ's defined above Eq. (2.38). The state $|\mathrm{Det}_{n,d}\rangle$ has $\Lambda^2_{\max} = 1/(d^p)!$.

Although the above states were discussed in terms of the GME [38], we shall, in the following section, show the rather surprising fact that the relative entropy of entanglement of these example states, is given by the corresponding expression: $-2\log_2\Lambda_{\max}$.

3.3 Connection between the two measures

In bi-partite systems, due to the existence of Schmidt decompositions, the relative entropy of entanglement of a pure state is simply the von Neumann entropy of its reduced density matrix. However, for multi-partite systems there is, in general, no such decomposition, and how to calculate the relative entropy of entanglement for an arbitrary pure state remains an open question. We now connect the relative entropy of entanglement to the geometric measure of entanglement for arbitrary pure states by giving a lower bound on the former in terms of the latter or, more specifically, via the entanglement eigenvalue.

3.3.1 Pure states: lower bound on relative entropy of entanglement

Let us begin with the following theorem:

Theorem 1. For any pure state $|\psi\rangle$ with entanglement eigenvalue $\Lambda_{\max}(\psi)$ the quantity $-2\log_2\Lambda_{\max}(\psi)$ is a lower bound on the relative entropy of entanglement of $|\psi\rangle$, i.e.,

$$E_{\rm R}(|\psi\rangle\langle\psi|) \geq -2\log_2\Lambda_{\max}(\psi). \tag{3.12}$$

Proof: From the definition (3.3) of the relative entropy of entanglement we have, for a pure state $|\psi\rangle$,

$$E_{\rm R}(|\psi\rangle\langle\psi|) = \min_{\sigma\in\mathcal{D}} -\langle\psi|\log_2\sigma|\psi\rangle = -\max_{\sigma\in\mathcal{D}}\langle\psi|\log_2\sigma|\psi\rangle. \tag{3.13}$$

Using the concavity of the log function, we have

$$\langle\psi|\log_2\sigma|\psi\rangle \leq \log_2(\langle\psi|\sigma|\psi\rangle) \tag{3.14}$$

and, furthermore,

$$\max_{\sigma\in\mathcal{D}}\langle\psi|\log_2\sigma|\psi\rangle \leq \max_{\sigma\in\mathcal{D}}\log_2(\langle\psi|\sigma|\psi\rangle), \tag{3.15}$$

although the σ's maximizing the left- and right-hand sides are not necessarily identical. We then conclude that

$$E_{\rm R}(|\psi\rangle\langle\psi|) \geq -\max_{\sigma\in\mathcal{D}}\log_2(\langle\psi|\sigma|\psi\rangle). \tag{3.16}$$

As any $\sigma\in\mathcal{D}$ can be expanded as $\sigma=\sum_i p_i|\phi_i\rangle\langle\phi_i|$, where $|\phi_i\rangle$'s are separable pure states, one has

$$\langle\psi|\sigma|\psi\rangle = \sum_i p_i|\langle\phi_i|\psi\rangle|^2 \leq \Lambda^2_{\max}(\psi), \tag{3.17}$$

and hence we arrive at the sought result

$$E_{\rm R}(|\psi\rangle\langle\psi|) \geq -2\log_2\Lambda_{\max}(\psi). \tag{3.18}$$

We wish to point out that such an inequality was previously established and exploited in Refs. [58].

When does the inequality becomes an equality? The demand that Eq. (3.14) hold as an equality

implies that σ (un-normalized) can be decomposed into either (a)

$$\sigma = \sum_i |i\rangle\langle i|, \tag{3.19a}$$

where $\{|i\rangle\}$ are mutually orthogonal but *not* orthogonal to $|\psi\rangle$, or (b)

$$\sigma = |\psi\rangle\langle\psi| + \tau^{\perp}, \tag{3.19b}$$

where $\tau^{\perp}$ (either pure or mixed) is orthogonal to ψ, i.e., $\langle\psi|\tau^{\perp}|\psi\rangle = 0$. However, the separable σ that has either property is not necessarily the one that maximizes both sides of the inequality (3.15), unless $|\psi\rangle$ (and hence σ) has high symmetry. On the other hand, a corollary arises from Thereom 1 which says that for any multi-partite pure state $|\psi\rangle$, if one can find a separable mixed state σ such that $S(\rho||\sigma)|_{\rho=|\psi\rangle\langle\psi|} = -2\log_2\Lambda_{\max}\big(|\psi\rangle\big)$ then $E_{\rm R} = -2\log_2\Lambda_{\max}\big(|\psi\rangle\big)$. This result follows directly from the fact that when the lower bound on $E_{\rm R}$ given in Eq. (3.12) equals an upper bound, the relative entropy of entanglement is immediate. In all the examples we shall consider for which this lower bound is saturated, it turns out that

$$\sigma^* \equiv \sum_i p_i\,|\phi_i\rangle\langle\phi_i| \tag{3.20}$$

is a closest separable mixed state, in which $\{|\phi_i\rangle\}$ are separable pure states closest to $|\psi\rangle$. (The distribution p_i is uniform, and can be either discrete or continuous, and $\{|\phi_i\rangle\}$ are not necessarily mutually orthogonal.)

We now examine several illustrative states in the light of the above corollary, thus obtaining $E_{\rm R}$ for each of them. We begin with the permutation-invariant states $|S(n,k)\rangle$ of Eq. (3.6), for which $\Lambda_{\max}$ was given in Eq. (3.7). The above theorem guarantees that $E_{\rm R}\big(|S(n,k)\rangle\big) \geq -2\log_2\Lambda_{\max}(n,k)$. To find an *upper* bound we construct a separable mixed state

$$\sigma^* \equiv \int \frac{d\phi}{2\pi}|\xi(\phi)\rangle\langle\xi(\phi)|, \tag{3.21a}$$

$$|\xi(\phi)\rangle \equiv \Big(\sqrt{p}|0\rangle + e^{i\phi}\sqrt{1-p}|1\rangle\Big)^{\otimes n}, \tag{3.21b}$$

with p chosen to maximize $||\langle\xi|S(n,k)\rangle|| = \sqrt{C_k^n\, p^k(1-p)^{n-k}}$, which gives $p = k/n$. Direct evaluation then gives

$$\sigma^* = \sum_{k=0}^{n} C_k^n p^k (1-p)^{(n-k)} |S(n,k)\rangle\langle S(n,k)|, \tag{3.22}$$

and $S(\rho||\sigma) = -2\log_2 \Lambda_{\max}(n,k)$, where $\rho = |S(n,k)\rangle\langle S(n,k)|$ and $\Lambda_{\max}(n,k)$ is given in Eq. (3.7). The upper and lower bounds on $E_{\rm R}$ coincide, and hence we have that

$$E_{\rm R}\big(|S(n,k)\rangle\big) = -2\log_2 \Lambda_{\max}(n,k). \tag{3.23}$$

The closest separable mixed state σ^* belongs to the case (b), i.e., Eq. (3.19b). Similar equalities can be established for the generalized permutation-invariant n-party $(d+1)$-dit states $|S(n,\{k\})\rangle$ of Eq. (3.8). We remark that the entanglements of the symmetric states $|S(n,k)\rangle$ (which are also known as *Dicke* states) have been analyzed via other approaches; see Ref. [39].

For our next example we consider the totally anti-symmetric states $|{\rm Det}_n\rangle$ of Eq. (3.10). It was shown in Ref. [40] that for these states $\Lambda_{\max}^2 = 1/n!$, and hence it is straightforward to see that each of the $n!$ basis states $|i_1,\ldots,i_n\rangle$ is a closest separable pure state. Thus, one can construct a separable mixed state from these separable pure states [cf. Eq. (3.20)]:

$$\sigma_1 \equiv \frac{1}{n!} \sum_{i_1,\ldots,i_n} |i_1,\ldots,i_n\rangle\langle i_1,\ldots,i_n|. \tag{3.24}$$

Then, by direct calculation one gets $S(\rho_{{\rm Det}_n}||\sigma_1) = \log_2(n!)$, which is identical to $-2\log_2\Lambda_{\max}$, as mentioned above. As in our previous examples, upper and lower bounds on $E_{\rm R}$ coincide, and hence we have that $E_{\rm R}(|{\rm Det}_n\rangle) = \log_2(n!)$. The closest separable mixed state σ_1 belongs to the case (a), i.e., Eq. (3.19a). Similarly, for the generalized determinant state (3.11) one can show that $E_{\rm R} = \log_2(d^p!)$.

We now focus our attention on three-qubit settings. Of these, the states $|S(3,0)\rangle = |000\rangle$ and $|S(3,3)\rangle = |111\rangle$ are not entangled and are, respectively, the components of the the 3-GHZ state: $|{\rm GHZ}\rangle \equiv \big(|000\rangle + |111\rangle\big)/\sqrt{2}$. Although the GHZ state is not of the form $|S(n,k)\rangle$, it has $\Lambda_{\max} = 1/\sqrt{2}$, and two of its closest separable pure states are $|000\rangle$ and $|111\rangle$ [38]. From these one

can construct a separable mixed state

$$\sigma_2 \;=\; \frac{1}{2}\big(|000\rangle\langle 000| + |111\rangle\langle 111|\big), \tag{3.25}$$

From the discussion given after Eq. (3.18), one concludes that $E_{\rm R}({\rm GHZ}) = -2\log_2\Lambda_{\rm max} = 1$ and that σ_2 is one of the closest separable mixed states to $|{\rm GHZ}\rangle$. This closest separable mixed state σ_2 belongs to the case (a), i.e., Eq. (3.19a). With some rewriting, it can also be classified as case (b), i.e.,

$$\sigma_2 = \frac{1}{2}|{\rm GHZ}\rangle\langle{\rm GHZ}| + \frac{1}{2}|{\rm GHZ}^-\rangle\langle{\rm GHZ}^-|, \tag{3.26}$$

where $|{\rm GHZ}^-\rangle \equiv \big(|000\rangle - |111\rangle\big)/\sqrt{2}$.

The states

$$|{\rm W}\rangle \;\equiv\; |S(3,2)\rangle = \big(|001\rangle + |010\rangle + |100\rangle\big)/\sqrt{3}, \tag{3.27a}$$

$$|\widetilde{\rm W}\rangle \;\equiv\; |S(3,1)\rangle = \big(|110\rangle + |101\rangle + |011\rangle\big)/\sqrt{3}, \tag{3.27b}$$

are equally entangled, and have $\Lambda_{\rm max} = 2/3$ [38]. Again, from the discussion after Eq. (3.18) we have $E_{\rm R} = \log_2(9/4)$, and one of the closest separable mixed states to the W state can be constructed from

$$\sigma_3 \;\equiv\; \int \frac{d\phi}{2\pi}|\psi(\phi)\rangle\langle\psi(\phi)|, \quad \text{with} \tag{3.28}$$

$$|\psi(\phi)\rangle \;\equiv\; \big(\sqrt{2/3}|0\rangle + e^{i\phi}\sqrt{1/3}|1\rangle\big)^{\otimes 3}, \tag{3.29}$$

which gives the result

$$\sigma_3 = \frac{4}{9}|{\rm W}\rangle\langle{\rm W}| + \frac{2}{9}|\widetilde{\rm W}\rangle\langle\widetilde{\rm W}| + \frac{8}{27}|000\rangle\langle 000| + \frac{1}{27}|111\rangle\langle 111|. \tag{3.30}$$

We remark that the mixed state σ_3 is not the only closest separable mixed state to the W state; the following state σ_4 is another example (as would be any mixture of σ_3 and σ_4):

$$\sigma_4 \equiv \frac{1}{3}\sum_{k=0}^{2}|\psi(2\pi k/3)\rangle\langle\psi(2\pi k/3)| = \frac{4}{9}|{\rm W}\rangle\langle{\rm W}| + \frac{2}{9}|\widetilde{\rm W}\rangle\langle\widetilde{\rm W}| + \frac{1}{3}|\xi\rangle\langle\xi|, \tag{3.31a}$$

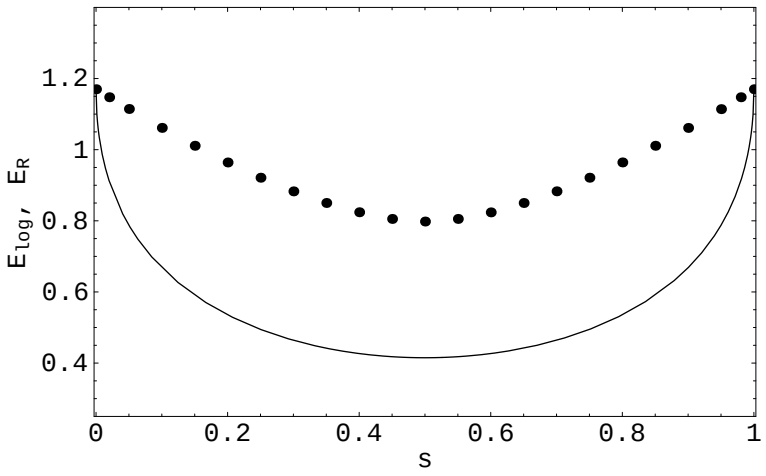

Figure 3.1: The solid curve represents $E_{\log_2}(s)$ of the pure state $\sqrt{s}\,|\mathrm{W}\rangle + \sqrt{1-s}\,|\widetilde{\mathrm{W}}\rangle$ vs. s. The dots are the corresponding relative entropies of entanglement, obtained numerically.

where $3|\xi\rangle \equiv 2\sqrt{2}|000\rangle + |111\rangle$. These closest separable mixed states of W state belong to the case (b), i.e., Eq. (3.19b).

Having obtained REE for W and $\widetilde{\mathrm{W}}$, it is interesting to examine the REE of the following superposition of the two: $|\mathrm{W}\widetilde{\mathrm{W}}(s)\rangle \equiv \sqrt{s}\,|\mathrm{W}\rangle + \sqrt{1-s}\,|\widetilde{\mathrm{W}}\rangle$. We have not been able to find an analytical result for REE, but we can compare the analytical expression for $-2\log_2\Lambda_{\max}(\mathrm{W}\widetilde{\mathrm{W}}(s))$ with the numerical evaluation of $E_{\mathrm{R}}(\mathrm{W}\widetilde{\mathrm{W}}(s))$, and we do this in Fig. 3.1. As we see in this figure, the qualitative behavior of the two functions is similar, but $-2\log_2\Lambda_{\max}$ and E_{R} only coincide at the two end-points, $s = 0$ and $s = 1$.

3.3.2 Mixed states: upper bound on relative entropy of entanglement

In Chapter 2 the procedure was given to find the geometric measure of entanglement, $E_{\sin^2}$, for the mixed state comprising symmetric states:

$$\rho(\{p\}) = \sum_k p_k\,|S(n,k)\rangle\langle S(n,k)|. \tag{3.32}$$

Here, we focus instead on the quantity $E_{\log_2}$, but the basic procedure is the same. The first step is to find the entanglement eigenvalue $\Lambda_n(\{q\})$ for the pure state

$$\sum_k \sqrt{q_k}\,|S(n,k)\rangle, \tag{3.33}$$

thus arriving at the quantity

$$\mathcal{E}(\{q\}) \equiv -2\log_2 \Lambda_n(\{q\}). \tag{3.34}$$

Then the quantity $E_{\log_2}$ for the mixed state (3.32) is actually the convex hull of the expression (3.34):

$$E_{\log_2}\left(\rho(\{p\})\right) = \mathrm{co}\,\mathcal{E}(\{p\}). \tag{3.35}$$

This prompts us to ask the question: Can we find REE for the mixture of $|S(n,k)\rangle$ in Eq. (3.32)? To answer it, we shall first construct an upper bound to REE, and then compare this bound with the numerically evaluated REE. To accomplish the first step, bearing in mind the fact that any separable mixed state will yield an upper bound, we consider the state formed by mixing the separable pure states $|\xi(\theta,\phi)\rangle$ [cf. Eq. (3.22)]:

$$\sigma(\theta) = \int \frac{d\phi}{2\pi} |\xi(\theta,\phi)\rangle\langle\xi(\theta,\phi)| = \sum_{k=0}^{n} C_k^n \cos^{2k}\theta \sin^{2(n-k)}\theta |S(n,k)\rangle\langle S(n,k)|, \tag{3.36}$$

where

$$|\xi(\theta,\phi)\rangle \equiv \Big(\cos\theta|0\rangle + e^{i\phi}\sin\theta|1\rangle\Big)^{\otimes n}. \tag{3.37}$$

We then minimize the relative entropy between $\rho(\{p\})$ and $\sigma(\theta)$,

$$S\left(\rho(\{p\})||\sigma(\theta)\right) = \sum_k p_k \log \frac{p_k}{C_k^n \cos^{2k}\theta \sin^{2(n-k)}\theta}, \tag{3.38}$$

with respect to θ, obtaining the stationarity condition

$$\tan^2\theta \equiv \frac{\sum_k p_k\,(n-k)}{\sum p_k\,k}. \tag{3.39}$$

Due to the convexity of the relative entropy,

$$S\left(\sum_i q_i\rho_i \| \sum_i q_i\sigma_i\right) \leq \sum_i q_i S(\rho_i||\sigma_i), \tag{3.40}$$

we can further tighten the expression of the relative entropy by taking its convex hull. (Via the convexification process, i.e., the convex hull construction, the corresponding separable state can

also be obtained.) Therefore, we arrive at an upper bound for the relative entropy of entanglement of the mixed state $\rho(\{p\})$:

$$E_{\rm R}\left(\rho(\{p\})\right) \leq {\rm co}F(\{p\}), \tag{3.41}$$

where

$$F(\{p\}) \equiv \sum_k p_k \log_2 \frac{p_k}{C_k^n \cos^{2k}\theta \sin^{2(n-k)}\theta} = \sum_k p_k \log_2 \frac{p_k\, n^n}{C_k^n \alpha^k (n-\alpha)^{n-k}}, \tag{3.42}$$

where the angle θ satisfies Eq. (3.39), $C_k^n \equiv n!/\big(k!(n-k)!\big)$, and $\alpha \equiv \sum_k p_k\, k$.

Having established an upper bound for REE for the state $\rho(\{p\})$, we now make the restriction to mixtures of two distinct n-qubit states $|S(n,k_1)\rangle$ and $|S(n,k_2)\rangle$ (with $k_1 \neq k_2$):

$$\rho_{n;k_1,k_2}(s) \equiv s|S(n,k_1)\rangle\langle S(n,k_1)| + (1-s)|S(n,k_2)\rangle\langle S(n,k_2)|. \tag{3.43}$$

One trivial example is $\rho_{n;0,n}(s)$, which is obviously unentangled as it is the mixture of two separable pure states $|0^{\otimes n}\rangle$ and $|1^{\otimes n}\rangle$. Other mixtures are generally entangled, except possibly at the end-points $s = 0$ or $s = 1$ when the mixture contains either $|S(n,0)\rangle$ or $|S(n,n)\rangle$. We first investigate the two-qubit (i.e. $n = 2$) case. Besides the trivial mixture, $\rho_{2;0,2}$, there is only one inequivalent mixture, $\rho_{2;0,1}(s)$ [which is equivalent to $\rho_{2;2,1}(s)$], which is—up to local basis change—the so-called *maximally entangled mixed state* [59, 46] (for a certain range of s)

$$\rho_{2;0,1} = s\,|11\rangle\langle 11| + (1-s)|\Psi^+\rangle\langle\Psi^+|, \tag{3.44}$$

where $|\Psi^+\rangle \equiv (|01\rangle + 10)/\sqrt{2}$. The function F for this state [denoted by $F_{2;0,1}(s)$] is

$$F_{2;0,1}(s) = s\,\log_2 \frac{4s}{(1+s)^2} + (1-s)\log_2 \frac{2}{1+s}\,, \tag{3.45}$$

which is convex in s. It is exactly the expression for the relative entropy of entanglement for the state $\rho_{2;0,1}$ found by Vedral and Plenio [26] (see their Eq. (56) with λ replaced by $1-s$).

For $n = 3$ there are three other inequivalent mixtures: $\rho_{3;0,1}(s)$ [equivalent to $\rho_{3;3,2}(s)$], $\rho_{3;0,2}(s)$ [to $\rho_{3;3,1}(s)$], and $\rho_{3;1,2}(s)$ [to $\rho_{3;2,1}(s)$]. In Fig. 3.2 we compare the function F in Eq. (3.42),

its convex hull co F, and numerical values of $E_{\rm R}$ obtained using the general scheme described in Ref. [26] extended beyond the two-qubit case. The agreement between co F and the numerical values of $E_{\rm R}$ appears to be exact.

For $n = 4$ there are five inequivalent nontrivial mixtures: $\rho_{4;0,1}(s)$, $\rho_{4;0,2}(s)$, $\rho_{4;0,3}(s)$, $\rho_{4;1,2}(s)$, and $\rho_{4;1,3}(s)$. In Figs. 3.3 and 3.4 we again compare the function F in Eq. (3.42), its convex hull co F, and numerical values of $E_{\rm R}$. Again the agreement between co F and the numerical values of $E_{\rm R}$ appears to be exact.

From these agreements, we are led to the following conjecture:

Conjecture 1: The relative entropy of entanglement $E_{\rm R}\left(\rho(\{p\})\right)$ for the mixed states $\rho(\{p\})$ is given exactly by co$F(\{p\})$.

For the states that we have just considered, we now pause to give the formulas for $E_{\rm R}$ suggested by the conjecture. For the three-qubit mixed state $\rho_{3;2,1}(s)$, its conjectured $E_{\rm R}$ is

$$s \log_2 \frac{9s}{(1+s)^2(2-s)} + (1-s) \log_2 \frac{9(1-s)}{(2-s)^2(1+s)}. \tag{3.46a}$$

For $\rho_{3;0,1}(s)$, it is

$$s \log_2 \frac{27s}{(2+s)^3} + (1-s) \log_2 \frac{9}{(2+s)^2}. \tag{3.46b}$$

For $\rho_{4;0,1}(s)$, it is

$$s \log_2 \frac{256s}{(3+s)^4} + (1-s) \log_2 \frac{64}{(3+s)^3}. \tag{3.47a}$$

For $\rho_{4;1,2}(s)$, it is

$$s \log_2 \frac{64s}{(2-s)(2+s)^3} + (1-s) \log_2 \frac{128(1-s)}{3(2-s)^2(2+s)^2}. \tag{3.47b}$$

For $\rho_{4;1,3}(s)$, it is

$$s \log_2 \frac{64s}{(3-2s)(1+2s)^3} + (1-s) \log_2 \frac{64(1-s)}{(3-2s)^3(1+2s)}. \tag{3.47c}$$

For states such as $\rho_{3;0,2}$, $\rho_{4;0,2}$, and $\rho_{4;0,3}$, convexifications (i.e. convex hull constructions) are needed; see Figs. 3.2, 3.3, and 3.4. In Fig. 3.5 we give an example of a seven-qubit state, viz., $\rho_{7;2,5}(s)$.

Although we have not been able to prove our conjecture, we have observed some supporting evidence, in addition to the numerical evidence presented above. We begin by noting that the

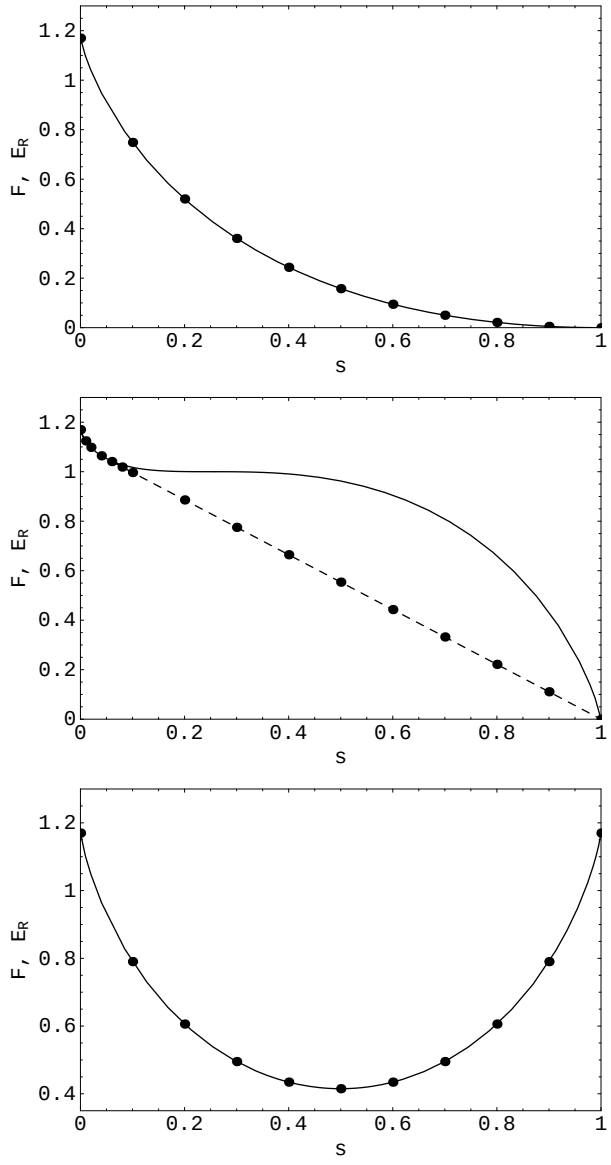

Figure 3.2: Comparison of F (solid curve), $\mathrm{co}\, F$ (convexification, indicated by dashed line) and the numerical value of E_{R} (dots) for the states $\rho_{3;0,1}(s)$, $\rho_{3;0,2}(s)$, and $\rho_{3;1,2}(s)$ (from top to bottom). Note that the log function is implicitly base-2.

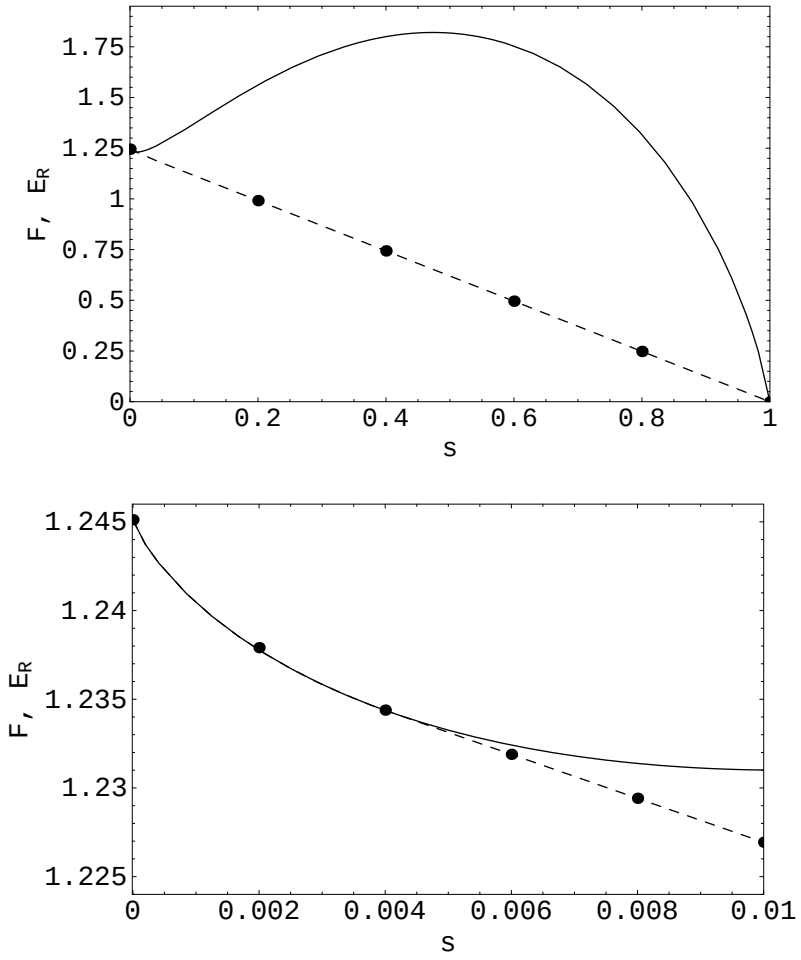

Figure 3.3: Comparison of F (solid curve), its convex hull (dash line), and the numerical value of E_{R} for the state $\rho_{4;0,3}(s)$. Upper panel shows the whole range $s \in [0, 1]$, whereas the lower panel shows a blow-up of the range $s \in [0, 0.01]$.

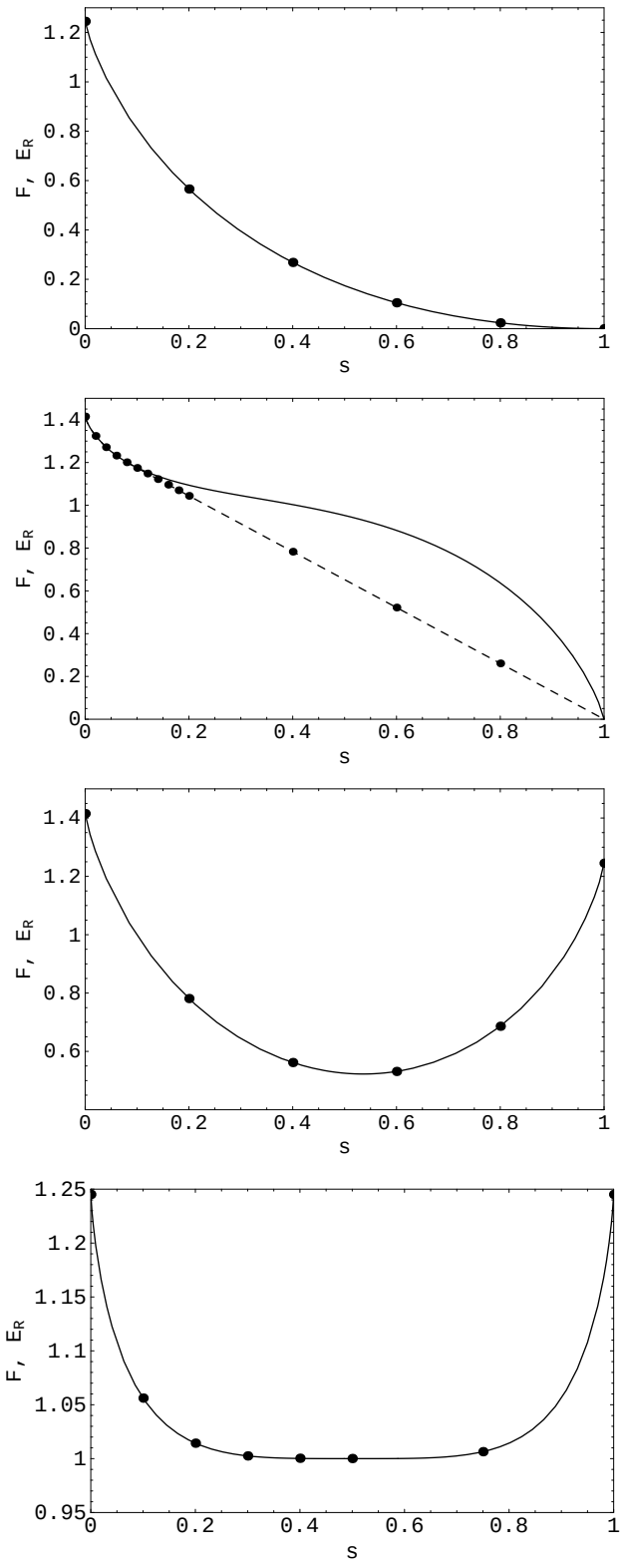

Figure 3.4: Comparison of F (solid curve), its convex hull (dashed line), and the numerical value of E_{R} for the states $\rho_{4;0,1}(s)$, $\rho_{4;0,2}(s)$, $\rho_{4;1,2}(s)$, and $\rho_{4;1,3}(s)$ (from top to bottom).

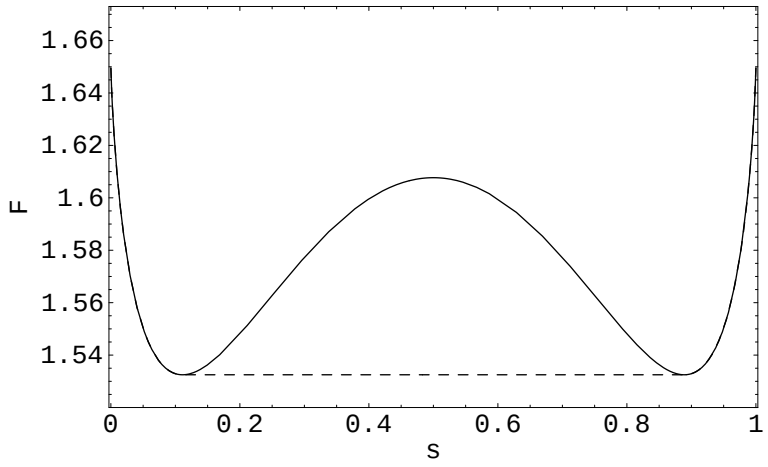

Figure 3.5: The function F (solid curve) and its convex hull (dashed line indicates convexification) for the seven-qubit mixed state $\rho_{7;2,5}(s)$.

states $\rho(\{p\})$ are invariant under the projection

$$\mathrm{P} : \rho \to \int \frac{d\phi}{2\pi} U(\phi)^{\otimes n} \rho\, U(\phi)^{\dagger \otimes n} \tag{3.48}$$

with $U(\phi)\big\{|0\rangle, |1\rangle\big\} \to \big\{|0\rangle, \mathrm{e}^{-i\phi}|1\rangle\big\}$. Vollbrecht and Werner [24] have shown that in order to find the closest separable mixed state for a state that is invariant under projections such as P, it is only necessary to search within the separable states that are also invariant under the projection. We can further reduce the set of separable states to be searched by invoking another symmetry property possessed by $\rho(\{p\})$: these states are also, by construction, invariant under permutations of all parties. Let us denote by Π_i one of the permutations of parties, and by $\Pi_i(\rho)$ the state obtained from ρ by permuting the parties under Π_i. We now show that the set of separable states to be searched can be reduced to the separable states that are invariant under the permutations. To see this, suppose that ρ is a mixed state in the family (3.32), and that σ^* is one of the closest separable states to ρ, i.e.,

$$E_{\mathrm{R}}(\rho) \equiv \min_{\sigma \in \mathcal{D}} S(\rho||\sigma) = S(\rho||\sigma^*). \tag{3.49}$$

As ρ is invariant under all Π_i, we have

$$E_{\mathrm{R}}(\rho) = \frac{1}{N_\Pi} \sum_i S\left(\rho \big\| \Pi_i(\sigma^*)\right), \tag{3.50}$$

where N_Π is the number of permutations. By using the convexity of the relative entropy we have

$$E_{\rm R}(\rho) \geq S\left(\rho \Big\| \big[\sum_i \Pi_i(\sigma^*)/N_\Pi\big]\right). \tag{3.51}$$

However, because of the extremal property, Eq. (3.49), the inequality must be saturated, as the left-hand side is already minimal. This shows that

$$\sigma^{**} \equiv \frac{1}{N_\Pi}\sum_i \Pi_i(\sigma^*) \tag{3.52}$$

also a closest separable mixed state to ρ, and is manifestly invariant under all permutations. Thus, we only need to search within this restricted family of separable states.

It is not difficult to see that the set $\mathcal{D}_S$ of all separable mixed states that are diagonal in the basis of $\{|S(n,k)\rangle\}$ can be constructed from a convex mixture of separable states in Eq. (3.36). That is, for any $\sigma_s \in \mathcal{D}_S$ we have a decomposition

$$\sigma_s = \sum_i t_i\, \sigma(\theta_i), \tag{3.53}$$

where $t_i \geq 0$, $\sum_i t_i = 1$, and $\sigma(\theta_i)$ is of the form (3.36). This is because the separability of the states (3.32) implies that there exists a decomposition into pure states such that each pure state is a separable state. Furthermore, because $\{|S(n,k)\rangle\}$ are eigenstates of $\rho(\{p\})$, the most general form of the pure state in its decomposition is

$$\sum_k \sqrt{q_k}\, e^{i\phi_k}|S(n,k)\rangle. \tag{3.54}$$

This pure state is separable if and only if it is of the form (3.37), up to an overall irrelevant phase. As $\rho(\{p\})$ is invariant under the projection P (3.48), a pure state in Eq. (3.37) will be projected to the mixed state in Eq. (3.36) under P. Thus, every separable state that is diagonal in $\{|S(n,k)\rangle\}$ basis can be expressed in the form (3.53).

Hence, our conjecture (3.41) ensures (via any necessary convexification) that it is at least the minimum (of the relative entropy) when the separable mixed states are restricted to $\mathcal{D}_S$. However, in order to prove the conjecture, one would still need to show that the expression is also the

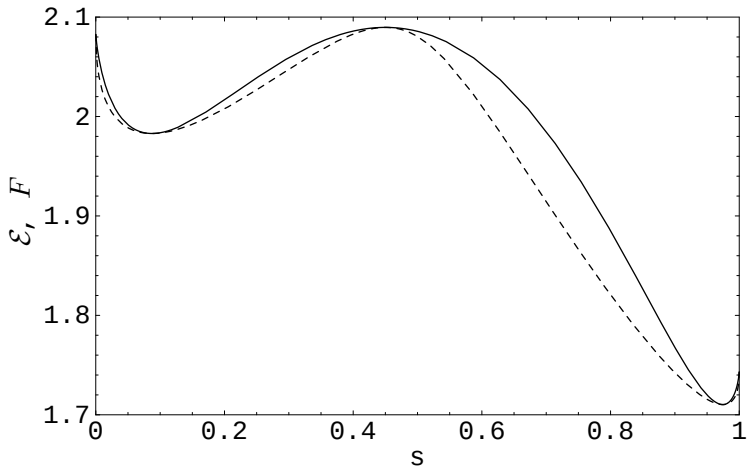

Figure 3.6: Comparision of $\mathcal{E}$ (dashed curve) and F (solid curve) for the eleven-qubit mixed state $\rho_{11;2,6}(s)$.

minimum when the restriction to $\mathcal{D}_S$ is relaxed.

We remark that our conjecture is consistent with the results of Ishizaka [60], in that our conjectured σ^* satisfies the condition that $[\rho, \sigma^*] = 0$ and that σ^* has the same reduction as ρ for every party. Furthermore, suppose σ^* (diagonal in the basis $\{|S(n,k)\rangle\}$) represents the separable state that gives the conjectured value of REE:

$$\sigma^* = \sum_k r_k |S(n,k)\rangle\langle S(n,k)|, \tag{3.55}$$

where the r's can be obtained by finding the convex hull of the function F in Eq. (3.42). Now consider any separable state τ in the Hilbert space *orthogonal* to the subspace spanned by $\{S(n,k)\}$. We need to show that the separable state $\sigma(x) \equiv x\sigma^* + (1-x)\tau$, for any $x \in [0,1]$, gives greater relative entropy with $\rho(\{p\})$ in Eq. (3.32) than σ^* does with $\rho(\{p\})$, i.e.,

$$S\left(\rho(\{p\})\|\sigma(x)\right) \geq S\left(\rho(\{p\})\|\sigma^*\right). \tag{3.56}$$

Writing out the expression explicitly, we have that

$$S\left(\rho(\{p\})\|\sigma(x)\right) = \sum_k p_k \log \frac{p_k}{x\, r_k} \geq \sum_k p_k \log \frac{p_k}{r_k} = S\left(\rho(\{p\})\|\sigma^*\right). \tag{3.57}$$

Note that τ gives no contribution in the relative entropy, as it is orthogonal to $\rho(\{p\})$, and that we have not used the fact that τ is separable. But to prove Conjecture 1 we need to show that Eq. (3.56) holds if separable τ is not orthogonal to the subspace spanned by $\{S(n,k)\}$.

Recall that for pure states we found the inequality $E_{\log_2} \leq E_{\rm R}$. Does this inequality hold for mixed states? We do not know the complete answer to this question, but for the mixed state $\rho(\{p\})$ we shall at least find that this inequality would hold if Conjecture 1 holds. To see this, we first establish that $\mathcal{E}(\{q\})$ is a lower bound on $F(\{q\})$; see the example in Fig. 3.6. The proof is as follows. Recall that

$$\mathcal{E}(\{p\}) = -2\log_2\left[\max_\theta \sum_k \sqrt{p_k}\,\sqrt{C_k^n}\cos^k\theta\sin^{n-k}\theta\right]. \tag{3.58a}$$

By the concavity of log, we then have

$$-2\log_2\left[\sum_k \sqrt{p_k}\,\sqrt{C_k^n}\cos^k\theta\sin^{n-k}\theta\right] \leq \sum_k p_k \log_2 \frac{p_k}{C_k^n\cos^{2k}\theta\sin^{2(n-k)}\theta}. \tag{3.58b}$$

Hence

$$\min_\theta -2\log_2\left[\sum_k \sqrt{p_k}\,\sqrt{C_k^n}\cos^k\theta\sin^{n-k}\theta\right] \leq \min_\theta \sum_k p_k \log_2 \frac{p_k}{C_k^n\cos^{2k}\theta\sin^{2(n-k)}\theta}, \tag{3.58c}$$

or equivalently

$$\mathcal{E}(\{p\}) \leq F(\{p\}). \tag{3.58d}$$

If Conjecture 1 is correct then by taking the convex hull of both sides of this inequality we would have

$$E_{\log_2} \leq E_{\rm R} \tag{3.58e}$$

for the family of states (3.32). Notice that we have also shown that this relation holds for arbitrary pure states. It would be interesting to know whether it also holds for arbitrary mixed states.

3.4 Concluding remarks

We have provided a lower bound on the relative entropy of entanglement for arbitrary multi-partite pure states in terms of their geometric measure of entanglement. For several families of pure states we have shown that the bound is in fact saturated, and thus provides the exact value of the relative entropy of entanglement. For mixtures of certain permutation-invariant states we have conjectured analytic expressions for the relative entropy of entanglement.

It is possible that our results on the relative entropy of entanglement might be applicable to the checking of the consistency of some equalities and inequalities [48, 61, 62] regarding minimal reversible entanglement generating sets (MREGSs). Consider, e.g., the particular family of n-qubit pure states $\{|S(n,k)\rangle\}$, the relative entropy of entanglement of which we have given in Eq. (3.23). Now, if we trace over one party we get a mixed $(n-1)$-qubit state:

$$\mathrm{Tr}_1|S(n,k)\rangle\langle S(n,k)| = \frac{n-k}{n}|S(n-1,k)\rangle\langle S(n-1,k)| + \frac{k}{n}|S(n-1,k-1)\rangle\langle S(n-1,k-1)|. \quad (3.59)$$

We have also given a conjecture for the relative entropy of entanglement for this mixed state. If we trace over m parties, the reduced mixed state would be a mixture of $\{|S(n-m,q)\rangle\}$ [with $q \leq (n-m)$], and again we have given a conjecture for its relative entropy of entanglement. For example, if we start with $|S(4,1)\rangle$, and trace over one party and then another, we get the sequence:

$$|S(4,1)\rangle \to \rho_{3;0,1}(1/4) \to \rho_{2;0,1}(1/2), \quad (3.60)$$

for which we have given the corresponding relative entropies of entanglement in Eqs. (3.23), (3.46b) and (3.45). (To be precise, the second formula is a conjecture; the others are proven.) The aforementioned equalities and inequalities concerning MREGS usually involve only the von Neumann entropy and the regularized (i.e. asymptotic) relative entropy of entanglement of the pure state and its reduced density matrices. The regularized relative entropy of entanglement is defined as

$$E_{\mathrm{R}}^{\infty}(\rho) \equiv \lim_{n\to\infty} \frac{1}{n} E_{\mathrm{R}}(\rho^{\otimes n}). \quad (3.61)$$

The calculation of the regularized relative entropy of entanglement is, in general, much more difficult

than for the non-regularized case, and the (in)equalities involving the regularized relative entropy of entanglement are thus difficult to check. Nevertheless, it is known that $E_{\rm R}^{\infty} \leq E_{\rm R}$, so we can check their weaker forms by replacing $E_{\rm R}^{\infty}$ by $E_{\rm R}$, and the corresponding (in)equalities by weaker inequalities.

Plenio and Vedral [48] have derived a lower bound on the REE of a tripartite pure state $\rho_{\rm ABC} = |\psi\rangle\langle\psi|$ in terms of the the entropies and REE's of the reduced states of two parties:

$$\max\{E_{\rm R}(\rho_{\rm AB}) + S(\rho_{\rm AB}), E_{\rm R}(\rho_{\rm AC}) + S(\rho_{\rm AC}), E_{\rm R}(\rho_{\rm BC}) + S(\rho_{\rm BC})\} \leq E_{\rm R}(\rho_{\rm ABC}), \tag{3.62}$$

where $\rho_{\rm AB} = {\rm Tr}_C(\rho_{\rm ABC})$ (and similarly for $\rho_{\rm AC}$ and $\rho_{\rm BC}$) and $S(\rho) \equiv -{\rm Tr}\rho\log_2\rho$ is the von Neumann entropy. They have further found that this lower bound is saturated by $|{\rm GHZ}\rangle$ and $|{\rm W}\rangle$. This raises an interesting question: is the above lower bound (for n-partite pure states) saturated by the states that saturate the lower bound $E_{\log_2} = -2\log_2\Lambda_{\max}(\psi) \leq E_{\rm R}(\psi)$? Numerical tests seem to suggest that the Plenio-Vedral bound is tighter than $E_{\log_2}$. If this is the case then all states that saturate the lower bound $E_{\log_2}$ on $E_{\rm R}$ will saturate the Plenio-Vedral bound. Based on Conjecture 1, we can show that for $\rho_{12\ldots n} = |S(n,k)\rangle\langle S(n,k)|$ the inequality

$$\max_i\{E_{\rm R}(\rho_{12\ldots\hat{i}\ldots n}) + S(\rho_{12\ldots\hat{i}\ldots n})\} \leq E_{\rm R}(\rho_{12\ldots n}) \tag{3.63}$$

is saturated, where $\rho_{12\ldots\hat{i}\ldots n} \equiv {\rm Tr}_i(\rho_{12\ldots n})$ is the reduced density matrix obtained from $\rho_{12\ldots n}$ by tracing out the i-th party. The proof is as follows. As $|S(n,k)\rangle$ is permutation-invariant, there is no need to maximize over all parties, and we can simply take $i = 1$, obtaining the reduced state $\rho_{n-1;k-1,k}(k/n)$ as in Eq. (3.59). As the corresponding function $F_{n-1;k-1,k}(s)$ of $\rho_{n-1;k-1,k}(s)$ is convex for $s \in [0,1]$, we immediately obtain from Conjecture 1 that, for $\rho_{n-1;k-1,k}(k/n)$,

$$\begin{aligned} E_{\rm R}\left(\rho_{n-1;k-1,k}(k/n)\right) &= \log_2\left[C_k^n\left(\frac{k}{n}\right)^k\left(\frac{n-k}{n}\right)^{n-k}\right] + \frac{k}{n}\log_2\frac{k}{n} + \frac{n-k}{n}\log_2\frac{n-k}{n} &\text{(3.64a)}\\ &= E_{\rm R}\left(|S(n,k)\rangle\right) - S\left(\rho_{n-1;k-1,k}(k/n)\right). &\text{(3.64b)}\end{aligned}$$

Therefore, the bound in Eq. (3.63) is saturated for $\rho_{12\ldots n} = |S(n,k)\rangle\langle S(n,k)|$.

A major challenge is to extend the ideas contained in the present Paper from the relative

entropy of entanglement to its regularized version, the latter in fact giving tighter upper bound on the entanglement of distillation than the former in the bi-partite settings. The alternative way of defining the relative entropy via the optimization over PPT states may also been used, in view of the recent progress on the bi-partite regularized relative entropy of entanglement [57].

We now explore the possibility that the geometric measures can provide lower bounds on yet another entanglement measure—the entanglement of formation. If the relationship $E_{\rm R} \leq E_{\rm F}$ between the two measures of entanglement—the relative entropy of entanglement $E_{\rm R}$ and the entanglement of formation $E_{\rm F}$—should continue to hold for *multi-partite* states (at least for pure states), and if $E_{\rm F}$ should remain a convex hull construction for mixed states, then we would be able to construct a lower bound on the entanglement of formation:

$$\begin{aligned} E_{\log_2}(\rho) &\equiv \min_{p_i,\psi_i} \sum_i p_i E_{\log_2}(|\psi_i\rangle) \leq \min_{p_i,\psi_i} \sum_i p_i E_{\rm R}(|\psi_i\rangle) \\ &\leq \min_{p_i,\psi_i} \sum_i p_i E_{\rm F}(|\psi_i\rangle) \equiv E_{\rm F}(\rho), \end{aligned} \tag{3.65}$$

where $\{p_i\}$ and $\{\psi_i\}$ are such that $\rho = \sum_i p_i |\psi_i\rangle\langle\psi_i|$. Thus, $E_{\log_2}(\rho)$ is a lower bound on $E_{\rm F}(\rho)$. By using the inequality $(1-x^2)\log_2 e \leq -2\log_2 x$ (for $0 \leq x \leq 1$), one further has has that $(\log_2 e) E_{\sin^2}(\rho) \leq E_{\log_2}(\rho) \leq E_{\rm F}(\rho)$.

We remark that $E_{\sin^2}$ has been shown to be an entanglement monotone [37, 38], i.e., it is not increasing under local operations and classical communication (LOCC). However, $E_{\log_2}$ is *not* a monotone, as the following example shows. Consider the bi-partite pure state

$$|\psi\rangle \equiv \frac{1}{\sqrt{1+Nx^2}}|00\rangle + \frac{x}{\sqrt{1+Nx^2}}\big(|11\rangle + |22\rangle + \cdots + |NN\rangle\big), \tag{3.66}$$

with $|x| \leq 1$, for which $E_{\log_2} = \log_2(1+Nx^2)$. Suppose that one party makes the following measurement:

$$\mathcal{M}_1 \equiv |0\rangle\langle 0|, \quad \mathcal{M}_2 \equiv |1\rangle\langle 1| + |2\rangle\langle 2| + \cdots + |N\rangle\langle N|. \tag{3.67}$$

With probability $P_1 = 1/(1+Nx^2)$ the output state becomes $|\psi_1\rangle = |00\rangle$; with probability $P_2 = Nx^2/(1+Nx^2)$ the output state becomes $|\psi_2\rangle = \big(|11\rangle + |22\rangle + \cdots + |NN\rangle\big)/\sqrt{N}$, for which $E_{\log_2} =$

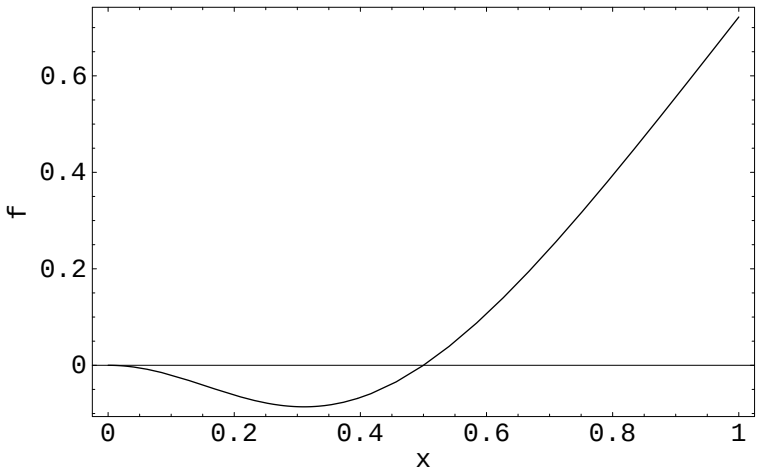

Figure 3.7: The function $f(4, x)$. It shows the violation of monotone condition (3.69) when the function is negative.

$\log_2 N$. For $E_{\log_2}$ to be a monotone it would be necessary that

$$E_{\log_2}(\psi) \geq P_1 E_{\log_2}(\psi_1) + P_2 E_{\log_2}(\psi_2). \tag{3.68}$$

Putting in the corresponding values for the P's and $E_{\log_2}$'s, we find that this inequality is equivalent to

$$f(N, x) \equiv \log_2(1 + Nx^2) - \frac{Nx^2}{1 + Nx^2} \log_2 N \geq 0. \tag{3.69}$$

As this is violated for certain values of x with $N > 2$, as exemplified in Fig. 3.7 for the plot of $f(4, x)$, we arrive at the conclusion that $E_{\log_2}$ is, in general, not a monotone.

We conclude by mentioning that certain results reported in the present chapter have recently been applied by Vedral [63] to the macroscopic entanglement of η-paired superconductivity.

Chapter 4

Bound entanglement

4.1 Introduction

As we have discussed above, we are motivated to study the quantification of entanglement for the basic reason that entanglement has been identified as a *resource* central to much of quantum information processing. As we have also discussed above, to date, progress in the quantification of entanglement for mixed states has resided primarily in the domain of bi-partite systems. For multi-partite systems in pure and mixed states, the characterization and quantification of entanglement presents even greater challenges.

We have introduced previously the notion of the entanglement of distillation, entanglement cost, and entanglement of formation. The entanglement of distillation ($E_{\rm D}$) is the optimal asymptotic *yield* of Bell states, given an infinite supply of replicas of an identical quantum state shared between two distant parties. The entanglement cost ($E_{\rm C}$) is the minimum asymptotic cost ratio of Bell states *consumed* to create an large number of copies of a certain quantum state shared between two distant parties. For pure states shared between two distant parties the two processes are reversible, i.e., $E_{\rm D} = E_{\rm C}$. For mixed states it is expected that $E_{\rm D} \leq E_{\rm C}$; otherwise recycling the two processes would churn out more entanglement than there was initially. The quantity entanglement of formation $E_{\rm F}$ is an averaged version of $E_{\rm C}$.

All these three quantities, $E_{\rm D}$, $E_{\rm C}$, and $E_{\rm F}$, especially the first two, are very difficult to calculate. The calculation of these quantities for general quantum states remains a challenge in quantum information theory. Another challenge regarding $E_{\rm F}$ concerns the question of whether or not $E_{\rm F}$, defined in an average sense, is equal to $E_{\rm C}$, which is defined for asymptotically large numbers of

copies. This is the so-called additivity problem for entanglement of formation, mentioned earlier.

There is, however, some progress in small dimensions, especially for two-qubit systems. Wootters' formula [22] for two-qubit entanglement of formation is the most prominent example. It sets an upper bound on the entanglement cost. It is obvious that an entangled state has nonzero $E_{\rm C}$ and $E_{\rm F}$. It was also shown by Horodecki and co-workers [18] that all two-qubit entangled states can be distilled into Bell states, and hence have nonzero $E_{\rm D}$. It was then thought that all entangled states, however small the entanglement, could be distilled. But shortly after, Horodecki and co-workers [19, 64] showed that in dimensions higher than two-qubit ($C^2 \otimes C^2$) and qubit-qubtrit ($C^2 \otimes C^3$) [such as $C^2 \otimes C^4$ and $C^3 \otimes C^3$] there exist entangled states that have *zero* entanglement of distillation. These states, however entangled, cannot be distilled into any pure entangled states. The entanglement used to create them is somehow bound and inextractable! Such states are called *bound entangled states*, and their entanglement is called bound entanglement. The bound entangled states that Horodecki constructed are bi-partite and have zero negativity, i.e., have positve partial transpose (PPT). Bound entanglement is not limited to bi-partite states. Bennett and co-workers [65] constructed both bi- and multi-partite bound entangled states using the technique of unextendible product bases; see also Appendix F. Other multi-partite bound entangled states have also been found [66], including the two [67, 68, 69] that we shall discuss in this chapter.

Although bound entanglement seems useless, as it cannot be used alone for quantum communication, Horodecki and co-workers [70] found that, surprisingly, a certain threshold fidelity of a teleportation process that cannot be achieved via a single copy of non-maximally entangled pure state *can* actually be achieved if combined with a supply of bound entanglement. Recently, Shor and co-workers [68] have shown that two multi-partite bound entangled states (of Smolin's), tensored together, can be be distilled (via LOCC) into a Bell state shared between two of the parties. Bound entanglement clearly has richer properties than was thought initially.

We have seen that bound entangled states are states that are entangled, but from which no pure entangled state can be distilled, provided all parties are allowed only local operations and classical communication (LOCC). The distillable entanglement ($E_{\rm D}$) is thus zero by definition. Bound entangled states can be either bi-partite or multi-partite, the latter possibly exhibiting more structure than the former. However, it does take nonzero entanglement to *create* bound entangled

states under LOCC. But exactly how much entanglement is bound in these strange states is not known analytically. In the present chapter, we study the entanglement content of two distinct types of bound entangled state: Smolin's four-party unlockable bound entangled state [67, 68] and Dür's N-party Bell-inequality-violating bound entangled states [69]. For each, we determine analytically their geometric measure of entanglement $E_{\sin^2}$ and the related quantity $E_{\log_2}$. We have shown in the previous chapter that, under certain circumstances, these give lower bounds on their multi-partite $E_{\rm F}$. In particular, we showed that $E_{\sin^2}(\rho)\log_2 e \leq E_{\log_2}(\rho) \leq E_{\rm F}(\rho)$. In addition, we make conjectures concerning the relative entropies of entanglement for these bound entangled states. Although quantities such as the geometric measure or the relative entropy of entanglement may not be able to reveal the exact nature of bound entanglement, they nevertheless quantify for these bound entangled states the content of entanglement that is inextractable. The discussion in the present chapter is based on Ref. [54].

We now turn to the calculations of entanglement for the two bound entangled states: Smolin's and Dür's.

4.2 Smolin's four-party unlockable bound entangled state

Consider the four-qubit mixed state

$$\rho^{ABCD} \equiv \frac{1}{4}\sum_{i=0}^{3} \big(|\Psi_i\rangle\langle\Psi_i|\big)_{\rm AB} \otimes \big(|\Psi_i\rangle\langle\Psi_i|\big)_{\rm CD}, \tag{4.1}$$

where the $|\Psi\rangle$'s are the four Bell states: $(|00\rangle \pm |11\rangle)/\sqrt{2}$ and $(|01\rangle \pm |10\rangle)/\sqrt{2}$. Now, the state ρ^{ABCD} can be conveniently rewritten as

$$\rho^{ABCD} = \frac{1}{4}\sum_{i=0}^{3} |X_i\rangle\langle X_i|, \tag{4.2}$$

where $|X\rangle$'s are the four orthogonal GHZ-like states:

$$|X_0\rangle \equiv \frac{1}{\sqrt{2}}\big(|0000\rangle + |1111\rangle\big),\ |X_1\rangle \equiv \frac{1}{\sqrt{2}}\big(|0011\rangle + |1100\rangle\big),$$
$$|X_2\rangle \equiv \frac{1}{\sqrt{2}}\big(|0101\rangle + |1010\rangle\big),\ |X_3\rangle \equiv \frac{1}{\sqrt{2}}\big(|0110\rangle + |1001\rangle\big).$$

From the decomposition in Eq. (4.2) we immediately see that the state ρ^{ABCD} is invariant under any permutations of the four parties.

If any two of the four parties, say C and D, get together, they can do a Bell-measurement (namely, measurement done in the basis of $|\Psi_i\rangle$'s). Depending on the result $i = 0, \ldots, 3$, they broadcast the outcome to A and B, from which A and B can then establish a definite Bell state. This shows that the state ρ^{ABCD} must be entangled. But if all the four parties are far apart, they have no way of distilling any pure entangled states. This can be seen from the fact proven in Ref. [20] that if two parties are on opposite sides of a separable cut, then they will remain in a separable cut under any local quantum operations and classical communication. From the form in Eq. (4.1) we see that A cannot establish any entanglement between either C or D, as A is in the opposite side of a separable cut from C and D. But from Eq. (4.2) we know that the state is invariant under any permutation of the parties, hence, A cannot establish any entanglement with B (by exchanging C with B), either. Therefore, the state ρ^{ABCD} is bound entangled.

Our goal here is to calculate how much entanglement is bound in the state. As the state is bound entangled, it is equivalent to ask how entangled is the state? For the purpose of using GME to quantify entanglement, we need to characterize all decompositions of the mixed state into pure states. The most general decomposition of a mixed state ρ into pure states can be expressed as

$$\rho = \sum_{k=1}^{\mathcal{M}} |\tilde{\varphi}_k\rangle\langle\tilde{\varphi}_k|, \quad \text{with } |\tilde{\varphi}_k\rangle = \sum_{i=1}^{n} \mathcal{U}_{ki}\sqrt{\lambda_i}\,|\xi_i\rangle, \tag{4.3}$$

where $\mathcal{M}$ is an integer not smaller than n, the number of orthonormal eigenvectors $\{|\xi_i\rangle\}$ (with nonzero eigenvalues $\{\lambda_i\}$) of ρ, $|\tilde{\varphi}\rangle$'s are *un-normalized*, and $\mathcal{U}$ satisfies $\sum_{k=1}^{\mathcal{M}} \mathcal{U}_{ki}\,\mathcal{U}_{kj}^{*} = \delta_{ij}$. Thus, the most general pure state that appears in the decomposition of Smolin's state is

$$|\tilde{\varphi}_k\rangle = \sum_{i=0}^{3} \frac{1}{2}\,\mathcal{U}_{ki}|X_i\rangle. \tag{4.4}$$

Our goal is to minimize $\sum_k p_k\, E_{\text{pure}}\big(|\varphi_k\rangle\big)$ over all possible $\mathcal{U}$'s, where E_{pure} is some pure-state entanglement ($E_{\sin^2}$ or $E_{\log_2}$ in our considerations), $p_k \equiv \langle\tilde{\varphi}_k|\tilde{\varphi}_k\rangle$, and $|\varphi_k\rangle$ is the normalized state $|\varphi_k\rangle \equiv |\tilde{\varphi}_k\rangle/\sqrt{p_k}$. Making a general minimization for an arbitrary mixed state is extremely difficult. However, for the mixed state ρ^{ABCD} we shall show that the decomposition in Eq. (4.2) does indeed

minimize the average entanglement over pure-state decompositions. As in Eq. (4.4), $|\varphi\rangle$ can be explicitly written as $|\varphi\rangle = \sum_{i=0}^{3} \sqrt{q_i}\, e^{i\,\phi_i} |X_i\rangle$, where the q's are non-negative, satisfying $\sum_i q_i = 1$, and the ϕ's are phases. For fixed q's, the state has a maximal entanglement eigenvalue when all phases are zero. We shall show shortly that its maximal entanglement eigenvalue is $1/\sqrt{2}$, which is achieved by the $|X\rangle$'s.

The entanglement eigenvalue of the state $|\varphi\rangle = \sum_{i=0}^{3} \sqrt{q_i}\, |X_i\rangle$ is the maximal overlap with the separable state $|\Phi\rangle = \otimes_{i=1}^{4} \big(c_i|0\rangle + s_i|1\rangle\big)$, where $c_i \equiv \cos\theta_i$ and $s_i \equiv \sin\theta_i$ with $0 \leq \theta_i \leq \pi/2$. Thus

$$\begin{aligned} \langle\Phi|\varphi\rangle &= \sqrt{q_0/2}\,(c_1c_2c_3c_4 + s_1s_2s_3s_4) + \sqrt{q_1/2}\,(c_1c_2s_3s_4 + s_1s_2c_3c_4) \\ &+ \sqrt{q_2/2}\,(c_1s_2c_3s_4 + s_1c_2s_3c_4) + \sqrt{q_3/2}\,(c_1s_2s_3c_4 + s_1c_2c_3s_4), \end{aligned}$$

which has maximum $1/\sqrt{2}$. To see this, use the Cauchy-Schwarz inequality, treating as one vector $\big\{\sqrt{q_0/2}, \sqrt{q_1/2}, \sqrt{q_2/2}, \sqrt{q_3/2}\big\}$ (whose modulus is $1/\sqrt{2}$), and the corresponding coefficients as another vector, whose modulus can be shown to be no greater than 1:

$$\begin{aligned} &(c_1c_2c_3c_4 + s_1s_2s_3s_4)^2 + (c_1c_2s_3s_4 + s_1s_2c_3c_4)^2 \\ &+(c_1s_2c_3s_4 + s_1c_2s_3s_4)^2 + (c_1s_2s_3c_4 + s_1c_2c_3s_4)^2 \leq 1. \end{aligned}$$

By subtracting the left-hand side from 1 and making some algebraic manipulation, we arrive at the non-negative expression (hence the sought result):

$$\begin{aligned} &(c_1c_2c_3s_4 - s_1s_2s_3c_4)^2 + (c_1c_2s_3s_4 - s_1s_2c_3s_4)^2 + \\ &(c_1s_2c_3c_4 - s_1c_2s_3s_4)^2 + (s_1c_2c_3c_4 - c_1s_2s_3s_4)^2 \geq 0. \end{aligned}$$

The states $|X_i\rangle$ are GHZ-like states and have $\Lambda_{\max} = 1/\sqrt{2}$ and they clearly saturate $|\langle\Phi|\varphi\rangle| \leq 1/\sqrt{2}$. Hence, we have

$$E_{\sin^2}(\rho^{ABCD}) = 1/2, \quad E_{\log_2}(\rho^{ABCD}) = 1. \tag{4.5}$$

This suggests that although bound entangled, Smolin's state has a very high degree of entanglement, the same as that of a 4-partite GHZ state. This high degree of entanglement seems to manifest in

some bi-partite partitioning, e.g., {A:BCD} (as we discuss below).

To compare the results with other measures of entanglement, we conjecture (and later prove) that $E_{\mathrm{R}}=1$ for this state and one of its closest separable mixed states is

$$\frac{1}{8}\big(|0000\rangle\langle 0000|+|1111\rangle\langle 1111|+|0011\rangle\langle 0011|+|1100\rangle\langle 1100|$$
$$+|0101\rangle\langle 0101|+|1010\rangle\langle 1010|+|0110\rangle\langle 0110|+|1001\rangle\langle 1001|\big).$$

The negativity $\mathcal{N}$ (a value used to quantify the degree of bi-partite inseparability of states and defined as twice the absolute sum of negative eigenvalues of the partial transpose (PT) of the density matrix with respect to some bi-partite partitioning) is zero for any 2/2 partitioning, e.g., {AB : CD}, but nonzero for 1/3 partitioning, e.g.,{A:BCD}. (This nonzero negativity also demonstrates that the state ρ^{ABCD} is entangled.) Specifically, $\mathcal{N}_{\mathrm{A:BCD}}=1$ but $\mathcal{N}_{\mathrm{AB:CD}}=0$.

Let us now turn to Dür's bound entangled states.

4.3 Dür's N-party bound entangled states

Dür [69] found that for $N\geq 4$ the following state is bound entangled:

$$\rho_N \equiv \frac{1}{N+1}\left(|\Psi_G\rangle\langle\Psi_G| + \frac{1}{2}\sum_{k=1}^{N}\left(P_k+\bar{P}_k\right)\right), \tag{4.6}$$

where $|\Psi_G\rangle \equiv \left(|0^{\otimes N}\rangle + e^{i\alpha_N}|1^{\otimes N}\rangle\right)/\sqrt{2}$ is a N-partite GHZ state; $P_k \equiv |u_k\rangle\langle u_k|$ is a projector onto the state $|u_k\rangle \equiv |0\rangle_1|0\rangle_2\ldots|1\rangle_k\ldots|0\rangle_N$; and $\bar{P}_k \equiv |v_k\rangle\langle v_k|$ projects onto $|v_k\rangle \equiv |1\rangle_1|1\rangle_2\ldots|0\rangle_k\ldots|1\rangle_N$. For $N\geq 8$ this state violates the Mermin-Klyshko-Bell inequality [69]; violation was pushed down to $N\geq 7$ by Kaszlikowski and co-workers [71] for a three-setting Bell inequality; it was pushed further down to $N\geq 6$ by Sen and co-workers [72] for a functional Bell inequality. For these inequalities, see Appendix E for more detail. These results are interesting and somewhat surprising, as one might expect that bound entangled states has low entanglement that they could not violate any Bell inequality. So how entangled are Dür's bound entangled states?

We remark that the phase α_N in $|\Psi_G\rangle$ can be eliminated by local unitary transformations, and

hence we shall take $\alpha_N = 0$ in the following discussion. In fact, if we consider the family of states

$$\rho_N(x) \equiv x|\Psi_G\rangle\langle\Psi_G| + \frac{1-x}{2N}\sum_{k=1}^{N}\big(P_k + \bar{P}_k\big), \tag{4.7}$$

we find that for $N \geq 4$ the state is bound entangled if $0 < x \leq 1/(N+1)$ and is still entangled but not bound entangled if $x > 1/(N+1)$. This can be seen from the fact that the negativities of $\rho_N(x)$ with respect to the two different partitions $(1 : 2\cdots N)$ and $(12 : 3\cdots N)$ are

$$\mathcal{N}_{1:2\cdots N}\big(\rho_N(x)\big) = \max\{0, [(N+1)\,x - 1\,]/N\,\}, \tag{4.8a}$$

$$\mathcal{N}_{12:3\cdots N}\big(\rho_N(x)\big) = x. \tag{4.8b}$$

By applying arguments similar to those used to calculate entanglement for Smolin's state, we have that the general pure state in the decomposition of $\rho_N(x)$ is

$$\sqrt{y}\,e^{i\phi_0}|\Psi_G\rangle + \sqrt{1-y}\sum_{k=1}^{N}\big(\sqrt{q_k}e^{i\phi_i}|u_i\rangle + \sqrt{r_k}e^{i\phi'_i}|v_i\rangle\big),$$

where q's and r's are non-negative and satisfy $\sum_k(q_k + r_k) = 1$. In this family, the state with the least entanglement (or maximum $\Lambda_{\max}$) for fixed $\{y, q_k, r_k\}$ is the one with all phase factors zero:

$$|\Psi\big(y, \{q, r\}\big)\rangle \equiv \sqrt{y}|\Psi_G\rangle + \sqrt{1-y}\sum_{k=1}^{N}\big(\sqrt{q_k}|u_i\rangle + \sqrt{r_k}|v_i\rangle\big).$$

Next, we ask: For fixed y, what is the least entanglement that the above state can have? Take a separable state of the form $|\Phi\rangle = \otimes_{i=1}^{N}\big(c_i|0\rangle + s_i|1\rangle\big)$; its overlap with $|\Psi\big(y, \{q, r\}\big)\rangle$ is then

$$\langle\Psi|\Phi\rangle = \sqrt{y/2}\,(c_1\cdots c_N + s_1\cdots s_N) + \sqrt{1-y}\sum_{k=1}^{N}(\sqrt{q_k}\,c_1\cdots s_k\cdots c_N + \sqrt{r_k}\,s_1\cdots c_k\cdots s_N).$$

This can be shown to no greater than $\sqrt{(2-y)/2}$, again by a Cauchy-Schwarz inequality, taking

$$\Big\{\sqrt{y/2}, \big\{\sqrt{(1-y)q_k}\big\}, \big\{\sqrt{(1-y)r_k}\big\}\Big\}$$

as the first $(2N{+}1)$-component vector (with modulus $\sqrt{(2-y)/2}$) and the corresponding coefficients

as the second one, whose modulus can be shown to be no greater than 1 for $N \geq 4$:

$$f_N \equiv \left(c_1 \cdots c_N + s_1 \cdots s_N\right)^2 + \sum_{k=1}^{N} \left\{(c_1 \cdots s_k \cdots c_N)^2 + (s_1 \cdots c_k \cdots s_N)^2\right\} \leq 1.$$

First, making similar arguments as previously, one can show that $f_4 \leq 1$. One can also show that $f_{N+1} \leq f_N$. Thus by induction, we have proved the inequality.

The bound can be saturated, e.g., by

$$|\psi_{\pm,u,k}(y)\rangle \equiv \sqrt{y}|\Psi_G\rangle \pm \sqrt{1-y}|u_k\rangle, \tag{4.9a}$$

$$|\psi_{\pm,v,k}(y)\rangle \equiv \sqrt{y}|\Psi_G\rangle \pm \sqrt{1-y}|v_k\rangle, \tag{4.9b}$$

for which $\Lambda_{\max}(y) = \sqrt{(2-y)/2}$ [73]. This can be seen as follows. As one can make local relative phase shifts to transform $\sqrt{y}|\Psi_G\rangle + \sqrt{1-y}|u_k\rangle$ to $\sqrt{y}|\Psi_G\rangle - \sqrt{1-y}|u_k\rangle$, they have the same entanglement. The change from $\sqrt{y}|\Psi_G\rangle \pm \sqrt{1-y}|u_k\rangle$ to $\sqrt{y}|\Psi_G\rangle \pm \sqrt{1-y}|v_k\rangle$ is simply a flipping of 0 to 1, and vice versa. The mapping from k to k' is just a relabelling of parties. Thus, we need only consider the state

$$\sqrt{y/2}\,(|00\cdots0\rangle + |11\cdots1\rangle) + \sqrt{1-y}|10\cdots0\rangle.$$

As this state is invariant under permutation of all parties except the first one, and as the coefficients are non-negative, in order to find the maximal overlap we can make the hypothesis that the closest separable state is of the form

$$\left(\sqrt{p}|0\rangle + \sqrt{1-p}|1\rangle\right) \otimes (\sqrt{q}|0\rangle + \sqrt{1-q}|1\rangle)^{\otimes N-1}.$$

We further see that in order for the overlap to be maximal, q must be either 1 or 0. For the former case, we can further maximize the overlap to get $\sqrt{(2-y)/2}$. For the latter case, the maximum overlap is $\sqrt{y/2}$, which is less than $\sqrt{(2-y)/2}$ (as $0 \leq y \leq 1$). Hence, the state $\sqrt{y}|\Psi_G\rangle \pm \sqrt{1-y}|u_k\rangle$ has the entanglement eigenvalue $\sqrt{(2-y)/2}$.

As $1-\Lambda_{\max}^2(y)$ is linear in y and $-2\log_2\Lambda_{\max}(y)$ is convex in y, one gets

$$E_{\sin^2}(\rho_N(x)) = \frac{x}{2}, \quad E_{\log_2}(\rho_N(x)) = \log_2\frac{2}{2-x}, \tag{4.10}$$

and one of the optimal decompositions is

$$\rho_N(x) = \frac{1}{4N}\sum_{k=1}^{N}\sum_{\alpha=\pm}\sum_{\beta=u,v}|\psi_{\alpha,\beta,k}(x)\rangle\langle\psi_{\alpha,\beta,k}(x)|. \tag{4.11}$$

The above calculations show that for $\rho_N(x)$, the entanglement depends on the portion x of the GHZ in states $|\psi_{\alpha,\beta,k}(x)\rangle\langle\psi_{\alpha,\beta,k}(x)|$ and it never becomes zero unless there is no GHZ mixture.

We conjecture that, for $N \geq 4$, $\rho_N(x)$ has $E_R(x) = x$, with one closest separable mixed state being

$$\frac{x}{2}\big(|0..0\rangle\langle 0..0| + |1..1\rangle\langle 1..1|\big) + \frac{1-x}{2N}\sum_{k=1}^{N}\big(P_k + \bar{P}_k\big),$$

which seems plausible as $\big(|0..0\rangle\langle 0..0| + |1..1\rangle\langle 1..1|\big)$ is a closest separable mixed state to $|\Psi_G\rangle$.

4.4 Concluding remarks

We have presented analytical results on how much entanglement is bounded in two distinct multi-partite bound entangled states. The measure we have used to quantify their entanglement is the geometric measure of entanglement (GME), whose construction, similiar to the entanglement of formation ($E_{\rm F}$), is via convex hull. In contrast to GME, $E_{\rm F}$ has not been explicitly generalized to multi-partite states, and hence is still unavailable for these bound entangled states. However, under the circumstances discussed previously, the results of $E_{\sin^2}$ as well as a related quantity, $E_{\log_2}$, might provide lower bounds on $E_{\rm F}$. For the Smolin state, its bound entanglement is as large as that of a four-partite GHZ state, whereas that for Dür states is related to the portion of the N-partite GHZ state. For each case, an optimal decomposition is given. Furthermore, we have conjectured that the relative entropy of entanglement ($E_{\rm R}$) for the Smolin state is unity (proved below), whereas we conjecture that $E_{\rm R}$ for Dür's state is equal to the portion that is N-GHZ.

For Smolin's state we can establish its $E_{\rm F}$, $E_{\rm D}$, $E_{\rm R}$ and $E_{\sin^2}$ for certain bi-partite partitionings.

For example, if we group the four parties ABCD in two, A:BCD, we can write the state as

$$\rho^{A:BCD} = \frac{1}{4}\sum_{i=0}^{3} |\bar{X}_i\rangle\langle\bar{X}_i|, \tag{4.12}$$

with the 3-qubit states of BCD mapped on to the 8-level system ($000 \to \underline{0}, 001 \to \underline{1}, ..., 111 \to \underline{7}$), involving the locally orthogonal and convertible states (by BCD)

$$|\bar{X}_0\rangle = \big(|0\underline{0}\rangle + |1\underline{7}\rangle\big)/\sqrt{2}, \quad |\bar{X}_1\rangle = \big(|0\underline{3}\rangle + |1\underline{4}\rangle\big)/\sqrt{2},$$
$$|\bar{X}_2\rangle = \big(|0\underline{5}\rangle + |1\underline{2}\rangle\big)/\sqrt{2}, \quad |\bar{X}_3\rangle = \big(|0\underline{6}\rangle + |1\underline{1}\rangle\big)/\sqrt{2}.$$

In order to find the entanglement of this bi-partite state (in $C^2 \otimes C^8$), we need to consider the entanglement of the general (properly normalized) pure state

$$|\psi\rangle \equiv \sum\nolimits_i \sqrt{x_i}\, e^{i\phi_i} |\bar{X}_i\rangle$$

that appears in the pure-state decompositions. In fact, regardless of the values of the x_i's, this pure state has a reduced density matrix (tracing over BCD) of the form $\left(|0\rangle\langle 0| + |1\rangle\langle 1|\right)/2$. This shows that $\rho^{A:BCD}$ has $E_{\rm F} = 1$, $E_{\sin^2} = 1/2$, and $E_{\log_2} = 1$. In fact, there is a general result due to Horodecki and co-workers [74] that $E_{\rm D} = E_{\rm F}$ for mixture of locally orthogonal bi-partite states, e.g., $C^2 \otimes C^{2m}$ states that are derived from mixing Bell-like states

$$|\Psi_k^{\pm}\rangle \equiv (|0, \underline{k}\rangle \pm |1, \underline{2m-k-1}\rangle)/\sqrt{2}, \tag{4.13}$$

having *distinct* k's, where $k = 0, 1, \ldots, m-1$. As $E_{\rm D} \leq E_{\rm R} \leq E_{\rm F}$, we have that $E_{\rm R}(\rho^{\rm A:BCD}) = 1$ as well. What about the original four-partite state $\rho^{\rm ABCD}$? As $E_{\rm R}(\rho^{\rm ABCD}) \geq E_{\rm R}(\rho^{\rm A:BCD})$, we have $E_{\rm R}(\rho^{\rm ABCD}) \geq 1$. But we also have that $E_{\rm R}(\rho^{\rm ABCD}) \leq 1$, as our previous conjecture gives at least an upper bound; we thus have that $E_{\rm R}(\rho^{\rm ABCD}) = 1$ and the conjecture is proved. Naively, we expect that any arbitrary $\rho^{\rm ABCD}$ has greater entanglement than $\rho^{\rm A:BCD}$. However, for the Smolin state, they have the same entanglement as quantified by both GME and the relative entropy of entanglement.

Although Dür's bound entangled state violates a Bell inequality, it has nonzero negativity under

certain partitionings. One may raise the question: Does there exist a bound entangled state that has positive PT (PPT) under all partitionings but that still violates a Bell's inequality? For example, does a UPB bound entangled state [65] violate a Bell inequality? We shall see shortly that the answer is "No", at least for the three different Bell inequalities [69, 71, 72] mentioned earlier. Acín has shown [75] that if an N-qubit state violates a two-setting Bell inequality then it is distillable under certain bi-partite partitioning. Using the results of Refs. [76, 77] regarding distillability, we can repeat the same analysis for the other two inequalities [71, 72] and indeed obtain the same conclusion. We analyze this as follows.

It was shown by Dür and Cirac [77] that an arbitrary N-qubit state ρ can be locally depolarized into the form

$$\rho_N = \lambda_0^+ |\Psi_0^+\rangle\langle\Psi_0^+| + \lambda_0^- |\Psi_0^-\rangle\langle\Psi_0^-| + \sum_{j=1}^{2^{N-1}-1} \lambda_j \big(|\Psi_j^+\rangle\langle\Psi_j^+| + |\Psi_j^-\rangle\langle\Psi_j^-|\big),$$

while preserving $\lambda_0^\pm = \langle\Psi_0^\pm|\rho|\Psi_0^\pm\rangle$ and $\lambda_j = \langle\Psi_j^+|\rho|\Psi_j^+\rangle + \langle\Psi_j^-|\rho|\Psi_j^-\rangle$, where $|\Psi_0^\pm\rangle \equiv (|0^{\otimes N}\rangle \pm |1^{\otimes N}\rangle)/\sqrt{2}$, and the $|\Psi_j^\pm\rangle$'s are GHZ-like states, i.e., the states in (4.13), unfolded into qubit notation. Normalization gives the condition

$$\lambda_0^+ + \lambda_0^- + 2\sum_j \lambda_j = 1.$$

Now define $\Delta \equiv \lambda_0^+ - \lambda_0^-$, which we assume to be non-negative (w.l.o.g). The condition that there is no bi-partite distillability for some bi-partite partitioning P_j is [76]

$$2\lambda_j \geq \Delta.$$

Assuming non-distillability for *all* bi-partite splittings, we have

$$2\sum_j \lambda_j = 1 - (\lambda_0^+ + \lambda_0^-) \geq (2^{N-1} - 1)\Delta.$$

As $\lambda_0^+ + \lambda_0^- \geq \Delta$, we have further that

$$1 - \Delta \geq (2^{N-1} - 1)\Delta. \tag{4.14}$$

For the Mermin-Klyshko-Bell inequality, violation implies $\Delta > 1/2^{(N-1)/2}$. For the three-setting Bell inequality considered in [71], violation implies $\Delta > \sqrt{3}\,(2^N/3^N)$. For the functional Bell inequality in [72], violation implies $\Delta > 2\,(2^N/\pi^N)$. One can easily check that the three Bell inequalities considered are inconsistent with non-bipartite-distillability condition, Eq. (4.14). Hence, the violating of these three Bell inequalities implies the existence of some bi-partite distillability.

This bi-partite distillability then implies a negative PT (NPT) under that bi-partite partitioning according to Horodecki and co-workers [19]. Hence, violating these Bell inequalities implies NPT under certain bi-partite partitioning. Said equivalently, if an N-qubit state has PPT under all bi-partite partitionings then the state never violates these Bell inequalities. This seems to suggest that PPT bound entangled states are truly bound in nature that cannot give deviation from local theories.

Chapter 5

Global entanglement and quantum criticality in spin chains

5.1 Introduction

Entanglement has been recognized in the past decade as a useful resource in quantum information processing. Very recently, it has emerged as an actor on the nearby stage of quantum many-body physics, especially for systems that exhibit quantum phase transitions [78, 79, 80, 81, 82], where it can play the role of a diagnostic of quantum correlations. Quantum phase transitions [83] are transitions between qualitatively distinct phases of quantum many-body systems, driven by quantum fluctuations. In view of the connection between entanglement and quantum correlations, one anticipates that entanglement will furnish a dramatic signature of the quantum critical point. On the other hand, the more entangled a state is, the more useful it is likely to be as resource for quantum information processing. It is thus desirable to study and quantify the degree of entanglement near quantum phase transitions. By employing entanglement to diagnose many-body quantum states one may obtain fresh insight into the quantum many-body problem.

To date, progress in quantifying entanglement has taken place primarily in the domain of bi-partite systems. Much of the previous work on entanglement in quantum phase transitions has been based on bi-partite measures, i.e., focus has been on entanglement either between pairs of parties [78, 79] or between a part and the remainder of a system [80]. For multi-partite systems, however, the complete characterization of entanglement requires the consideration of multi-partite entanglement, for which a consensus measure has not yet emerged.

Singular and scaling behavior of entanglement near quantum critical points was discovered in

important work by Osterloh and co-workers [79], who invoked Wootters' *bi-partite* concurrence [22] as a measure of entanglement. The drawback of concurrence is that it can deal with only two spins (each with spin-1/2) even though the system may contain an infinite number of spins. Although attempts have been made to generalize concurrence to many spin-1/2 systems via the time reversal operation, the generalized concurrence loses its connection to the entanglement of formation [84].

Another approach is to consider the von Neumann entropy of a subsystem of L spins with the rest $N-L$ spins of the system. It is found that for critical spin chains the entropy scales logarithmically with the subsystem size L for $N \to \infty$, with a prefactor that is related to the central charge of the corresponding conformal theory [80, 81]. However, the entanglement addressed in this case is not truly many-body, but only between a subsystem and the rest of the system, although the connection to central charge is interesting.

Quite recently, Barnum and co-workers [82] have developed an entanglement measure, which they call generalized entanglement. Instead of using subsystems they use different algebras and generalized coherent states to define the entanglement. They have also applied the generalized entanglement to systems exhibiting quantum phase transitions. Their approach opens a new approach to multi-partite entanglement. However, there is no *a priori* choice of which algebra, amongst all possible ones, is the most natural one to use.

In addtion to spin chains other models that have been studied by using either the von Neumann entropy or the concurrence as the entanglement measure include: (i) the super-radiance model, in which many two-level atoms interact with a single-mode photon field [85]; and (ii) the one-dimensional extended Hubbard model, in which electrons can hop between the nearest neighbors and there are Coulomb interactions among electrons on the same site and with nearest-neighbor electrons as well [86]. Verstraete and co-workers [87] have recently defined an entanglement length, viz., the distance at which two sites can establish a pure-state entanglement at the cost of measuring all other sites. They found that this entanglement length is usually greater than the correlation length. All these, including the theme of the present chapter, are aimed at approaching many-body problems from different, and hopefully fresh, prespectives.

In the present chapter, we apply the *global* measure that we have developed in previous chapters, based on a geometric picture; it provides a *holistic*, rather than bi-partite, characterization of

the entanglement of quantum many-body systems. Our focus is on one-dimensional spin systems, specifically ones that are exactly solvable and exhibit quantum criticality. For these systems, we are able to determine the entanglement analytically, and to observe that it varies in a singular manner near the quantum critical line. This supports the view that entanglement—the non-factorization of wave functions—reflects quantum correlations. Moreover, the boundaries between different phases can be detected by the entanglement.

5.2 Global measure of entanglement

We quickly review the global measure that we shall use in the present chapter. Consider a general, n-partite, normalized pure state: $|\Psi\rangle = \sum_{p_1 \cdots p_n} \Psi_{p_1 p_2 \cdots p_n} |e_{p_1}^{(1)} e_{p_2}^{(2)} \cdots e_{p_n}^{(n)}\rangle$. If the parties are all spin-1/2 then each can be taken to have the basis $\{|\uparrow\rangle, |\downarrow\rangle\}$. Our scheme for analyzing the entanglement involves considering how well an entangled state can be approximated by some unentangled (normalized) state (e.g., the state in which every spin points in a definite direction): $|\Phi\rangle \equiv \otimes_{i=1}^{n} |\phi^{(i)}\rangle$. The proximity of $|\Psi\rangle$ to $|\Phi\rangle$ is captured by their overlap; the entanglement of $|\Psi\rangle$ is revealed by the maximal overlap [38]

$$\Lambda_{\max}(\Psi) \equiv \max_{\Phi} |\langle \Phi | \Psi \rangle| \,; \tag{5.1}$$

the larger $\Lambda_{\max}$ is, the less entangled is $|\Psi\rangle$. (Note that for a product state, $\Lambda_{\max}$ is unity.) If the entangled state consists of two separate entangled pairs of subsystems, $\Lambda_{\max}$ is the product of the maximal overlaps of the two. Hence, it makes sense to quantify the entanglement of $|\Psi\rangle$ via the following *extensive* quantity

$$E_{\log_2}(\Psi) \equiv -\log_2 \Lambda_{\max}^2(\Psi), \tag{5.2}$$

This normalizes to unity the entanglement of EPR-Bell and N-party GHZ states, as well as giving zero for unentangled states. Finite-N entanglement is interesting in the context of quantum information processing. To characterize the properties of the quantum critical point we use the

thermodynamic quantity $\mathcal{E}$ defined by

$$\mathcal{E} \equiv \lim_{N\to\infty} \mathcal{E}_N, \tag{5.3a}$$

$$\mathcal{E}_N \equiv N^{-1} E_{\log_2}(\Psi), \tag{5.3b}$$

where $\mathcal{E}_N$ is the *entanglement density*, i.e., the entanglement per particle.

5.3 Quantum XY spin chains and entanglement

We consider the family of models governed by the Hamiltonian

$$\mathcal{H}_{\rm XY} = -\sum_{j=1}^{N} \left(\frac{1+r}{2}\sigma_j^x \sigma_{j+1}^x + \frac{1-r}{2}\sigma_j^y \sigma_{j+1}^y + h\,\sigma_j^z \right), \tag{5.4}$$

where r measures the anisotropy between x and y couplings, h is the transverse external field, lying along the z-direction, and we impose periodic boundary conditions, namely, a ring geometry. At $r = 0$ we have the isotropic XY limit (also known as the XX model) and at $r = 1$, the Ising limit. All anisotropic XY models ($0 < r \leq 1$) belong to the same universality class, i.e., the Ising class, whereas the isotropic XX model belongs to a different universality class. XY models exhibit three phases (see Fig. 5.1): oscillatory, ferromagnetic and paramagnetic. In contrast to the paramagnetic phase, the first two are ordered phases, with the oscillatory phase being associated with a characteristic wavevector, reflecting the modulation of the spin correlation functions (see, e.g., Ref. [88]). We shall see that the global entanglement detects the boundaries between these phases, and that the universality class dictates the behavior of entanglement near quantum phase transitions.

Before we solve the entanglement of the XY model, we give perturbative analysis of, as an illustration of how entanglement arises and vanishes, the Ising model in a transverse field (viz. $r = 1$)

$$\mathcal{H} = -\sum_{i=1}^{N} \left(\sigma_i^x \sigma_{i+1}^x + h\sigma_i^z \right). \tag{5.5}$$

At $h = 0$ the ground state is that with all spins pointing up in the x-direction $|{\rightarrow}{\rightarrow}\cdots{\rightarrow}\rangle$ or down $|{\leftarrow}{\leftarrow}\cdots{\leftarrow}\rangle$, which is manifestly unentangled. The ground state can be any superposition

of ($|\rightarrow\rightarrow\cdots\rightarrow\rangle$ and $|\leftarrow\leftarrow\cdots\leftarrow\rangle$ when the Z_2 symmetry is not spontaneously broken. For example, the states $(|\rightarrow\rightarrow\cdots\rightarrow\rangle \pm |\leftarrow\leftarrow\cdots\leftarrow\rangle)/\sqrt{2}$ are actually the two lowest levels obtained from solving the models using Jordan-Wigner and Bogoliubov transformations and they both have $E_{\log_2} = 1$. (For small h the entanglement rises quadratically in the case of unbroken symmetry instead of quartically, as we shall show shortly.) We shall see later that whether or not we use a broken-symmetry state has no effect in the thermodynamic limit. For small h (i.e., $h \ll 1/\sqrt{N}$) one can obtain the ground state by treating the $h\sigma_i^z$ terms as perturbations. Take the ground state at $h = 0$ to be $|\rightarrow\rightarrow\cdots\rightarrow\rangle$. Then first-order perturbation theory for the ground state gives

$$\frac{1}{\sqrt{1+\frac{Nh^2}{4}}}\Big(|\rightarrow\rightarrow\cdots\rightarrow\rangle + \frac{h}{2}\sum_i |\rightarrow\cdots\leftarrow_i\cdots\rightarrow\rangle\Big). \tag{5.6}$$

Using the method described in Sec. 2.2 we obtain $E_{\log_2} \approx N(N-1)h^4/32$ to leading order in h. At $h = \infty$ the ground state is a quantum paramagnet with all spins aligning along the external field: $|\uparrow\uparrow\ldots\uparrow\rangle$, and once more is unentangled. To $\mathcal{O}(1/h)$ perturbation theory gives (treating $\sigma_i^z\sigma_{i+1}^z$ terms small)

$$\frac{1}{\sqrt{1+\frac{N}{16h^2}}}\Big(|\uparrow\uparrow\ldots\uparrow\rangle + \frac{1}{4h}\sum_i |\uparrow\ldots\downarrow_i\downarrow_{i+1}\ldots\uparrow\rangle\Big), \tag{5.7}$$

for which $E_{\log_2} \approx N/(16h^2)$, to leading order of $1/h$. The quantum phase transition from a ferromagnetic to a paramagnetic phase occurs at $h = 1$ [83]. The two lowest levels, which we denote by $|\Psi_{1/2}\rangle$ and $|\Psi_0\rangle$ (for reasons to be explained later) are, respectively, the ground and first excited states, and they are asymptotically degenerate for $0 \le h \le 1$ when $N \to \infty$.

As is well known [83, 88, 89], the energy eigenproblem for the XY spin chain can be solved via a Jordan-Wigner transformation, through which the spin degrees of freedom are recast as fermionic ones, followed by a Bogoliubov transformation, which diagonalizes the resulting quadratic Hamiltonian.

The Jordan-Wigner transformation that we shall make from spins (σ's) to fermion particles

(c's) is

$$\sigma_i^z = 1 - 2c_i^\dagger c_i, \tag{5.8a}$$

$$\sigma_i^x = \prod_{j=1}^{i-1} \left(1 - 2c_j^\dagger c_j\right)\left(c_i + c_i^\dagger\right), \tag{5.8b}$$

$$\sigma_i^y = -i \prod_{j=1}^{i-1} \left(1 - 2c_j^\dagger c_j\right)\left(c_i - c_i^\dagger\right). \tag{5.8c}$$

One has to pay attention to the boundary conditions that are to be imposed on the c's. Although periodic in the σ's, one cannot simply take

$$\sigma_{N+1}^z = \prod_{j=1}^{N} \left(1 - 2c_j^\dagger c_j\right)\left(c_{N+1} + c_{N+1}^\dagger\right) = \sigma_1 = \left(c_1 + c_1^\dagger\right), \tag{5.9}$$

and conclude that either (i) $\prod_{j=1}^N \left(1-2c_j^\dagger c_j\right) = 1$ and $c_{N+1} = c_1$, or (ii) $\prod_{j=1}^N \left(1-2c_j^\dagger c_j\right) = -1$ and $c_{N+1} = -c_1$, neither of which are correct if one wishes to obtain the correct spectrum and eigenstates for arbitrary finite N. Instead one should impose that (as the $(N+1)$-th site is identified as the first site)

$$\sigma_N^x \sigma_{N+1}^x = \sigma_N^x \sigma_1^x, \tag{5.10}$$

which then leads to

$$\left(c_N + c_N^\dagger\right)\left(c_{N+1} + c_{N+1}^\dagger\right) = \prod_{j=1}^{N} \left(1 - 2c_j^\dagger c_j\right)\left(c_N + c_N^\dagger\right)\left(c_1 + c_1^\dagger\right). \tag{5.11}$$

The two possible conditions that satisfy this are either (I) $\prod_{j=1}^N \left(1 - 2c_j^\dagger c_j\right) = -1$ and $c_{N+1} = c_1$, or (II) $\prod_{j=1}^N \left(1 - 2c_j^\dagger c_j\right) = 1$ and $c_{N+1} = -c_1$. The operator

$$\prod_{j=1}^{N} \left(1 - 2c_j^\dagger c_j\right) = e^{i\pi \sum_j c_j^\dagger c_j} \tag{5.12}$$

counts whether the total number of particles is even $(+1)$ or odd (-1). For c's that are periodic, the number is odd, whereas for antiperiodic c's, this number is even.

To incoporate these two boundary conditions on the c's, we take

$$c_j = \frac{1}{\sqrt{N}} \sum_{m=0}^{N-1} e^{i\frac{2\pi}{N} j(m+b)} \tilde{c}_m^{(b)}, \tag{5.13}$$

where $b = 0$ for periodic c's; $b = 1/2$ for anti-periodic c's. (This explains why we label the lowest two states by $|\Psi_{1/2}\rangle$ and $|\Psi_0\rangle$.) The momentum index m ranges from 0 to $N-1$. In terms of these fermion operators the Hamiltonian becomes

$$\mathcal{H} = -Nh - \sum_{m=0}^{N-1} \left\{ \Big[2\cos\frac{2\pi}{N}(m+b) - 2h \Big] \tilde{c}_m^{(b)\dagger} \tilde{c}_m^{(b)} + ir \sin\frac{2\pi}{N}(m+b) \Big[\tilde{c}_m^{(b)} \tilde{c}_{N-m-2b}^{(b)} + \tilde{c}_m^{(b)\dagger} \tilde{c}_{N-m-2b}^{(b)\dagger} \Big] \right\}. \tag{5.14}$$

Upon using the Bogoliubov transformation

$$\tilde{c}_m^{(b)} = \cos\theta_m^{(b)} \gamma_m^{(b)} + i \sin\theta_m^{(b)} \gamma_{N-m-2b}^{(b)\dagger}, \tag{5.15}$$

with

$$\tan 2\theta_m^{(b)} = r \sin\frac{2\pi\,(m+b)}{N} \Big/ \left(h - \cos\frac{2\pi\,(m+b)}{N} \right), \tag{5.16}$$

one arrives at the diagonal the Hamiltonian:

$$\mathcal{H} = \sum_{m=0}^{N-1} \varepsilon_m^{(b)} \Big(\tilde{\gamma}_m^{(b)\dagger} \tilde{\gamma}_m^{(b)} - \frac{1}{2} \Big), \tag{5.17a}$$

$$\varepsilon_m^{(b)} = 2\sqrt{\left(h - \cos\frac{2\pi\,(m+b)}{N} \right)^2 + r^2 \sin^2\frac{2\pi\,(m+b)}{N}}, \tag{5.17b}$$

except for the special case that $\varepsilon_0^{(0)} = 2(h-1)$.

We remark that we have not left out any constant in diagonalizing the Hamiltonian in either case, so the energy spectrum is exact. For each value of b the diagonalization gives 2^N energy eigenvalues, so there are 2^{N+1} in total. Half of them are spurious. In determining the correct 2^N states from the 2^{N+1} solutions, one has to impose a constraint from the boundary conditions. Namely, in case I there can be only odd number of fermions, whereas in case II there can be only even number of fermions.

For $b = 0$, viz, the odd-number-fermion case, the lowest state $|\Psi_0\rangle$ is such that $\langle \tilde{\gamma}_m^{(0)\dagger} \tilde{\gamma}_m^{(0)} \rangle = 0$

except that $\langle\tilde{\gamma}_0^{(0)\dagger}\tilde{\gamma}_0^{(0)}\rangle = 1$. Its energy eigenvalue is

$$E_0^{(0)}(r,h) = (h-1) - \sum_{m=1}^{N-1}\sqrt{\Big(h-\cos\frac{2\pi\,m}{N}\Big)^2 + r^2\sin^2\frac{2\pi\,m}{N}}. \tag{5.18}$$

For $b = 1/2$, namely, the even-number-fermion case, the lowest state $|\Psi_{1/2}\rangle$ is such that $\langle\tilde{\gamma}_m^{(1/2)\dagger}\tilde{\gamma}_m^{(1/2)}\rangle = 0$ for all m. Its eigen-energy is

$$E_0^{(1/2)}(r,h) = -\sum_{m=0}^{N-1}\sqrt{\Big(h-\cos\frac{2\pi\,(m+1/2)}{N}\Big)^2 + r^2\sin^2\frac{2\pi\,(m+1/2)}{N}}. \tag{5.19}$$

We see that, as $N\to\infty$, the above two energy levels are degenerate for $h \le 1$. Furthermore, as $N\to\infty$ the difference between the two energy levels becomes

$$E_0^{(0)}(r,h) - E_0^{(1/2)}(r,h) = 2(h-1)\Theta(h-1), \tag{5.20}$$

where $\Theta(x) = 1$ if $x > 0$ and zero otherwise. The way the energy gap vanishes as $h\to 1^+$ gives a relation betweem two exponents

$$z\nu = 1; \tag{5.21}$$

z is the dynamical exponent (defined via the vanishing of energy gap $\Delta\sim|h-h_c|^{z\nu}$) and ν is the correlation-length exponent (defined via $L_c\sim|h-h_c|^{-\nu}$).

Having found the lowest two eigenstates, the quantity $\Lambda_{\max}$ of Eq. (5.1)—and hence the entanglement—can be found, at least in principle. To do this, we parametrize the separable states via

$$|\Phi\rangle \equiv \bigotimes_{i=1}^{N}\big[\cos(\xi_i/2)|\uparrow\rangle_i + e^{i\phi_i}\sin(\xi_i/2)|\downarrow\rangle_i\big], \tag{5.22}$$

where $|\uparrow/\downarrow\rangle$ denote spin states parallel/antiparallel to the z-axis. Instead of maximizing the overlap with respect to the $2N$ real parameters $\{\xi_i,\phi_i\}$, for the lowest two states it is adequate to appeal to the translational symmetry of and the reality of the ground-state wavefunctions. Thus taking $\xi_i = \xi$ and $\phi_i = 0$ we make the Ansatz:

$$|\Phi(\xi)\rangle \equiv e^{-i\frac{\xi}{2}\sum_{j=1}^{N}\sigma_j^y}|\uparrow\uparrow\ldots\uparrow\rangle \tag{5.23}$$

for searching for the maximal the overlap $\Lambda_{\max}(\Psi)$ [90]. This form shows that this separable state can be constructed as a global rotation of the ground state at $h = \infty$, viz., the separable state $|\uparrow\uparrow \ldots \uparrow\rangle$. In this particular limit the boundary condition on the c's is irrelevant, as the dominant term in the Hamiltonian is $-\sum_j h(1 - 2c_j^\dagger c_j)$.

The energy eigenstates are readily expressed in terms of the Jordan-Wigner fermion operators, and so too is the family of the Ansatz states $|\Phi(\xi)\rangle$. By working in this fermion basis we are able to evaluate the overlaps between the two lowest states and the Ansatz states. With $|\Psi_0\rangle$ ($|\Psi_{1/2}\rangle$) denoting the lowest state in the odd (even) fermion-number sector, we arrive at the overlaps

$$\langle \Psi_b(r,h)|\Phi(\xi)\rangle = f_N^{(b)}(\xi) \prod_{m=1-2b}^{m<\frac{N-1}{2}} \left[\cos\theta_m^{(b)}(r,h)\cos^2(\xi/2) + \sin\theta_m^{(b)}(r,h)\sin^2(\xi/2)\cot(k_{m,N}^{(b)}/2)\right], \tag{5.24}$$

with

$$k_{m,N}^{(b)} \equiv \frac{2\pi}{N}(m+b), \quad \tan 2\theta_m^{(b)}(r,h) \equiv r\sin k_{m,N}^{(b)}/(h - \cos k_{m,N}^{(b)}); \tag{5.25a}$$

$$f_N^{(1/2)}(\xi) \equiv 1, \quad f_N^{(0)}(\xi) \equiv \sqrt{N}\sin(\xi/2)\cos(\xi/2), \ (N \text{ even}); \tag{5.25b}$$

$$f_N^{(1/2)}(\xi) \equiv \cos(\xi/2), \quad f_N^{(0)}(\xi) \equiv \sqrt{N}\sin(\xi/2), \quad (N \text{ odd}); \tag{5.25c}$$

where $b = 0, 1/2$ and $m \in [0, N-1]$ is the (integer) momentum index. The above results are *exact* for arbitrary N, obtained with periodic boundary conditions on spins rather than in the so-called c-cyclic approximation [89]. Given these overlaps, we can readily obtain the entanglement of the ground state, the first excited state, and any linear superposition, $\cos\alpha|\Psi_0\rangle + \sin\alpha|\Psi_1\rangle$ of the two lowest states, for arbitrary (r,h) and N, by maximizing the magnitude of the overlap with respect to the single, real parameter ξ. For the derivation of the above results, see Appendix G.

The formulas [in Eqs. (5.24) and (5.25)] contain all the results that we shall explore shortly. By analyzing the structure of Eq. (5.24), we find that the global entanglement does provide information on the phase structure and critical properties of the quantum spin chains. Two of our key results, as captured in Figs. 5.1 and 5.2, are: (i) although the entanglement itself is, generically, not maximized at the quantum critical line in the (r,h) plane, *the field-derivative of the entanglement diverges as the critical line $h = 1$ is approached*; and (ii) the entanglement *vanishes* at the disorder

line $r^2 + h^2 = 1$, which separates the oscillatory and ferromagnetic phases.

As is to be expected, at finite N the two lowest states $|\Psi_0\rangle$ and $|\Psi_{1/2}\rangle$ featuring in Eq. (5.24) do not spontaneously break the Z_2 symmetry. However, in the thermodynamic limit they are degenerate for $h \leq 1$, and linear combinations are also ground states. The question then arises as to whether linear combinations that explicitly break Z_2 symmetry, i.e., the physically relevent states with finite spontaneous magnetization, show the same entanglement properties. In fact, we see from Eq. (5.24) that, in the thermodynamic limit, overlaps for $|\Psi_0\rangle$ and $|\Psi_{1/2}\rangle$ are identical, up to the prefactors $f_N^{(0)}$ and $f_N^{(1/2)}$. These prefactors do not contribute to the entanglement density, and the entanglement density is therefore the same for both $|\Psi_0\rangle$ and $|\Psi_{1/2}\rangle$. It further follows that, in the thermodynamic limit, the results for the entanglement density are insensitive to the replacement of a symmetric ground state by a broken-symmetry one.

5.4 Entanglement and quantum criticality

Before we discuss the thermodynamic limit of the entanglement density, we compare the entanglement obtained via the results in Eq. (5.24) and that obtained via numerically diagonalizing the Hamiltonian and calculating the maximal overlap. In Figure 5.3 the results via each method are shown for the Ising case ($r = 1$) with small numbers of spins ($N = 13$ through 22), it is seen that our analytical results are exact even for small N, both even and odd.

From Eq. (5.24) it follows that the thermodynamic limit of the entanglement density is given by

$$\mathcal{E}(r,h) = -\frac{2}{\ln 2} \max_{\xi} \int_0^{\frac{1}{2}} d\mu \, \ln \left[\cos\theta(\mu,r,h) \cos^2(\xi/2) + \sin\theta(\mu,r,h) \sin^2(\xi/2) \cot \pi\mu \right], \quad (5.26)$$

where $\tan 2\theta(\mu,r,h) \equiv r \sin 2\pi\mu/(h - \cos 2\pi\mu)$.

Figure 5.2 shows the thermodynamic limit of the entanglement density $\mathcal{E}(r,h)$ and its h-derivative in the ground state, as a function of h for three values of r, i.e., three slices through the surface shown in Fig. 5.1. As the $r = 1$ slice shows, in the Ising limit the entanglement density is small for both small and large h. It increases with h from zero, monotonically, albeit very slowly for small h, then swiftly rising to a maximum at $h \approx 1.13$ before decreasing monotonically upon

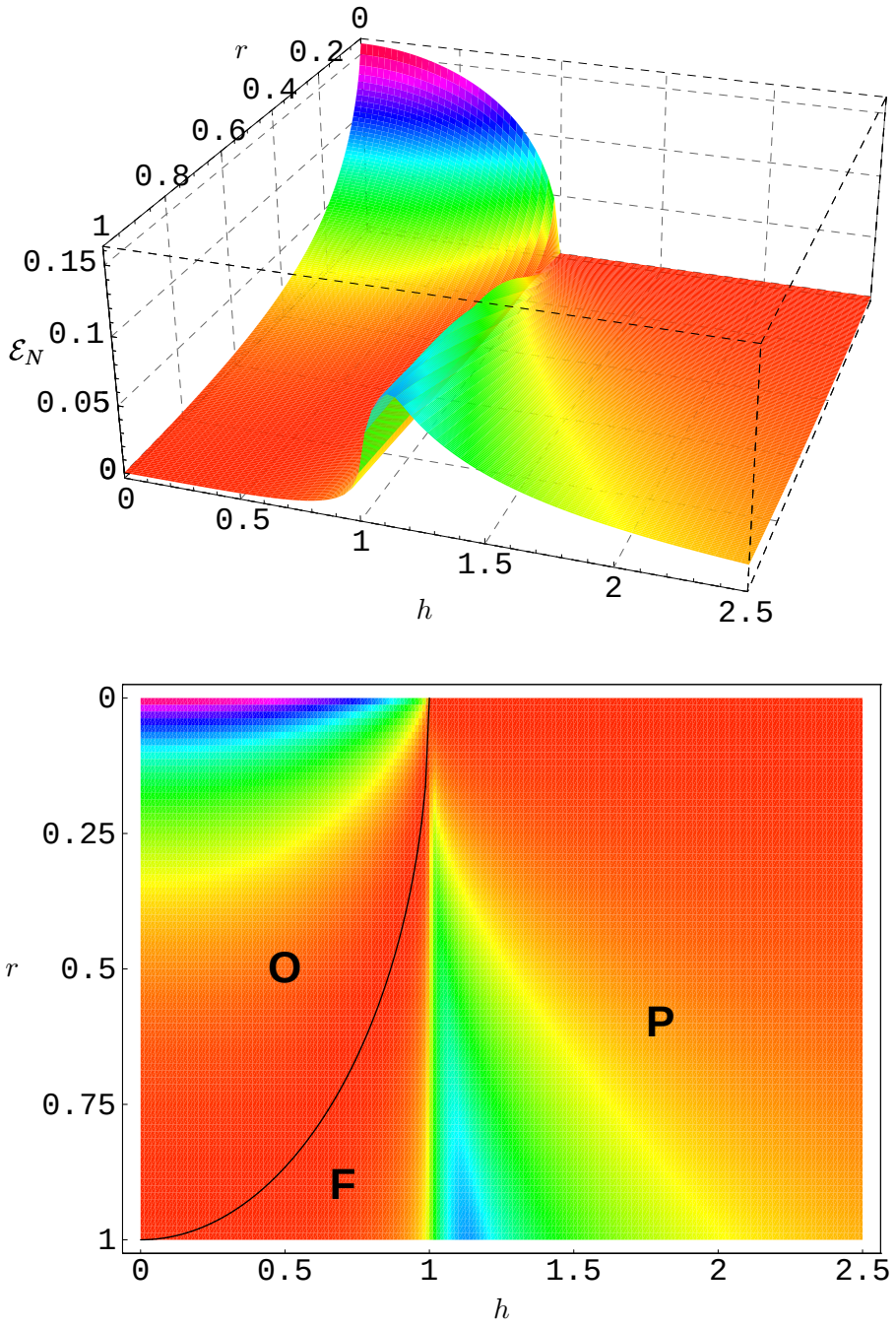

Figure 5.1: Entanglement density (upper) and phase diagram (lower) vs. (r, h) for the XY model with $N = 10^4$ spins, which is essentially in the thermodynamic limit. There are three phases: **O**: ordered oscillatory, for $r^2 + h^2 < 1$ and $r \neq 0$; **F**: ordered ferromagnetic, between $r^2 + h^2 > 1$ and $h < 1$; **P**: paramagnetic, for $h > 1$. As is apparent, there is a sharp rise in the entanglement across the line $h = 1$, which signifies a quantum phase transition. The arc $h^2 + r^2 = 1$, along which the entanglement density is zero (see also Fig. 5.2), separates phases **O** and **F**. Along $r = 0$ lies the XX model, which belongs to a different universality class from the anisotropic XY model.

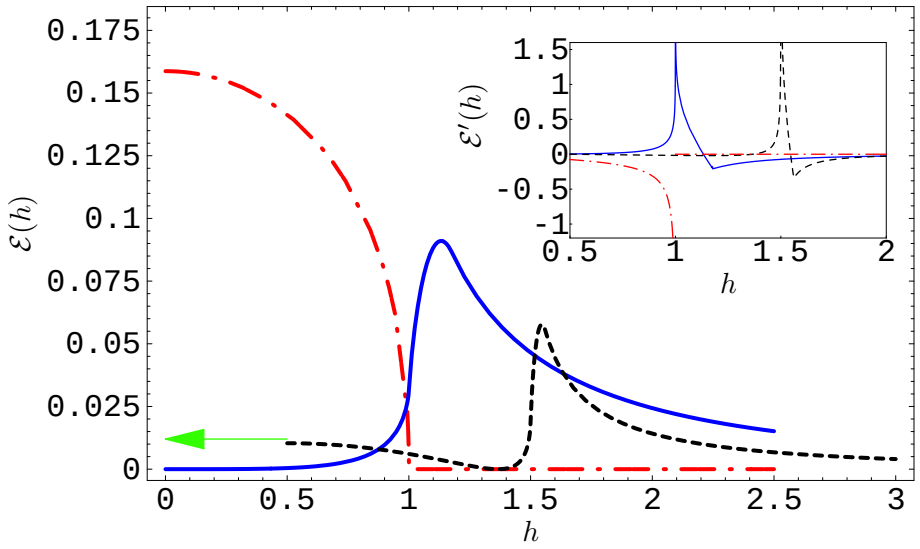

Figure 5.2: Entanglement density and its h-derivative (inset) for the ground state of three systems at $N = \infty$. Solid line: Ising ($r = 1$) limit; dashed line: anisotropic ($r = 1/2$) XY model; dash-dotted line: ($r = 0$) XX model. For the sake of clarity, the XY-case curves are shifted to the right by 0.5, indicated by the arrow. For the $r = 1/2$ case, at the entanglement density vanishes at $h = \sqrt{1 - r^2}$, which is a general property for the anisotropic XY model. Note that whilst the entanglement itself has a nonsingular maximum at $h \approx 1.1$ (Ising), $h \approx 1.04$ ($r = 1/2$ XY), and $h = 0$ (XX), respectively, it has a singularity at the quantum critical point at $h = 1$, as revealed by the divergence of its derivative.

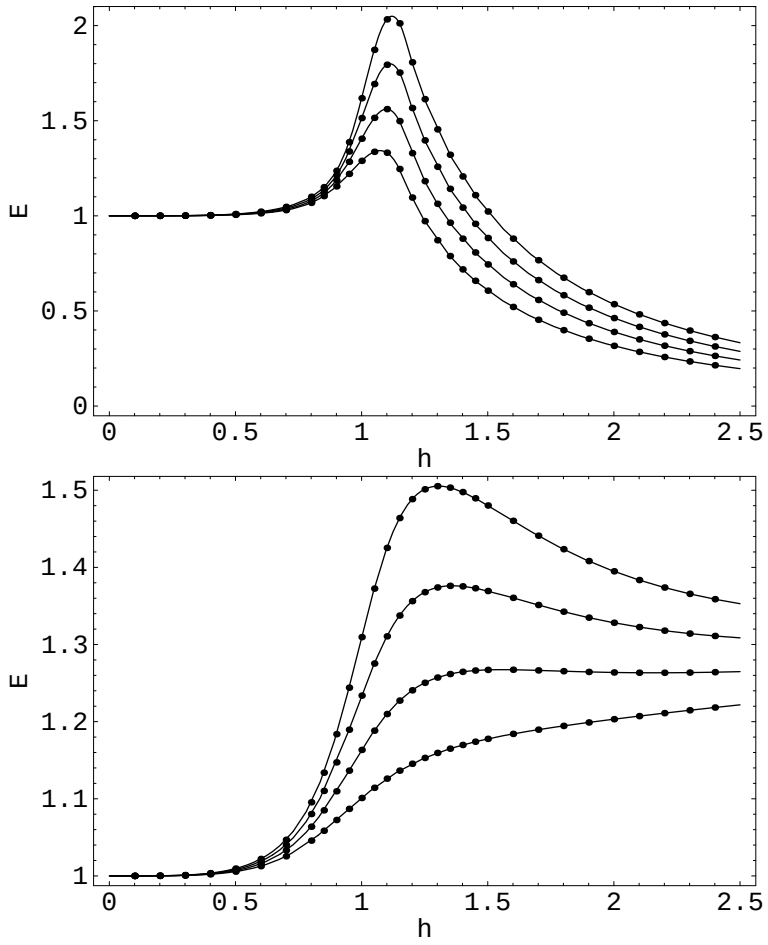

Figure 5.3: Entanglement vs. magnetic field h for ground (upper panel) and first excited (lower panel) states with small $N = 13, 16, 19, 22$ (from bottom to top) for the transverse Ising model ($r = 1$). The numerical results are shown as discrete points whereas the analytical results are shown as lines. This demonstrates that the analytical results are exact, even for small N, both even and odd.

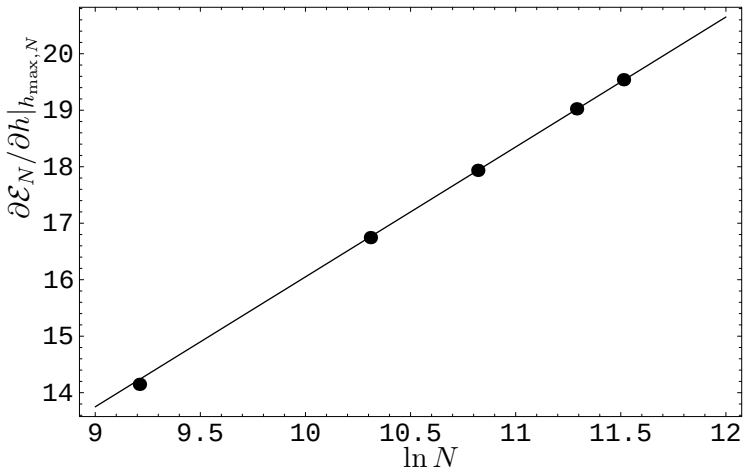

Figure 5.4: Finite-size scaling. $\partial\mathcal{E}_N/\partial h|_{h_{\max,N}}$ vs. $\ln N$, for $N = 10^4, 3\times10^4, 5\times10^4, 8\times10^4$, and 10^5 (points) with $r = 0.1$. The solid line represents the fit $\partial\mathcal{E}_N/\partial h|_{h_{\max,N}} \approx 2.30\ln N - 6.95$.

further increase of h, asymptotically to zero. The entanglement maximum *does not* occur at the quantum critical point. However, the derivative of the entanglement with respect to h *does* diverge at the critical point $h = 1$, as shown in the inset. The slice at $r = 1/2$ (for clarity, shifted half a unit to the right) shows qualitatively similar behavior, except that it is finite (although small) at $h = 0$, and starts out by decreasing to a shallow minimum of zero at $h = \sqrt{1-r^2}$. By constrast, the slice at $r = 0$ (XX) starts out at $h = 0$ at a maximum value of $1 - 2\gamma_C/(\pi\ln 2) \approx 0.159$. (where $\gamma_C \approx 0.9160$ is the *Catalan* constant), the globally maximal value of the entanglement over the entire (r, h) plane. For larger h it falls monotonically until it vanishes at $h = 1$, remaining zero for larger h.

We find that along the line $r^2+h^2 = 1$ the entanglement density vanishes in the thermodynamic limit. In fact, this line exactly corresponds to the boundary separating the oscillatory and ferromagnetic phases; the boundary can be characterized by a set of ground states with total entanglement of order unity, and thus of zero entanglement density. The entanglement density is also able to track the phase boundary ($h = 1$) between the ordered and disordered phases. Associated with the quantum fluctuations accompanying the transition, the entanglement density shows a drastic variation across the boundary and the field-derivative diverges all along $h = 1$. The two boundaries separating the three phases coalesce at $(r, h) = (0, 1)$, i.e., the XX critical point. Figures 5.1 and 5.2 reveal all these features.

In Appendix H.1 we analyze the singular behavior of the field-derivative of the entanglement density (5.26) in the vicinity of the quantum critical line, and we find that the asymptotic behavior (for $r \neq 0$)

$$\frac{\partial \mathcal{E}}{\partial h} \approx -\frac{1}{2\pi r \ln 2} \ln |h-1|, \text{ for } |h-1| \ll 1. \tag{5.27}$$

From the arbitrary-N results (5.24) of the entanglement we analyze the approach to the thermodynamic limit, in order to develop further connections with quantum criticality. We focus on the exponent ν, which governs the divergence at criticality of the correlation length: $L_c \sim |h-1|^{-\nu}$. To do this, we compare the divergence of the slope $\partial \mathcal{E}_N / \partial h$ (i) near $h = 1$ (at $N = \infty$), given above, and (ii) for large N at the value of h for which the slope is maximal (viz. $h_{\max,N}$), i.e., $\partial \mathcal{E}_N / \partial h|_{h_{\max,N}} \approx 0.230 r^{-1} \ln N + \text{const.}$, obtained by analyzing Eq. (5.24) for various values of r; see Fig. 5.4 for the example of $r = 0.1$ case. Then, noting that $(2\pi \ln 2)^{-1} \approx 0.2296$ and that the logarithmic scaling hypothesis [91] (or see Appendix I) identifies ν with the ratio of the amplitudes of these divergences, $0.2296/0.230 \approx 1$, we recover the known result that $\nu = 1$. Moreover, from Eq. (5.21) we can extract the value of the dynamical exponent: $z = 1$.

We derive in Appendix H.2 the divergence behavior of the field-derivative of the entanglement density for the isotropic ($r = 0$) case. Compared with $r \neq 0$ case, the nature of the divergence of $\partial \mathcal{E} / \partial h$ at $r = 0$ belongs to a different universality class:

$$\frac{\partial}{\partial h} \mathcal{E}(0, h) \approx -\frac{\log_2(\pi/2)}{\sqrt{2\,\pi}} \frac{1}{\sqrt{1-h}}, \qquad (h \to 1^-). \tag{5.28}$$

From this divergence, the scaling hypothesis, and the assumption that the entanglement density is intensive, we can infer the known result [83] that the critical exponent $\nu = 1/2$ for the XX model. Moreover, from Eq. (5.21) we can extract the value of the dynamical exponent $z = 2$ for the XX model.

In keeping with the critical features of the XY-model phase diagram, for any small but nonzero value of the anisotropy, the critical divergence of the entanglement derivative is governed by Ising-type behavior. It is only at the $r = 0$ point that the critical behavior of the entanglement is governed by the XX universality class. For small r, XX behavior ultimately crosses over to Ising behavior.

We have mentioned that along the disorder line, $r^2+h^2=1$, the entanglement density vanishes. One extreme limit is the Ising case, i.e., $r=1$ and $h=0$, where the ground state is either $|\rightarrow\rightarrow\cdots\rightarrow\rangle$ or $|\leftarrow\leftarrow\cdots\leftarrow\rangle$, both of these being unentangled. Any superposition of them is also a valid ground state, but it has entanglement of order unity. In the thermodynamic limit the entanglement per spin is identically zero. Is this a general feature along the disorder line? Before we establish this, recall that the energies of the lowest two levels are given in Eqs. (5.18) and (5.19). Evaluating them at $r^2=1-h^2$, we immediately find that both are $-N$.

Now let us evaluate the expectation value of the Hamiltonian (5.4) with respect to a separable state with all spins pointing in the same direction:

$$\langle\mathcal{H}\rangle=-N\left(\frac{1+r}{2}\langle\sigma^x\rangle^2+\frac{1-r}{2}\langle\sigma^y\rangle^2+h\langle\sigma^z\rangle\right). \tag{5.29}$$

Denoting $x\equiv\langle\sigma^x\rangle$, $y\equiv\langle\sigma^y\rangle$, $z\equiv\langle\sigma^z\rangle$, we find that the above expression achieves its minimum value $-N$ at $r^2+h^2=1$ when

$$(x,y,z)=\left(\pm\sqrt{\frac{2r}{1+r}},0,\sqrt{\frac{1-r}{1+r}}\right). \tag{5.30}$$

Therefore, the separable state satisfying the above conditions is the ground state, and there is a Z_2 degeneracy. Hence, along the disorder line the entanglement density vanishes.

5.5 Concluding remarks

In summary, we have quantified the global entanglement of the quantum XY spin chain. This model exhibits a rich phase structure, the qualitative features of which are reflected by this entanglement measure. Perhaps the most interesting aspect is the divergence in the field-derivative of the entanglement as the critical line ($h=1$) is crossed. The behavior of the divergence is dictated by the universality class of the model. Furthermore, in the thermodynamic limit, the entanglement density vanishes on the disorder line ($r^2+h^2=1$). The structure of the entanglement surface, as a function of the parameters of the model (the magnetic field h and the coupling anistotropy r), is surprisingly rich.

We close by pointing towards a deeper connection between the global measure of entanglement and the correlations among quantum fluctuations. The maximal overlap (5.1) can be decomposed in terms of correlation functions (see Sec. 2.2.4):

$$\Lambda^2_{\max} = \frac{1}{2^N} + \frac{N}{2^N} \max_{|\vec{r}|=1} \Big\{ \langle \vec{r} \cdot \vec{\sigma}_1 \rangle + \frac{1}{2} \sum_{j=2}^{N} \langle \vec{r} \cdot \vec{\sigma}_1 \otimes \vec{r} \cdot \vec{\sigma}_j \rangle + \cdots \Big\},$$

where translational invariance is assumed and the Cartesian coordinates of $\vec{r}$ can be taken to be $(\sin\xi, 0, \cos\xi)$. The two-point correlations appearing in the decomposition are related to a bi-partite measure of entanglement, namely, the concurrence, which shows similar singular behavior [79] to Eq. (5.27). It would be interesting to establish the connection between the global entanglement and correlations more precisely, e.g., by identifying which correlators are responsible for the singular behavior in the entanglement and how they relate to the better known critical properties.

Appendix A

Local hidden variable theories and Bell-CHSH inequality

Local hidden variable (LHV) theories were conceived as alternatives for quantum mechanics and were constructed in order to explain the predictions of quantum mechanics in a statistical way without invoking the nonlocal features that quantum mechanics allows. The most natural quantity for two observers at a distance to measure is the correlation. Local hidden variable theories dictate that the outcome of some measurement is predetermined by the combination of measurement setting and some unknown local hidden variable, and that the result at one site should not be influenced by that at the other. Suppose A and B are operators to be measured at the two different sites, respectively. The correlation predicted by the LHV theories is

$$E_L(a,b) \equiv \int d\lambda\, \rho(\lambda) A(a,\lambda) B(b,\lambda), \tag{A.1}$$

where $A(a,\lambda) = \pm 1$ and $B(b,\lambda) = \pm 1$ are predetermined results for the measurement settings a for A and b for B depending on the local hidden variable λ; $\rho(\lambda)$ is the distribution for the local hidden variable. Locality requires that the outcome $A(a,\lambda)$ does not depend on b and that of $B(b,\lambda)$ does not depend on a. For two different settings at each site one arrives at the inequality

$$|E_L(a,b) + E_L(a,b') + E_L(a',b) - E_L(a',b')| \leq 2. \tag{A.2}$$

We shall see shortly that quantum mechanics can violate this inequality. To be specific, the operators to be measured are the Pauli operators $\vec{\sigma}$. The correlation

$$E_Q(a,b) \equiv \langle \vec{\sigma}\cdot\vec{a} \otimes \vec{\sigma}\cdot\vec{b}\rangle, \tag{A.3}$$

where $\vec{a}$ and $\vec{b}$ are unit vectors indicating the directions of the Stern-Gerlach apparata at A and B, respectively. Define

$$2B \equiv \vec{\sigma}\cdot\vec{a}\otimes\vec{\sigma}\cdot\vec{b} + \vec{\sigma}\cdot\vec{a}\otimes\vec{\sigma}\cdot\vec{b'} + \vec{\sigma}\cdot\vec{a'}\otimes\vec{\sigma}\cdot\vec{b} - \vec{\sigma}\cdot\vec{a'}\otimes\vec{\sigma}\cdot\vec{b'}. \tag{A.4}$$

It is straightforward to see that for a separable state $\rho_s = \sum_i p_i \rho_A^i \otimes \rho_B^i$

$$\max_{a,a',b,b'} |2\mathrm{Tr}(B\rho_s)| \leq 2, \tag{A.5}$$

namely, it never violates the inequality. But for a singlet state $(|\uparrow\downarrow\rangle - |\downarrow\uparrow\rangle)/\sqrt{2}$, we have

$$\max_{a,a',b,b'} |\langle 2B\rangle| = 2\sqrt{2}. \tag{A.6}$$

This can be achieved for the settings $\theta_a = 0$, $\theta_a' = \pi/2$, $\theta_b = \pi/4$, and $\theta_b' = -\pi/4$, where the angles are measured from the z-axis in the $z-x$ plane.

Gisin [4] was the first to show that for any entangled pure state, e.g., $\alpha|\uparrow\uparrow\rangle + \beta|\downarrow\downarrow\rangle$ with $\alpha\beta \neq 0$, the inequality is also violated. Horodecki and co-workers [92] derived the maximal violation for any two-qubit mixed states. It was then clear that there exist many mixed states that are entangled but do not violate the CHSH inequality. The question remains open whether there exists a Bell-like inequality that is necessary and sufficient for a state being entangled.

Appendix B

Schumacher's quantum data compression

B.1 Quantum Data Compression

To communicate quantum information by directly transmitting qubits may be costly. The idea of quantum data compression (QDC) is to ask the question whether we can compress the message into fewer qubits so as to minimize the cost of transmission. Schmacher has provided an answer to achieve this [21]. One excellent review of quantum data compression is by Preskill [93], which we follow here.

Let us go straight to the procedure of QDC. Suppose Alice needs to communicate with Bob through some noiseless quantum channel as efficiently as possible, that is, she hopes to compress her message using as few qubits as possible. The message consists of letters represented by some states $|\phi_x\rangle$. Since on average, the frequency of each letter's appearance may not be equal but is some probability p_x, the message can be said to be drawn from an ensemble of states:

$$\{|\phi_x\rangle, p_x\}, \tag{B.1}$$

so each letter has a density matrix $\boldsymbol{\rho} = \sum_x p_x |\phi_x\rangle\langle\phi_x|$. As we will see in the following, the lowest number of qubits per letter needed to encode is set by the von Neumann entropy $S(\rho) = -\mathrm{tr}(\rho \log_2 \rho)$. If we try to compress into fewer qubits, the fidelity of compression will be ruined.

If the total length of the message is n, then the message has a density matrix which is a direct

product of n letter density matrices

$$\boldsymbol{\rho}^{\otimes n} \equiv \underbrace{\boldsymbol{\rho} \otimes \cdots \otimes \boldsymbol{\rho}}_{n\ \rho\text{'s}}. \tag{B.2}$$

The procedure for quantum data compression goes as follows,

1) Diagonalize $\boldsymbol{\rho}$. Work in the orthonormal basis in which $\boldsymbol{\rho}$ is diagonal. If $\boldsymbol{\rho}$ has eigenvalues (arranged decreasingly) $\lambda_1 \geq \lambda_2 \geq \cdots \geq \lambda_d$(the number d depends on whether the state $|\phi\rangle$ is a qubit, tri-bit, or d-bit), then $\boldsymbol{\rho}^{\otimes n}$ has eigenvalues of the form (i.e., the eigenvalues are obtained by choosing n values from $\lambda_1, \lambda_2, \ldots, \lambda_d$)

$$\lambda(\{k_i\}) \equiv \prod_{i=1}^{d} \lambda_i^{k_i} = \lambda_1^{k_1} \lambda_2^{k_2} \cdots \lambda_d^{k_d}, \tag{B.3}$$

where $\sum_i^d k_i = n$, and each eigenvalue $\lambda(\{k_i\})$ occurs $N(\{k_i\}) = n!/(k_1!k_2! \cdots k_d!)$ times. We will restrict ourselves to qubits, i.e., $d = 2$: $\lambda(k_1, k_2 = n - k_1) = \lambda_1^{k_1}\lambda_2^{k_2}$, and $N(k_1, k_2) = C_{k_1}^n$.

2) Given a set of tolerances δ (tolerance for using slightly more qubits than the asymptotically optimal case) and ϵ (tolerance for not projecting onto the "typical" subspace), find the typical subspace Λ and its dual subspace $\Lambda^\perp$:

2a) First find out the smallest number $D(n)$ of necessary largest eigenvalues (suppose they are $\lambda_{n,1} \geq \lambda_{n,2} \geq \cdots \geq \lambda_{n,D}$) and corresponding eigenvectors$(|\lambda_{n,1}\rangle, |\lambda_{n,2}\rangle, \cdots, |\lambda_{n,D}\rangle)$ of $\boldsymbol{\rho}^{\otimes n}$ such that the sum of these eigenvalues is larger than $1 - \epsilon$, but the value $D(n)$ may be larger than $2^{n(S(\rho)+\delta)}$. Increase n and repeat the step until when $n > n_0$

$$D(n) \leq 2^{n(S(\rho)+\delta)}, \tag{B.4}$$

where n_0 is the smallest number such that the above inequality is satisfied. Note that it is sufficient to use at most some $n(S(\rho) + \delta)$ qubits to represent any state in Λ. This means there exists a unitary transformation $\boldsymbol{U}$ which takes any state $|\phi_\Lambda\rangle$ in Λ to

$$\boldsymbol{U}|\phi_\Lambda\rangle = |\phi_{\text{compressed}}\rangle|0_{\text{rest}}\rangle, \tag{B.5}$$

where $|\phi_{\rm compressed}\rangle$ is a state of $n(S(\rho)+\delta)$ qubits, and $|0_{\rm rest}\rangle$ is a state $|0\rangle\otimes\cdots|0\rangle$ of $(n-n(S+\delta))$ qubits.

2b) Those eigenvectors corresponding to the first $D(n)$ largest eigenvalues span a typical subspace Λ, the remaining spanning a dual subspace $\Lambda^{\perp}$. Note this division into two subspaces can be represented by a projection operator $\boldsymbol{E}$ which projects onto Λ and the complement of which $\mathbf{1}-\boldsymbol{E}$ to $\Lambda^{\perp}$. The condition that the sum of eigenvalues of eigenvectors in Λ is larger than $1-\epsilon$ can be rewritten as

$$\mathrm{tr}(\boldsymbol{\rho}^n\boldsymbol{E}) > 1-\epsilon. \tag{B.6}$$

This means states in Λ have much higher overlap with any state drawn from the ensemble than those in $\Lambda^{\perp}$.

3) Prepare the input state $|\psi\rangle = |\phi_1\rangle\cdots|\phi_n\rangle$, where $|\phi_i\rangle$ belongs to the ensemble in the Eq.(B.1). Make the unitary transformation $\boldsymbol{U}$ on $|\psi\rangle$, and measure the state of the last $(n-n(S+\delta))$ qubits mentioned above. If the result is $|0_{\rm rest}\rangle$, Alice successfully compresses $|\psi\rangle$ onto $|\psi_{\rm compressed}\rangle|0_{\rm rest}\rangle$, and she simply sends $|\psi_{\rm compressed}\rangle$ to Bob. On the other hand, if Alice gets the results other than $|0_{\rm rest}\rangle$, she fails to compress her message and the best she can do is send a state $|0'_{\rm compressed}\rangle$ which is the compressed state corresponding to the largest eigenvector $|\lambda_{n,1}\rangle$ in Λ,

$$\boldsymbol{U}|\lambda_{n,1}\rangle = |0'_{\rm compressed}\rangle|0_{\rm rest}\rangle. \tag{B.7}$$

We note that the input state $|\psi\rangle$ has much higher overlap with states in Λ than any other states in $\Lambda^{\perp}$, the result for Alice to get $|0_{\rm rest}\rangle$ is of high probability (larger than $1-\epsilon$).

4)Bob, after receiving $|\psi_{\rm compressed}\rangle$, appends $|0_{\rm rest}\rangle$ to it, and applies the inverse unitary transformation $\boldsymbol{U^{-1}}$. On average, Bob receives a density matrix

$$\boldsymbol{\rho}'^n = \boldsymbol{E}|\psi\rangle\langle\psi|\boldsymbol{E} + |\lambda_{n,1}\rangle\langle\lambda_{n,1}|\langle\psi|(\mathbf{1}-\boldsymbol{E})|\psi\rangle. \tag{B.8}$$

The averaged fidelity $\overline{F}$ of this procedure over the ensemble of possible messages $\{|\psi_i\rangle, p'_i\}$ can be shown to be larger than $1-2\epsilon$. It can also be shown that if we try to compress the message

into $n(S(\rho)-\delta)$ qubits, the fidelity will be arbitrarily small for sufficient large n.

Finally, we note quantum data compression cannot compress messages drawn from a completely(maximally) mixed state, since $S(\rho_{\text{ completely mixed}}) = 1$.

B.2 An Example

The example we will discuss shortly is for a small n. From previous discussion, we know for any given δ and ϵ, we can always find a number n_0, such that for any $n > n_0$, the procedure succeeds with the prescibed tolerances. In fact, for a given n, as ϵ becomes smaller, the necessary δ increases, which means we need more qubits to compress, as can be seen from the average number of qubits necessary to encode is $n(S(\rho)+\delta)$. On the other hand, for a given n, as δ decreases (we require fewer qubits to encode), ϵ increases, which means the average fidelity decreases, as can be seen from $\overline{F} > 1-2\epsilon$. Hence, there is some tradeoff between δ, and ϵ for a fixed finite n.

Suppose the ensemble consists of $\{(|H\rangle, p_H = \frac{1}{2}), (|D\rangle, p_D = \frac{1}{2})\}$, where $|H\rangle$ is the state of horizontal polarization while $|D\rangle$ is 45°,

$$|H\rangle = \begin{pmatrix} 1 \\ 0 \end{pmatrix},\ |D\rangle = \frac{1}{\sqrt{2}}\begin{pmatrix} 1 \\ 1 \end{pmatrix}. \tag{B.9}$$

The density matrix is

$$\rho = \frac{1}{2}|H\rangle\langle H| + \frac{1}{2}|D\rangle\langle D| = \begin{pmatrix} \frac{3}{4} & \frac{1}{4} \\ \frac{1}{4} & \frac{1}{4} \end{pmatrix}, \tag{B.10}$$

where the matrix is in $|H\rangle$ and $|V\rangle$ basis, and has two eigenvectors and eigenvalues

$$\begin{aligned} |Q\rangle = |22.5°\rangle &= \begin{pmatrix} \cos\frac{\pi}{8} \\ \sin\frac{\pi}{8} \end{pmatrix},\ \lambda_Q = \cos^2\frac{\pi}{8} \\ |\overline{Q}\rangle = |112.5°\rangle &= \begin{pmatrix} -\sin\frac{\pi}{8} \\ \cos\frac{\pi}{8} \end{pmatrix},\ \lambda_{\overline{Q}} = \sin^2\frac{\pi}{8}. \end{aligned} \tag{B.11}$$

The von Neumann entropy $S(\rho)$ is

$$S(\rho) = -\lambda_Q \log_2 \lambda_Q - \lambda_{\overline{Q}} \log_2 \lambda_{\overline{Q}} \approx 0.60088, \tag{B.12}$$

so the minimal number of qubits per letter needed to encode is about 0.6009.

Suppose Alice needs to send 3 letters to Bob, but she can afford only two qubits. Since $3{*}S(\rho) \approx 1.8$, it's possible to compress 3 letters using only 2 qubits with high fidelity. Note this means $\delta \approx 0.2$ and $D(n=3) = 2$. The eigenvalues and eigenvectors of ρ^3 are

$$\begin{aligned} &\lambda_1 = \cos^3 \tfrac{\pi}{8},\ \lambda_2 = \lambda_3 = \lambda_4 = \cos^2 \tfrac{\pi}{8} \sin \tfrac{\pi}{8}, \\ &\lambda_5 = \lambda_6 = \lambda_7 = \cos \tfrac{\pi}{8} \sin^2 \tfrac{\pi}{8},\ \lambda_8 = \sin^3 \tfrac{\pi}{8}. \end{aligned}$$

$$\begin{aligned} &|1\rangle = |QQQ\rangle,\ |2\rangle = |QQ\overline{Q}\rangle,\ |3\rangle = |Q\overline{Q}Q\rangle,\ |4\rangle = |\overline{Q}QQ\rangle, \\ &|5\rangle = |Q\overline{QQ}\rangle,\ |6\rangle = |\overline{Q}Q\overline{Q}\rangle,\ |7\rangle = |\overline{QQ}Q\rangle,\ |8\rangle = |\overline{QQQ}\rangle. \end{aligned} \tag{B.13}$$

The subspace Λ is spanned by $\{|1\rangle, |2\rangle, |3\rangle, |4\rangle\}$, while its dual subspace $\Lambda^\perp$ is by $\{|5\rangle, |6\rangle, |7\rangle, |8\rangle\}$, and

$$\begin{aligned} P_\Lambda &\equiv \mathrm{tr}(\rho^{\otimes 3} \boldsymbol{E}) = \sum_{i=1}^{4} \lambda_i \approx 0.9419 \\ P_\Lambda^\perp &\equiv \mathrm{tr}(\rho^{\otimes 3} (\mathbf{1} - \boldsymbol{E})) = \sum_{i=5}^{8} \lambda_i \approx 0.0581. \end{aligned} \tag{B.14}$$

Alice and Bob both agree on the form of the unitary transformation that they will use,

$$\mathrm{U} \begin{pmatrix} |1\rangle \\ |2\rangle \\ |3\rangle \\ |4\rangle \end{pmatrix} \rightarrow \begin{pmatrix} |HHH\rangle \\ |HVH\rangle \\ |VHH\rangle \\ |VVH\rangle \end{pmatrix} \quad \mathrm{U} \begin{pmatrix} |5\rangle \\ |6\rangle \\ |7\rangle \\ |8\rangle \end{pmatrix} \rightarrow \begin{pmatrix} |HHV\rangle \\ |HVV\rangle \\ |VHV\rangle \\ |VVV\rangle \end{pmatrix}; \tag{B.15}$$

this transformation is unitary since it is simply the transformation between two sets of orthonormal bases of 3 qubits.

Alice prepares her message in a state $|\psi\rangle$, which can be expanded in the basis of $|1\rangle \cdots |8\rangle$,

$$|\psi\rangle = \sum_{i=1}^{8} a_i |i\rangle, \tag{B.16}$$

where from Eq.(B.14) we have

$$\sum_{i=1}^{4} |a_i|^2 = P_\Lambda \gg \sum_{i=5}^{8} |a_i|^2 = P_\Lambda^\perp. \tag{B.17}$$

Then Alice applies the unitary transformation $\boldsymbol{U}$ on $|\psi\rangle$ followed by a measurement on the third qubit. If the result is $|H\rangle$, she sucessfully projects $|\psi\rangle$ into the likely subspace Λ. At this stage, the total state is

$$a_1|HHH\rangle + a_2|HVH\rangle + a_3|VHH\rangle + a_4|VVH\rangle = |\psi_{\text{compressed}}\rangle|H\rangle, \tag{B.18}$$

where $|\psi_{\text{compressed}}\rangle \equiv a_1|HH\rangle + a_2|HV\rangle + a_3|VH\rangle + a_4|VV\rangle$. She simply sends this two-qubit state $|\psi_{\text{compressed}}\rangle$ to Bob. Upon receiving $|\psi_{\text{compressed}}\rangle$, Bob appends a third qubit $|H\rangle$ to it, and does the inverse transformation $\boldsymbol{U^{-1}}$ to get

$$|\psi'\rangle = \boldsymbol{U^{-1}}(|\psi_{\text{compressed}}\rangle|H\rangle) = \sum_{i=1}^{4} a_i|i\rangle, \tag{B.19}$$

which has high resemblance to the initial $|\psi\rangle$, that is

$$F_1 \equiv |\langle\psi|\psi'\rangle|^2 = P_\Lambda \approx 0.9419. \tag{B.20}$$

On the other hand, if, when Alice measures the third qubit and gets $|V\rangle$, she fails to project $|\psi\rangle$ into Λ but $\Lambda^\perp$ instead, the best she can do is send a qubit state $|HH\rangle$. After Bob receives it and decompresses it, he gets

$$|\psi''\rangle = \boldsymbol{U^{-1}}(|HH\rangle|H\rangle) = |1\rangle, \tag{B.21}$$

which has overlap with the initial $|\psi\rangle$:

$$F_2 \equiv |\langle\psi|\psi''\rangle|^2 = |a_1|^2 = \lambda_1 \approx 0.6219. \tag{B.22}$$

The fidelity of this procedure is $F = P_\Lambda F_1 + P_\Lambda^\perp F_2 = 0.9234$.

How good is this? Let us compare it to the case when Alice sends the first two letters without compressing and asks Bob to guess the third letter. Since both $|H\rangle$ and $|D\rangle$ from the ensemble have higher overlap with $|Q\rangle$ than with $|\overline{Q}\rangle$, the best guess he can make is $|Q\rangle$. The fidelity of this procedure is

$$F = \frac{1}{2}|\langle H|Q\rangle|^2 + \frac{1}{2}|\langle D|Q\rangle|^2 = 0.8535, \tag{B.23}$$

which is smaller than the case when we do compression.

Appendix C

Wootters' formula

The entanglement of formation defined in Eq. (1.30) is, in general, difficult to calculate. However, for two-qubit systems, Wootters [22] has provided and proved the following formula:

$$E_{\mathrm{F}}(\rho) = h\left(\frac{1}{2}[1+\sqrt{1-C(\rho)^2}]\right), \tag{C.1}$$

where $h(x) \equiv -x\log_2 x - (1-x)\log_2(1-x)$, and $C(\rho)$, the *concurrence* of the state ρ, is defined as

$$C(\rho) \equiv \max\{0, \sqrt{\lambda_1} - \sqrt{\lambda_2} - \sqrt{\lambda_3} - \sqrt{\lambda_4}\}, \tag{C.2}$$

in which $\lambda_1, \ldots, \lambda_4$ are the eigenvalues of the matrix $\rho(\sigma_y \otimes \sigma_y)\rho^*(\sigma_y \otimes \sigma_y)$ in nonincreasing order and σ_y is a Pauli spin matrix. $E_{\mathrm{F}}(\rho)$, $C(\rho)$ and the *tangle* $\tau(\rho) \equiv C(\rho)^2$ are equivalent measures of entanglement, inasmuch as they are monotonic functions of one another. For pure state $a|00\rangle + b|01\rangle + c|10\rangle + d|11\rangle$ the concurrence C is $2|ad - bc|$.

Appendix D

Proof of entanglement monotone

In this appendix we prove in detail that the geometric measure of entanglement satisfies the criteria listed in Sec. 2.3, and hence it is an entanglement monotone. For convenience we list those criteria as follows

C1. (a) $E(\rho) \geq 0$; (b) $E(\rho) = 0$ if ρ is not entangled.

C2. Local unitary transformations do not change E.

C3. Local operations and classical communication (LOCC) (as well as post-selection) do not increase the expectation value of E.

C4. Entanglement is convex under the discarding of information, i.e., $\sum_i p_i\, E(\rho_i) \geq E(\sum_i p_i\, \rho_i)$.

From the definition (2.57)

$$E(\rho) \equiv (\mathrm{co}\, E_{\mathrm{pure}})(\rho) \equiv \min_{\{p_i, \psi_i\}} \sum\nolimits_i p_i\, E_{\mathrm{pure}}(|\psi_i\rangle),$$

it is evident that C1 and C2 are satisfied, provided that E_{pure} satisfies them, as it does for E_{pure} being any function of Λ_{max} consistent with C1. It is straightforward to check that C4 holds, by the convex hull construction. First, consider the case is which $\rho = \sum_i p_i |\psi_i\rangle\langle\psi_i|$. From the definition (2.57) of $E(\rho)$, which is the *minimum* over all decompositions, we have that $E(\rho) \leq \sum_i p_i E_{\mathrm{pure}}(|\psi_i\rangle)$. Hence we have that $E(\sum_i p_i |\psi_i\rangle\langle\psi_i|) \leq \sum_i p_i E(|\psi_i\rangle\langle\psi_i|)$, i.e., C4 is obeyed whenever the deomposition is into *pure* states. Second, allow ρ_i to be mixed. To deal with this case, express ρ_i as its optimal decomposition: $\rho_i = \sum_k q_{ik} |\psi_{ik}\rangle\langle\psi_{ik}|$, for which $E(\rho_i) = \sum_k q_{ik} E_{\mathrm{pure}}(|\psi_{ik}\rangle)$. Inserting the above

expression for ρ_i and $E(\rho_i)$ into the left hand side of the sought criterion, and using the pure-state result just proved, we find $\sum_i p_i E(\rho_i) = \sum_{ik} p_i\, q_{ik} E(|\psi_{ik}\rangle\langle\psi_{ik}|) \geq E(\sum_{ik} p_i\, q_{ik} |\psi_{ik}\rangle\langle\psi_{ik}|) = E(\sum_i p_i \rho_i)$. Thus we see that C4 is indeed obeyed.

The consideration of C3 seems to be more delicate. The reason is that our analysis of whether or not it holds depends on the explicit form of $E_{\rm pure}$. For C3 to hold, it is sufficient to show that the average entanglement is non-increasing under any trace-preserving, unilocal operation [1]: $\rho \to \sum_k V_k \rho V_k^\dagger$, where the Kraus operator V_k has the form $\mathbb{1} \otimes \cdots \mathbb{1} \otimes V_k^{(i)} \otimes \mathbb{1} \cdots \otimes \mathbb{1}$ and obeys $\sum_k V_k^\dagger V_k = \mathbb{1}$. Furthermore, it suffices to show that C3 holds for the case of a pure initial state, i.e., $\rho = |\psi\rangle\langle\psi|$.

We now prove that C3 holds for the particular (and by no means un-natural) choice $E_{\rm pure} = E_{\sin^2}$. To be precise, for any quantum operation on a pure initial state, i.e.,

$$|\psi\rangle\langle\psi| \to \sum\nolimits_k V_k |\psi\rangle\langle\psi| V_k^\dagger, \tag{D.1}$$

we aim to show that

$$\sum_k p_k\, E_{\sin^2}\left(V_k|\psi\rangle/\sqrt{p_k}\right) \leq E_{\sin^2}(|\psi\rangle), \tag{D.2}$$

where $p_k \equiv {\rm Tr}\, V_k|\psi\rangle\langle\psi|V_k^\dagger = \langle\psi|V_k^\dagger V_k|\psi\rangle$, regardless of whether the operation $\{V_k\}$ is state-to-state or state-to-ensemble. Let us denote by Λ and Λ_k the respective entanglement eigenvalues corresponding to $|\psi\rangle$ and the (normalized) pure state $V_k|\psi\rangle/\sqrt{p_k}$. Then our task is to show that $\sum_k p_k\, \Lambda_k^2 \geq \Lambda^2$, of which the left hand side is, by the definition of Λ_k, equivalent to

$$\sum_k p_k \max_{\xi_k \in D_s} \|\langle\xi_k|V_k|\psi\rangle/\sqrt{p_k}\|^2 = \sum_k \max_{\xi_k \in D_s} \|\langle\xi_k|V_k|\psi\rangle\|^2. \tag{D.3}$$

Without loss of generality, we may assume that it is the first party who performs the operation. Recall that the condition (2.9) for the closest separable state

$$|\phi\rangle \equiv |\tilde{\alpha}\rangle_1 \otimes |\tilde{\gamma}\rangle_{2\cdots n} \tag{D.4}$$

[1] What we mean by unilocal is that the operation is performed by only one of the parties. All general multi-party operations can be regarded as a sequence of unilocal operations

can be recast as

$$_{2\cdots n}\langle\tilde{\gamma}|\psi\rangle_{1\cdots n} = \Lambda|\tilde{\alpha}\rangle_1. \tag{D.5}$$

Then, by making the specific choice

$$\langle\xi_k| = (\langle\tilde{\alpha}|V_k^{(1)\dagger}/\sqrt{q_k}) \otimes \langle\tilde{\gamma}|, \tag{D.6}$$

where $q_k \equiv \langle\tilde{\alpha}|V_k^{(1)\dagger}V_k^{(1)}|\tilde{\alpha}\rangle$, we have the sought result

$$\sum_k p_k\Lambda_k^2 = \sum_k \max_{\xi_k\in D_s} \|\langle\xi_k|V_k|\psi\rangle\|^2 \geq \Lambda^2 \sum_k (\langle\tilde{\alpha}|V_k^{(1)\dagger}V_k^{(1)}|\tilde{\alpha}\rangle/\sqrt{q_k})^2 = \Lambda^2. \tag{D.7}$$

Hence, the form $1-\Lambda^2$, when generalized to mixed states, is an entanglement monotone. We note that a different approach to establishing this result has been used by Barnum and Linden [37]. Moreover, using the result that $\sum_k p_k\Lambda_k^2 \geq \Lambda^2$, one can further show that for any convex increasing function $f_c(x)$ with $x \in [0,1]$,

$$\sum_k p_k\, f_c(\Lambda_k^2) \geq f_c(\Lambda^2). \tag{D.8}$$

Therefore, the quantity $const. - f_c(\Lambda^2)$ (where the *const.* is to ensure the whole expression is non-negative), when extended to mixed states, is also an entanglement monotone, hence a good entanglement measure.

Appendix E

Three N-qubit Bell inequalities

E.1 Mermin-Klyshko-Bell inequality

In Appendix A we have discussed the Bell-CHSH inequality for two qubits. Here we will discuss its generalization to N qubits. The discussion here follows Dür [69]. First let us define a Pauli operator at arbitrary direction

$$\sigma_{a_k} \equiv \vec{\sigma} \cdot \vec{a}_k, \tag{E.1}$$

where $\vec{a}_k$ is a unit vector. The Mermin-Klyshko-Bell inequality is conveniently defined via Bell operators in a recursive way:

$$B_k = \frac{1}{2} B_{k-1} \otimes (\sigma_{a_k} + \sigma_{a'_k}) + \frac{1}{2} B'_{k-1} \otimes (\sigma_{a_k} - \sigma_{a'_k}), \tag{E.2}$$

with $B_1 \equiv \sigma_{a_1}$, $B'_1 \equiv \sigma_{a'_1}$, and B'_k is obtained from B_k by exchanging all a_k with a'_k and vice versa. For example,

$$B_2 = (\sigma_{a_1} \otimes \sigma_{a_2} + \sigma_{a'_1} \otimes \sigma_{a_2} + \sigma_{a_1} \otimes \sigma_{a'_2} - \sigma_{a'_1} \otimes \sigma_{a'_2})/2 \tag{E.3a}$$

$$B_3 = (\sigma_{a_1} \otimes \sigma_{a_2} \otimes \sigma_{a'_3} + \sigma_{a_1} \otimes \sigma_{a'_2} \otimes \sigma_{a_3} + \sigma_{a'_1} \otimes \sigma_{a_2} \otimes \sigma_{a_3} - \sigma_{a'_1} \otimes \sigma_{a'_2} \otimes \sigma_{a'_3})/2. \tag{E.3b}$$

It is easy to see that for real x, x', y, y' in the range $[-1, 1]$, we have that $|xy + xy' + x'y - x'y'| \leq 2$. As $\langle B_1 \rangle$ and $\langle B'_1 \rangle$ are evidently in the range $[-1, 1]$, local hidden variable theories will then predict that $|\langle B_2 \rangle| \leq 1$, and by induction $|\langle B_k \rangle| \leq 1$. However, quantum mechanics can violate this

inequality. In particular, for the N-partite GHZ state

$$|\mathrm{GHZ}\rangle = (|0\ldots0\rangle + |1\ldots1\rangle)/\sqrt{2}, \tag{E.4}$$

$|\langle B_N\rangle|$ can achieve the value $2^{(N-1)/2}$.

E.2 Three-setting Bell inequality

There are actually at least two approaches to define a three-setting Bell inequality. These all involve selecting three settings for measurement at each site. The first approach is to consider the linear combination of the joint probabilities or correlations $E_(\xi_1,\ldots,\xi_N)$, with ξ_i being chosen from three possible settings. The goal is to construct an inequality that is satisfied by local hidden variable theores whereas it can be violated by quantum mechanics. However, the number of such inequalities grows with the number of parties. It is only possible to exhaust all inequivalent inequalities for small number of parties, as investigated by Collins and Gisin [94] very recently. Here we shall focus on a second approach [1].

The basic idea of the second approach is that, for two vectors h and q, if $|\langle h|q\rangle| < ||q||^2$, this means that $h \neq q$. Specifically, h represents prediction from local hidden variables whereas q represents that from quantum mechanics. To be more precise, quantum mechanics predicts that for a state ρ_N the average outcome of the observables $\{O_i, i = 1,\ldots,N\}$ (with possible outcomes being ±1) at N locations is

$$E_Q(\xi_1,\ldots,\xi_N) \equiv \mathrm{Tr}(O_1\cdots O_N\rho_N), \tag{E.5}$$

where ξ_k is the measurement setting at the k-th location. A local hidden variable theory predicts

$$E_L(\xi_1,\ldots,\xi_N) = \int d\lambda\,\rho(\lambda)\prod_{k=1}^{N} I_k(\xi_k,\lambda), \tag{E.6}$$

where $\rho(\lambda)$ is the probability distribution for the local hidden variable λ, and $I_k(\xi_k,\lambda)$ is the outcome ascribed by the local hidden variable λ for the observable $O_k(\xi_k)$ measured with the

[1] It would be interesting to compare the difference between the two approaches.

apparatus setting ξ_k.

The inner product between $E(\xi_1, \ldots, \xi_N)$ and $E'(\xi_1, \ldots, \xi_N)$ is defined as

$$\langle E|E'\rangle \equiv \sum_{\xi_1,\ldots,\xi_N} E(\xi_1, \ldots, \xi_N)\, E'(\xi_1, \ldots, \xi_N), \tag{E.7}$$

where each ξ has three different values. If it can be shown that $|\langle E_Q|E_L\rangle|^2 < ||E_Q||^2$ then the two theories have different predictions. Zukowski and Kaszlikowski [95] considered the following basis to be measured:

$$|\pm, \xi_i\rangle_i \equiv (|0\rangle_i \pm |1\rangle_i)/\sqrt{2} \tag{E.8}$$

for party i. For the N-partite GHZ state they chose three values for ξ_1: $(\pi/6, \pi/2, 5\pi/6)$, and for ξ_i: $(0, \pi/3, 2\pi/3)$ for $i = 2, \ldots, N$. They showed that

$$|\langle E_L|E_Q\rangle| \leq 2^{N-1}\sqrt{3} < \|E_Q\|^2 = 3^N/2. \tag{E.9}$$

Thus, the two theories, LHV and quantum mechanics, have different predictions.

E.3 Functional Bell inequality

The idea of functional Bell inequality [72] is to consider a continuous range of measurement settings, instead of a finite number. The inner product between $E(\xi_1, \ldots, \xi_N)$ and $E'(\xi_1, \ldots, \xi_N)$ for the continuous setting is defined as

$$\langle E|E'\rangle \equiv \int [\prod_{i=1}^{N} d\xi_i] E(\xi_1, \ldots, \xi_N)\, E'(\xi_1, \ldots, \xi_N). \tag{E.10}$$

Similarly, if it can be shown that $|\langle E_Q|E_L\rangle|^2 < ||E_Q||^2$ then the two theories have different predictions. Sen and co-workers considered the same measurement basis as in Eq. (E.8), with $\xi_i \in [0, 2\pi]$. They showed that

$$|\langle E_L|E_Q\rangle| \leq 4^N < \|E_Q\|^2 = (2\pi)^N/2. \tag{E.11}$$

Thus again, the two theories, LHV and quantum mechanics, have different predictions.

To compare the three-setting and the functional inequalities, we mention that for the Dür's

bound entangled state (4.6) discussed in Sec. 4.3, violation is achieved using the three-setting one only when $N \geq 7$ whereas for the functional one $N \geq 6$, the latter being stronger.

Appendix F

Unextendible product bases and bound entangled states

To illustrate the idea of the unextendible product basis and its connection to bound entanglement, we shall give an explicit example. The discussion here follows Ref. [65]. product basis is a set S of pure orthogonal product states, which span a subspace $\mathcal{H}_S$ of $\mathcal{H}$, a bi- or multi-partite quantum system. For example, $S = \{|0,1,+\rangle, |1,+,0\rangle, |+,0,1\rangle, |-,-,-\rangle\}$ in a three-qubit system, where we have defined $|\pm\rangle \equiv (|0\rangle \pm |1\rangle)/\sqrt{2}$. It is straightforward to check that these basis states are orthogonal to one another.

This set has the peculiar property that it is not possible to add an additional basis vector that is a product state. Suppose we add $|a,b,c\rangle$. This then requires that

$$\langle a,b,c|0,1,+\rangle = \langle a,b,c|1,+,0\rangle = \langle a,b,c|+,0,1\rangle = \langle a,b,c|-,-,-\rangle = 0. \tag{F.1}$$

But each of $|a\rangle$, $|b\rangle$, and $|c\rangle$ can be, at most, orthogonal to any of the four states $|0\rangle$, $|1\rangle$, $|+\rangle$, and $|-\rangle$. Hence, together, $|a,b,c\rangle$ can be orthogonal to three of the four states in S. This means that the set S cannot be extended, hence, the name unextendible product basis (UPB). Therefore, the subspace that is orthogonal to the space by the UPB contains no product states, nor mixture of them.

What is the use of UPB? It turns out that it can be used to construct a bound entangled state.

Suppose $S = \{|\psi_1\rangle, \ldots, |\psi_n\rangle\}$ contains a UPB. Then the mixed state

$$\rho = \frac{1}{D-n}\left(\mathbb{1} - \sum_{j=1}^{n} |\psi_j\rangle\langle\psi_j|\right) \tag{F.2}$$

is a bound entangled state, where D is the total dimension (e.g., D=8 in the above three-qubit example).

The state ρ is entangled because it lies in the subspace $\mathcal{H} - \mathcal{H}_S$, in which, by construction, there is no product state, and hence, it cannot be written as a decomposition of pure product states. To see that its entanglement is bound, we can look at its partial transpose with respect to all bi-partite partitionings. As a product state is mapped to a product state under partial transpose and the identity is unchanged, ρ, under partial transpose, is mapped to a valid density matrix, which has non-negative eigenvalues. Therefore, ρ has PPT, and hence no entanglement can be established across any bi-partite cut via local operations and classical communication. We have then shown that the uniform mixture on the subspace complementary to that spanned by a UPB is a bound entangled state. In particular, the state

$$\rho = \frac{1}{4}\left(\mathbb{1} - |0,1,+\rangle\langle 0,1,+| - |1,+,0\rangle\langle 1,+,0| - |+,0,1\rangle\langle +,0,1| - |-,-,-\rangle\langle -,-,-|\right) \tag{F.3}$$

is bound entangled. We have shown previously in Sec. 4.4 that such a state cannot violate, e.g., the Mermin-Klyshko-Bell inequality.

Appendix G

Derivation of overlap of the ground state with the separable Ansatz state

In this appendix we derive the results shown in Eqs. (5.24) and (5.25). We first analyze $b = 1/2$ case, viz., the even-fermion case. The lowest state $|\Psi_{1/2}(r,h)\rangle$ has zero number of Bogoliubov fermions. It is related to the state that has no c-fermions, i.e., $|\Omega\rangle \equiv |\uparrow \cdots \uparrow\rangle$ via

$$|\Psi_{1/2}(r,h)\rangle = \prod_{m=0}^{m<\frac{N-1}{2}} \cos\theta_m^{(1/2)}(r,h) e^{i\tan\theta_m^{(1/2)}(r,h)\,\tilde{c}_m^{(1/2)\dagger}\tilde{c}_{N-m-1}^{(1/2)\dagger}}|\Omega\rangle \tag{G.1a}$$

$$= \prod_{m=0}^{m<\frac{N-1}{2}} \Big[\cos\theta_m(r,h) + i\sin\theta_m(r,h)\,\tilde{c}_m^\dagger\tilde{c}_{N-m-1}^\dagger\Big]|\Omega\rangle. \tag{G.1b}$$

The Ansatz state is then

$$|\Phi(\xi)\rangle = \prod_{j=1}^{N}\Big[\cos\frac{\xi}{2} + \sin\frac{\xi}{2}\prod_{1\le l<j}(1-2c_l^\dagger c_l)(c_j^\dagger - c_j)\Big]|\Omega\rangle \tag{G.2a}$$

$$= \prod_{j=1}^{N}\big(\cos\frac{\xi}{2} + \sin\frac{\xi}{2}\,c_j^\dagger\big)|\Omega\rangle \tag{G.2b}$$

$$= \cos^N\frac{\xi}{2}\, e^{\tan\frac{\xi}{2}c_1^\dagger}\cdots e^{\tan\frac{\xi}{2}c_N^\dagger}|\Omega\rangle \tag{G.2c}$$

$$= \cos^N\frac{\xi}{2}\, e^{\tan\frac{\xi}{2}\sum_{j=1}^N c_j^\dagger} e^{\tan^2\frac{\xi}{2}\sum_{j<l}c_j^\dagger c_l^\dagger}|\Omega\rangle, \tag{G.2d}$$

where we have suppressed the index (1/2). The term $\sum_{j<l}c_j^\dagger c_l^\dagger$ can be rewritten in momentum space as

$$\sum_{1\le j<l\le N} c_j^\dagger c_l^\dagger = i\sum_{m=0}^{m<\frac{N-1}{2}}\cot\frac{\pi(m+\frac{1}{2})}{N}\tilde{c}_m^\dagger\tilde{c}_{N-m-1}^\dagger. \tag{G.3}$$

Thus, for even N

$$|\Phi(\xi)\rangle = \left(1+\tan\frac{\xi}{2}\sum_{j=1}^{N}c_j^\dagger\right)\prod_{m=0}^{m<\frac{N-1}{2}}\left(\cos^2\frac{\xi}{2}+i\sin^2\frac{\xi}{2}\cot\frac{\pi(m+\frac{1}{2})}{N}\tilde{c}_m^\dagger\tilde{c}_{N-m-1}^\dagger\right)|\Omega\rangle, \tag{G.4a}$$

whereas for odd N

$$|\Phi(\xi)\rangle = \left(1+\tan\frac{\xi}{2}\sum_{j=1}^{N}c_j^\dagger\right)\cos\frac{\xi}{2}\prod_{m=0}^{m<\frac{N-1}{2}}\left(\cos^2\frac{\xi}{2}+i\sin^2\frac{\xi}{2}\cot\frac{\pi(m+\frac{1}{2})}{N}\tilde{c}_m^\dagger\tilde{c}_{N-m-1}^\dagger\right)|\Omega\rangle. \tag{G.4b}$$

Therefore, the overlap of the state $|\Psi_{1/2}(r,h)\rangle$ with $|\Phi(\xi)\rangle$ for even N is

$$\langle\Psi_{1/2}(r,h)|\Phi(\xi)\rangle = \prod_{m=0}^{m<\frac{N-1}{2}}\left(\cos\theta_m^{(1/2)}(r,h)\,\cos^2\frac{\xi}{2}+\sin\theta_m^{(1/2)}(r,h)\,\sin^2\frac{\xi}{2}\cot\frac{\pi(m+\frac{1}{2})}{N}\right), \tag{G.5a}$$

whereas for odd N

$$\langle\Psi_{1/2}(r,h)|\Phi(\xi)\rangle = \cos\frac{\xi}{2}\prod_{m=0}^{m<\frac{N-1}{2}}\left(\cos\theta_m^{(1/2)}(r,h)\,\cos^2\frac{\xi}{2}+\sin\theta_m^{(1/2)}(r,h)\,\sin^2\frac{\xi}{2}\cot\frac{\pi(m+\frac{1}{2})}{N}\right). \tag{G.5b}$$

Next, we discuss the $b=0$ (odd-fermion) case. The lowest allowed state is the one with one $\gamma_0^{(0)}=\tilde{c}_0^{(0)}$ fermion:

$$|\Psi_0(r,h)\rangle \equiv \gamma_0^{(0)\dagger}|G(r,h)\rangle = \tilde{c}_0^{(0)\dagger}|G(r,h)\rangle, \tag{G.6}$$

where $|G(r,h)\rangle$ is the state with no γ fermions:

$$|G(r,h)\rangle = \prod_{m=1}^{m<\frac{N}{2}}\left[\cos\theta_m^{(0)}(r,h)+i\sin\theta_m^{(0)}(r,h)\,\tilde{c}_m^{(0)\dagger}\tilde{c}_{N-m}^{(0)\dagger}\right]|\Omega\rangle. \tag{G.7}$$

Similar to the $b=1/2$ case, by using

$$\sum_{1\le j<l\le N}c_j^\dagger c_l^\dagger = i\sum_{m=1}^{m<\frac{N}{2}}\cot\frac{\pi m}{N}\tilde{c}_m^{(0)\dagger}\tilde{c}_{N-m}^{(0)\dagger}, \tag{G.8}$$

we obtain that for even N

$$|\Phi(\xi)\rangle = \left(1 + \sqrt{N}\tan\frac{\xi}{2}\,\tilde{c}_0^\dagger\right)\cos^2\frac{\xi}{2}\prod_{m=1}^{m<\frac{N}{2}}\left(\cos^2\frac{\xi}{2} + i\sin^2\frac{\xi}{2}\cot\frac{\pi m}{N}\tilde{c}_m^\dagger\tilde{c}_{N-m}^\dagger\right)|\Omega\rangle, \tag{G.9a}$$

whereas for odd N

$$|\Phi(\xi)\rangle = \left(1 + \sqrt{N}\tan\frac{\xi}{2}\,\tilde{c}_0^\dagger\right)\cos\frac{\xi}{2}\prod_{m=1}^{m<\frac{N}{2}}\left(\cos^2\frac{\xi}{2} + i\sin^2\frac{\xi}{2}\cot\frac{\pi m}{N}\tilde{c}_m^\dagger\tilde{c}_{N-m}^\dagger\right)|\Omega\rangle. \tag{G.9b}$$

Therefore, the overlap of $|\Psi_0(r,h)\rangle$ with $|\Phi(\xi)\rangle$ for even N is

$$\langle\Psi_0(r,h)|\Phi(\xi)\rangle = \sqrt{N}\sin\frac{\xi}{2}\prod_{m=1}^{m<\frac{N}{2}}\left(\cos\theta_m^{(0)}(r,h)\,\cos^2\frac{\xi}{2} + \sin\theta_m^{(0)}(r,h)\,\sin^2\frac{\xi}{2}\cot\frac{\pi m}{N}\right), \tag{G.10}$$

whereas for odd N

$$\langle\Psi_0(r,h)|\Phi(\xi)\rangle = \sqrt{N}\sin\frac{\xi}{2}\cos\frac{\xi}{2}\prod_{m=1}^{m<\frac{N}{2}}\left(\cos\theta_m^{(0)}(r,h)\,\cos^2\frac{\xi}{2} + \sin\theta_m^{(0)}(r,h)\,\sin^2\frac{\xi}{2}\cot\frac{\pi m}{N}\right). \tag{G.11}$$

Appendix H

Analysis of singular behavior of entanglement density

In this Appendix we investigate the singular behavior of the entanglement density near the critical line $h = 1$ for both anisotropic ($r \neq 0$) and isotropic ($r = 0$) cases. We begin with $r \neq 0$ case first.

H.1 Divergence of entanglement-derivative for the anisotropic XY models

The starting point is Eq. (5.26), in which there is a maximization over the variable ξ. The function to be maximized is

$$F(\xi, r, h) \equiv \int_0^{\frac{1}{2}} d\mu \, \ln \left[\cos\theta(\mu, r, h) \cos^2(\xi/2) + \sin\theta(\mu, r, h) \sin^2(\xi/2) \cot \pi\mu \right]. \tag{H.1}$$

To find the stationarity condition, we demand the derivative with respect to ξ vanishes:

$$\partial_\xi F(\xi, r, h)\Big|_{\xi=\xi*} = -\frac{1}{2} \sin\xi \int_0^{\frac{1}{2}} d\mu \, \frac{\cos\theta(\mu, r, h) - \sin\theta(\mu, r, h) \cot \pi\mu}{\cos\theta(\mu, r, h) \cos^2(\xi/2) + \sin\theta(\mu, r, h) \sin^2(\xi/2) \cot \pi\mu}\Big|_{\xi=\xi*} = 0. \tag{H.2}$$

Denote by $\xi^*(h)$ the solution for fixed r. Then the field-derivative of the entanglement is

$$\partial_h \mathcal{E}(r, h) = -\frac{2}{\ln 2} \partial_h F(\xi^*(h), h) = -\frac{2}{\ln 2} \left[\frac{\partial \xi^*(h)}{\partial h} \partial_\xi F(\xi, h)\Big|_{\xi^*} + \partial_h F(\xi^*, h) \right] = -\frac{2}{\ln 2} \partial_h F(\xi^*, h), \tag{H.3}$$

where the first term in the square bracket vanishes identically due to the condition (H.2). Thus

(dropping the * on ξ for convenience),

$$\begin{aligned}\partial_h \mathcal{E}(r,h) &= -\frac{2}{\ln 2}\partial_h F(\xi^*,h) &\text{(H.4)}\\ &= -\frac{2}{\ln 2}\int_0^{\frac{1}{2}} d\mu\, \frac{\partial_h \cos\theta(\mu,r,h)\cos^2(\xi/2)+\partial_h \sin\theta(\mu,r,h)\sin^2(\xi/2)\cot\pi\mu}{\cos\theta(\mu,r,h)\cos^2(\xi/2)+\sin\theta(\mu,r,h)\sin^2(\xi/2)\cot\pi\mu}. &\text{(H.5)}\end{aligned}$$

Recall that $\tan 2\theta(\mu,r,h) \equiv r\sin 2\pi\mu/(h-\cos 2\pi\mu)$ and thus

$$\cos\theta = \sqrt{(1+\cos 2\theta)/2},\ \sin\theta = \sqrt{(1-\cos 2\theta)/2}, \tag{H.6a}$$

$$\cos 2\theta(\mu,r,h) = \frac{h-\cos 2\pi\mu}{\sqrt{(r\sin 2\pi\mu)^2+(h-\cos 2\pi\mu)^2}}. \tag{H.6b}$$

Putting everything in Eq. (H.5), we get

$$\begin{aligned}\partial_h \mathcal{E}(r,h) &= -\frac{r}{\ln 2}\int_0^{\frac{1}{2}} d\mu\, \frac{\sin 2\pi\mu}{(r\sin 2\pi\mu)^2+(h-\cos 2\pi\mu)^2}\\ &\quad \frac{\sqrt{\sqrt{\quad}-(h-\cos 2\pi\mu)}\cos^2(\xi/2)-\sqrt{\sqrt{\quad}+(h-\cos 2\pi\mu)}\sin^2(\xi/2)\cot\pi\mu}{\sqrt{\sqrt{\quad}+(h-\cos 2\pi\mu)}\cos^2(\xi/2)+\sqrt{\sqrt{\quad}-(h-\cos 2\pi\mu)}\sin^2(\xi/2)\cot\pi\mu}, &\text{(H.7)}\end{aligned}$$

where $\sqrt{\quad} \equiv \sqrt{(r\sin 2\pi\mu)^2+(h-\cos 2\pi\mu)^2}$.

We aim to explore the behavior near $h=1$. First consider $h>1$ and define $\epsilon \equiv h-1$, which is the deviation from the critical point. Make the change of variables $t = h-\cos 2\pi\nu$, giving lower and upper limits ϵ and $2+\epsilon$, respectively. We further shift the integration variable by ϵ, arriving at

$$\begin{aligned}\partial_h \mathcal{E}(r,h) &= -\frac{r}{2\pi\ln 2}\int_0^2 d\,t\frac{1}{(1-r^2)t^2+2(r^2+\epsilon)t+\epsilon^2}\\ &\quad \frac{\sqrt{t}\sqrt{\sqrt{\quad}-(t+\epsilon)}\cos^2(\xi/2)-\sqrt{\sqrt{\quad}+(t+\epsilon)}\sin^2(\xi/2)\sqrt{2-t}}{\sqrt{t}\sqrt{\sqrt{\quad}+(t+\epsilon)}\cos^2(\xi/2)+\sqrt{\sqrt{\quad}-(t+\epsilon)}\sin^2(\xi/2)\sqrt{2-t}}, &\text{(H.8)}\end{aligned}$$

where $\sqrt{\quad} = \sqrt{(1-r^2)t^2+2(r^2+\epsilon)t+\epsilon^2}$.

As we inspect the limit $h\to 1$ or $\epsilon\to 0$, we see that the above expression diverges, with the contribution coming from t small, i.e., infrared divergence. Large $t(\le 2)$ does not contribute to the divergence. Note further that only the second term in the numerator contributes to the divergence.

We then proceed to evaluate the integral by separating it into two parts:

$$\int_0^2 = \int_0^\delta + \int_\delta^2, \tag{H.9}$$

with $\delta \ll 1$. In the first region we only need to keep t to first order at most. Also noting that for $t, \epsilon \ll 1$, the first term in the denominator is much smaller than the second term, we get

$$-\frac{r}{2\pi \ln 2} \int_0^\delta d\, t \frac{-1}{2r^2(t + \frac{\epsilon^2}{2r^2})} \frac{\sqrt{\sqrt{2(r^2+\epsilon)t + \epsilon^2} + (t+\epsilon)}}{\sqrt{\sqrt{2(r^2+\epsilon)t + \epsilon^2} - (t+\epsilon)}}. \tag{H.10}$$

Next, we simplify the second term (ignoring ϵ when there is no danger in doing so)

$$\frac{\sqrt{\sqrt{2(r^2+\epsilon)t + \epsilon^2} + (t+\epsilon)}}{\sqrt{\sqrt{2(r^2+\epsilon)t + \epsilon^2} - (t+\epsilon)}} = \frac{\sqrt{t + \frac{\epsilon^2}{2r^2}}}{\sqrt{t}} + \frac{t+\epsilon}{\sqrt{2r^2 t}}. \tag{H.11}$$

Observing that only the first term on the right-hand side contributes to the divergence, we have that the divergent part is

$$-\frac{r}{2\pi \ln 2} \int_0^\delta d\, t \frac{-1}{2r^2(t + \frac{\epsilon^2}{2r^2})} \frac{\sqrt{t + \frac{\epsilon^2}{2r^2}}}{\sqrt{t}} = \frac{1}{4r\pi \ln 2} \int_0^{\delta 2r^2/\epsilon^2} d\, t \frac{1}{\sqrt{t+1}} \frac{1}{\sqrt{t}}. \tag{H.12}$$

The divergence part is then (for $\delta 2r^2/\epsilon^2 \gg 1$)

$$\frac{1}{4r\pi \ln 2} 2 \sinh^{-1} \sqrt{\delta 2r^2/\epsilon^2} \approx \frac{1}{2r\pi \ln 2} \ln \left(2\sqrt{\delta 2r^2/\epsilon^2} \right) = -\frac{1}{2r\pi \ln 2} \ln \epsilon + \frac{\ln \left(2\sqrt{\delta 2r^2} \right)}{2r\pi \ln 2}. \tag{H.13}$$

As the integral (H.8) does not depend on the choice of δ, the part that involves δ must be cancelled by the second half of the integration $\int_\delta^2$, which can be verified by direct evaluation. Therefore, for h very close to $h_c = 1$, we have

$$\frac{\partial \mathcal{E}}{\partial h} \approx -\frac{1}{2\pi r \ln 2} \ln |h - 1|. \tag{H.14}$$

In deriving the above divergence form, we have assumed that $r \neq 0$. Similar consideration can be applied to the case when h approaches 1 from below, and the behavior is the same.

H.2 Divergence of entanglement-derivative for the XX limit of the model

We now analyze the $r = 0$ isotropic case. It turns out that the analysis for this case is much simpler. To see this, we first note when $r = 0$ we have the simplification

$$\cos 2\theta(\mu, h) = \mathrm{sgn}(h - \cos 2\pi\mu). \tag{H.15}$$

The above expression changes sign when $h = \cos 2\pi\nu$. So let us introduce the variable $\mu_0 \equiv (\cos^{-1} h)/(2\pi)$. The expression for the entanglement density Eq. (5.26) becomes

$$\begin{aligned} \mathcal{E}(h) &= -\frac{2}{\ln 2} \max_{\xi} \int_0^{\frac{1}{2}} d\mu \, \ln \left[\cos\theta(\mu, r, h) \cos^2(\xi/2) + \sin\theta(\mu, r, h) \sin^2(\xi/2) \cot \pi\mu \right] & \text{(H.16a)} \\ &= -\frac{2}{\ln 2} \max_{\xi} \left[\int_0^{\mu_0} d\mu \, \ln \sin^2(\xi/2) \cot \pi\mu + \int_{\mu_0}^{\frac{1}{2}} d\mu \, \ln \cos^2(\xi/2) \right]. & \text{(H.16b)} \end{aligned}$$

Demanding stationarity with respect to ξ gives the condition

$$[\mu_0 - \frac{1}{4}(1 - \cos\xi)] \sin\xi = 0. \tag{H.17}$$

The solution $\xi = 0$ gives the entanglement density for $h \geq 1$. It is straightforward to see from Eq. (H.16a) that the entanglement density is identically zero. The solution $\mu_0 - \frac{1}{4}(1 - \cos\xi) = 0$ gives

$$\cos\xi = 1 - \frac{2}{\pi} \cos^{-1} h. \tag{H.18}$$

This in turn gives the entanglement density for $0 \leq h \leq 1$:

$$\mathcal{E}(h) = -\frac{2}{\ln 2} \left[\mu_0(h) \ln \frac{2\mu_0(h)}{1 - 2\mu_0(h)} + \frac{1}{2} \ln(1 - 2\mu_0(h)) + \int_0^{\mu_0(h)} d\mu \ln \cot \pi\mu \right]. \tag{H.19}$$

Thus we have derived the entanglement density as a function of the magnetic field h in the XX limit. The result is shown in Fig. (5.2).

We see from the figure that the entanglement density at $h = 0$ is the highest, which being $\mathcal{E}(0) = 1 - 2\gamma_C/(\pi \ln 2) \approx 0.159$ by evaluating Eq. (H.19) at $h = 0$. The constant $\gamma_C \approx 0.9160$

is the *Catalan* constant. The entanglement density decreases monotonically as h increases until $h = 1$ beyond which it becomes zero identically. This qualitative behavior can be understood as follows. As the total z-component spin is conserved, increasing h simply increases the z-component spin of the ground state until $h = 1$ where all the spins are aligned with the field, hence there is no entanglement beyond this value of h.

By directly taking the derivative with respect to h, we get

$$\partial_h \mathcal{E}(h) = \frac{1}{\pi \ln 2\sqrt{1-h^2}} \ln \left[\frac{\cos^{-1} h}{\pi - \cos^{-1} h} \sqrt{\frac{1+h}{1-h}} \right]. \tag{H.20}$$

Near $h \approx 1$, we have (putting $1 + h = 2$ and evaluating the limit in the argument of log function)

$$\frac{\partial}{\partial h}\mathcal{E}(0,h) \approx -\frac{\log_2(\pi/2)}{\sqrt{2}\,\pi} \frac{1}{\sqrt{1-h}}, \qquad (h \to 1^-). \tag{H.21}$$

This completes our derivation of the singular behavior of the entanglement density near the critical points.

Appendix I

Finite-size scaling

The discussion here follows Barber [91]. In the vicinity of the bulk critical temperature T_C the behavior of a system should depend on $y \equiv L/\xi(T)$, where $\xi(T)$ is the bulk correlation length and L is the characteristic length of the system. How does the divergence of certain thermodynamic quantities emerge as the system size L grows?

I.1 Algebraic divergence

Assume that some thermodynamic quantity at $L \to \infty$ diverges as $t \equiv (T - T_C)/T_C \to \infty$:

$$P_\infty(T) \sim C_\infty t^{-\rho}. \tag{I.1}$$

Finite-size scaling hypothesis asserts that for finite L and T near T_C,

$$P_L(T) \sim l^\omega Q_P(l^{1/\nu}\tilde{t}), \quad l \to \infty, \ \tilde{t} \to 0, \tag{I.2}$$

where $l \equiv L/a$ (a is some microscopic length), $\tilde{t} \equiv [T - T_C(L)]$. The exponent ω can be determined by the requirement that the $P_L(T)$ reproduces $P_\infty(T)$ as $l \to \infty$. Thus,

$$Q_P(x) \sim C_\infty x^{-\rho}, \quad x \to \infty, \tag{I.3}$$

and $\omega = \rho/\nu$. We consider the case that the finite system does not exhibit a true transition, then

$$Q_P(x) \to Q_0, \quad x \to 0. \tag{I.4}$$

From this we have that at the peak or rounding temperature $T_m^*(l)$ (where P_L reaches the maximum or deviates significantly from the bulk value)

$$P_L(T_m^*(l)) \sim Q_0 l^{\rho/\nu}, \quad l \to \infty. \tag{I.5}$$

This means that the behavior of a thermodynamic quantity varies with the system size is determined by the bulk critical exponent.

I.2 Logarithmic divergence

Now assume the thermodynamic quantity $P(T)$ diverges logarithmically as

$$P_\infty(T) \sim C_\infty \ln t, \quad t \to 0, \tag{I.6}$$

as in the field-derivative of the entanglement density for anisotropic XY spin chains. The finite-size scaling hypothesis in this case is to assume

$$P_L(T) - P_L(T_0) \sim Q_P(l^{1/\nu}\tilde{t}) - Q_P(l^{1/\nu}\tilde{t}_0), \tag{I.7}$$

where T_0 is some non-critical temperature and $\tilde{t}_0 \equiv (T_0 - T_C(L))/T_C$. The hypothesis has to recover the $l \to \infty$ limit at fixed T, which requires

$$Q_P(x) \sim C_\infty \ln x, \quad x \to \infty. \tag{I.8}$$

Thus in the limit $\tilde{t} \to 0$ at fixed large l, we have

$$P_L(T_C(L)) \sim -\frac{C_\infty}{\nu} \ln l + O(1), \tag{I.9}$$

if $Q_P(x) = O(1)$ as $x \to 0$. This allows us to obtain the exponent ν by analyzing how the divergence develops as the system size l (which is N in our spin-chain entanglement problem) increases.

References

[1] J. F. Clauser, M. A. Horne, A. Shimony, R. A. Holt, Phys. Rev. Lett. **23**, 880 (1969).

[2] A. Aspect, J. Dalibard, G. Roger, Phys. Rev. Lett. **49**, 1804 (1982).

[3] P. G. Kwiat, E. Waks, A. G. White, I. Appelbaum, and P. H. Eberhard, Phys. Rev. A **60**, 773 (1999).

[4] N. Gisin, Phys. Lett. A **154**, 201 (1991).

[5] A. K. Ekert, Phys. Rev. Lett. **67**, 661 (1991).

[6] C. H. Bennett and S. J. Wiesner, Phys. Rev. Lett. **69**, 2881 (1992).

[7] C. H. Bennett, G. Brassard, C. Crépeau, R. Jozsa, A. Peres, and W. K. Wootters, Phys. Rev. Lett. **70**, 1895 (1993).

[8] P. W. Shor, in *Proceedings of the 35th Annual Symposium on the Foundations of Computer Science*, edited by S. Goldwasser (IEEE Computer Society, Los Alamitos, CA), p. 124; also in e-print quant-ph/9508027. A. Ekert and R. Jozsa, Rev. Mod. Phys. **68**, 733 (1996).

[9] L. K. Grover, Phys. Rev. Lett. **79**, 325 (1997); L. K. Grover, Phys. Rev. Lett. **80**, 4329 (1998).

[10] R. Raussendorf and H. J. Briegel, Phys. Rev. Lett. **86**, 5188 (2001).

[11] R. F. Werner, Phys. Rev. A **40**, 4277 (1989).

[12] A. Peres, Phys. Rev. Lett. **77**, 1413 (1996).

[13] M. Horodecki, P. Horodecki, and R. Horodecki, Phys. Lett. A **223**, 1 (1996).

[14] K. Życzkowski, P. Horodecki, A. Sanpera, and M. Lewenstein, Phys. Rev. A **58**, 883 (1998).

[15] G. Vidal and R. F. Werner, Phys. Rev. A **65**, 032314 (2002).

[16] C. H. Bennett, H. J. Bernstein, S. Popescu, and B. Schumacher, Phys. Rev. **A53**, 2046 (1996).

[17] C. H. Bennett, G. Brassard, S. Popescu, B. Schumacher, J. Smolin, and W. K. Wootters, Phys. Rev. Lett. **76**, 722 (1996).

[18] M. Horodecki, P. Horodecki, and R. Horodecki, Phys. Rev. Lett. **78**, 574 (1997).

[19] M. Horodecki, P. Horodecki, and R. Horodecki, Phys. Rev. Lett. **80**, 5239 (1998).

[20] C. H. Bennett, D. P. DiVincenzo, J. A. Smolin, and W. K. Wootters, Phys. Rev. **A54**, 3824 (1996).

[21] B. Schumacher, Phys. Rev. **A 51**, 2738 (1995).

[22] W. K. Wootters, Phys. Rev. Lett. **80**, 2245 (1998).

[23] B. M. Terhal and K. G. H. Vollbrecht, Phys. Rev. Lett. **85**, 2625 (2000).

[24] K. G. H. Vollbrecht and R. F. Werner, Phys. Rev. A **64**, 062307 (2001).

[25] P. W. Shor, e-print quant-ph/0305035.

[26] V. Vedral and M. B. Plenio, Phys. Rev. A**57**, 1619 (1998).

[27] V. Vedral, M. B. Plenio, M. A. Rippin, and P. L. Knight, Phys. Rev. Lett. **78**, 2275 (1997).

[28] M. Horodecki, P. Horodecki, and R. Horodecki, Phys. Rev. Lett. **84**, 2014 (2000).

[29] M. A. Nielsen already considered this simple two-spin model in his Ph.D. thesis, University of New Mexico (1998).

[30] B. M. Terhal, A. C. Doherty, and D. Schwab, Phys. Rev. Lett. **90**, 157903 (2003).

[31] P. G. Kwiat, S. Barraza-Lopez, A. Stefanov, and N. Gisin, Nature **409**, 1014 (2001).

[32] W. Dür, G. Vidal, and J. I. Cirac, Phys. Rev. A **62**, 062314 (2000).

[33] C. H. Bennett, S. Popescu, D. Rohrlich, J. A. Smolin, and A. V. Thapliyal, Phys. Rev. A **63**, 012307 (2001).

[34] F. Verstraete, J. Dehaene, and B. De Moor, Phys. Rev. A **65**, 032308 (2002).

[35] J. Eisert and H. J. Briegel, Phys. Rev. A **64**, 022306 (2001).

[36] A. Shimony, Ann. NY. Acad. Sci. **755**, 675 (1995).

[37] H. Barnum and N. Linden, J. Phys. A: Math. Gen. **34**, 6787 (2001).

[38] T.-C. Wei and P. M. Goldbart, Phys. Rev. A **68**, 042307 (2003).

[39] J. K. Stockton, J. M. Geremia, A. C. Doherty, and H. Mabuchi, Phys. Rev. A **67**, 022112 (2003).

[40] S. Bravyi, Phys. Rev. A **67**, 012313 (2003).

[41] O. Gühne, P. Hyllus, D. Bruß, A. Ekert, M. Lewenstein, C. Macchiavello, and A. Sanpera, Phys. Rev. A **66**, 062305 (2002).

[42] G. Vidal, J. Mod. Opt. **47**, 355 (2000).

[43] M. Horodecki and P. Horodecki, Phys. Rev. A **59**, 4206 (1999).

[44] G. Vidal, Phys. Rev. A **62**, 062315 (2000).

[45] See e.g., C. B. Barber, D. P. Dobkin, and H. T. Huhdanpaa, ACM Trans. on Mathematical Software **22**, 469 (1996).

[46] T.-C. Wei, K. Nemoto, P. M. Goldbart, P. G. Kwiat, W. J. Munro, and F. Verstraete, Phys. Rev. A **67**, 022110 (2003).

[47] This ordering difficulty has been discussed in the settings of two qubits in many places, e.g., Ref. [51]; J. Eisert and M. B. Plenio, J. Mod. Opt. **46**, 145 (1999); S. Virmani and M. B. Plenio, Phys. Lett. A **268**, 31 (2000); F. Verstraete, K. Audenaert, J. Dehaene, and B. De Moor, J. Phys. A **34**, 10327 (2001), as well as in Ref. [46].

[48] M. B. Plenio and V. Vedral, J. Phys. A **34**, 6997 (2001).

[49] A. Acín, D. Bruß, M. Lewenstein, and A. Sanpera, Phys. Rev. Lett **87**, 040401 (2001).

[50] J. Eisert, P. Hyllus, O. Gühne, M. Curty, e-print quant-ph/0407135.

[51] K. Życzkowski, Phys. Rev. A **60**, 3496 (1999).

[52] A. Peres, Phys. Lett. A **202**, 16 (1995).

[53] As we shall show later, this state has $E_{\mathrm{R}} = \log_2(9/4)$, exactly the value cited in Ref. [48] from a numerical result.

[54] T.-C. Wei, J. B. Altepeter, P. M. Goldbart, and W. J. Munro, Phys. Rev. A **70**, 022322 (2004).

[55] T.-C. Wei, M. Ericsson, P. M. Goldbart, and W. J. Munro, Quantum Inf. Comput. **4**, 252 (2004).

[56] S. Ishizaka, Phys. Rev. A **67**, 060301 (2003).

[57] K. Audenaert, J. Eisert, E. Jané, M. B. Plenio, S. Virmani, and B. De Moor, Phys. Rev. Lett. **87**, 217902 (2001); K. Audenaert, M. B. Plenio, and J. Eisert, Phys. Rev. Lett. **90**, 027901 (2003).

[58] A. Acín, G. Vidal, and J. I. Cirac, Quantum Inf. and Comput. **3**, 55 (2003). G. Vidal and J. I. Cirac, Phys. Rev. Lett. **86**, 5803 (2001).

[59] W. J. Munro, D. F. V. James, A. G. White, and P. G. Kwiat, Phys. Rev. A **64**, 030302 (2001).

[60] S. Ishizaka, J. Phys. A: Math. Gen., **35**, 8075 (2002).

[61] S. Wu and Y. Zhang, Phys. Rev. A **63**, 012308 (2000).

[62] E. F. Galvao, M. B. Plenio, and S. Virmani, J. Phys. A **33**, 8809 (2000).

[63] V. Vedral, e-print quant-ph/0405102.

[64] P. Horodecki, Phys. Lett. A **232**, 333 (1997).

[65] C. H. Bennett, D. P. DiVincenzo, T. Mor, P. W. Shor, J. A. Smolin, and B. M. Terhal, Phys. Rev. Lett. **82**, 5385 (1999).

[66] Dagmar Brußand Asher Peres Phys. Rev. A **61**, 030301 (2000).

[67] J. A. Smolin, Phys. Rev. A **63**, 032306 (2001).

[68] P. W. Shor, J. A. Smolin, and A. V. Thapliyal, Phys. Rev. Lett. **90**, 107901 (2003).

[69] W. Dür, Phys. Rev. Lett. **87**, 230402 (2001).

[70] P. Horodecki, M. Horodecki, and R. Horodecki, Phys. Rev. Lett. **82**, 1056 (1999).

[71] D. Kaszlikowski, J. L. Chen, C. H. Oh, and L. C. Kwek, Phys. Rev. A **66**, 052309 (2002).

[72] A. Sen(De), U. Sen, and M. Żukowski, Phys. Rev. A **66**, 062318 (2002).

[73] In arriving at this result we have made a hypothesis about the form of the closest separable pure state. The result has been verified numerically for the $N = 4$ case.

[74] P. Horodecki et al., Acta Phys. Slov. **48**, 144 (1998).

[75] A. Acín, Phys. Rev. Lett. **88**, 027901 (2002).

[76] W. Dür and J. I. Cirac, Phys. Rev. A **62**, 022302 (2000).

[77] W. Dür and J. I. Cirac, Phys. Rev. A **61**, 042314 (2000).

[78] T. J. Osborne and M. A. Nielsen, Phys. Rev. A **66**, 032110 (2002).

[79] A. Osterloh, L. Amico, G. Falci, and R. Fazio, Nature **416**, 608 (2002).

[80] G. Vidal, J. I. Latorre, E. Rico, and A. Kitaev, Phys. Rev. Lett. **90**, 227902 (2003).

[81] P. Calabrese and J. Cardy, e-print hep-th/0405152

[82] H. Barnum, Emanuel Knill, Gerardo Ortiz, Rolando Somma, and Lorenza Viola Phys. Rev. Lett. **92**, 107902 (2004).

[83] S. Sachdev, *Quantum phase transitions* (Cambridge University Press, 1999).

[84] A. Wong and N. Christensen, Phys. Rev. A **63**, 044301 (2001).

[85] N. Lambert, C. Emary, and T. Brandes, Phys. Rev. Lett. **92**, 073602 (2004).

[86] S.-J. Gu, S.-S. Deng, Y.-Q. Li, and H.-Q. Lin, e-print quant-ph/0405067.

[87] F. Verstraete, M. Popp, and J. I. Cirac, Phys. Rev. Lett. **92**, 027901 (2004). F. Verstraete, M. A. Martin-Delgado, and J. I. Cirac, Phys. Rev. Lett. **92**, 087201 (2004).

[88] M. Henkel, *Conformal Invariance and Critical Phenomena* (Springer, 1999).

[89] E. Lieb, T. Schultz, and D. Mattis, Ann. Phys. **60**, 407 (1961).

[90] We have confirmed this Ansatz numerically for small numbers of spins.

[91] M. N. Barber, in *Phase Transitions and Critical Phenomena*, Vol. 8, p.158-161, C. Domb and J. L. Lebowitz (eds.) (Academic, London, 1983).

[92] R. Horodecki, P. Horodecki, and M. Horodecki, Phys. Lett. A **200**, 340 (1995).

[93] J. Preskill, "http://www.theory.caltech.edu/people/preskill/ph229"

[94] D. Collins and N. Gisin, J. Phys. A **7**, 1775 (2004).

[95] M. Żukowski and D. Kaszlikowski, Phys. Rev. A **56**, 1682 (1997).

Vita

Tzu-Chieh Wei was born in Taichung, Taiwan on February 25, 1973. He received his B.S. in Physics with a minor in Mathematics in 1994 and M.S. in Physics in 1996, both from National Taiwan University. He fulfilled his obligatory military service from 1996 to 1998. He entered the Ph.D. program in Physics at the University of Illinois in 1999.

List of Publications

1. "Two-qubit mixed states and the entanglement-entropy frontier", T.-C. Wei, K. Nemoto, P.M. Goldbart, P.G. Kwiat, W.J. Munro, and F. Verstraete, Proceedings of the 6th international conference on quantum communication, measurement and computing, July 22-26, 2002, p.37-40, ed. J.H. Shapiro and O. Hirota, Rinton Press, 2003.

2. "Taming entanglement", P.G. Kwiat, J.B. Altepeter, D. Branning, E. Jeffrey, N. Peters, and T.-C. Wei, Proceedings of the 6th international conference on quantum communication, measurement and computing, July 22-26, 2002, p.117-122, ed. J.H. Shapiro and O. Hirota, Rinton Press, 2003.

3. "Quantum information with optics", T.-C. Wei, Physics Bimonthly, **25**, p.555-564 (2003), published by the Physical Society of the Republic of China, Taipei, Taiwan.

4. "Maximal entanglement versus entropy for mixed quantum states", T.-C. Wei, K. Nemoto, P. M. Goldbart, P. G. Kwiat, W. J. Munro, and F. Verstraete, Phys. Rev A **67**, 022110 (2003).

5. "Ancilla-assisted quantum process tomography", J. B. Altepeter, D. Branning, E. Jeffrey, T.-C. Wei, P. G. Kwiat, R. T. Thew, J. L. O'Brien, M. A. Nielsen, and A. G. White, Phys. Rev. Lett. **90**, 193601 (2003).

6. "Geometric measure of entanglement for bipartite and multipartite quantum states", T.-C. Wei and P. M. Goldbart, Phys. Rev. A **68**, 042307 (2003).

7. "Maximally entangled mixed states: creation and concentration", N. A. Peters, J. B. Altepeter, D. A. Branning, E. R. Jeffrey, T.-C. Wei, and P. G. Kwiat, Phys. Rev. Lett. **92**, 133601 (2004).

8. "Benchmarking and procrustean noise reduction of entangled mixed states", N. A. Peters, T.-C. Wei, P. G. Kwiat, Proc. SPIE Vol. **5468**, p.269-281, Fluctuations and Noise in Photonics and Quantum Optics II; Ed. Peter Heszler, 2004.

9. "h/e magnetic flux modulation of the energy gap in nanotube quantum dots", U. C. Coskun, T.-C. Wei, S. Vishveshwara, P. M. Goldbart, and A. Bezryadin, Science **304**, 1132 (2004).

10. "Connections between relative entropy of entanglement and geometric measure of entanglement", T.-C. Wei, M. Ericsson, P. M. Goldbart, and W. J. Munro, Quantum Info. Comput. **4**, 252 (2004).

11. "Measures of entanglement in bound entangled states", T.-C. Wei, J. B. Altepeter, P. M. Goldbart, and W. J. Munro, Phys. Rev. A **70**, 022322 (2004).

12. "Mixed state sensitivity of several quantum information benchmarks", N. A. Peters, T.-C. Wei, and P. G. Kwiat, to appear in Phy. Rev. A **70**; e-print quant-ph/0407172.

13. "Synthesizing arbitrary two-photon polarization mixed states", T.-C. Wei, J. B. Altepeter, D. A. Branning, P. M. Goldbart, D. F. V. James, E. Jeffrey, P. G. Kwiat, S. Mukhopadhyay, and N. A. Peters, submitted to Phys. Rev. A.

14. "Global entanglement and quantum criticality in spin chains", T.-C. Wei, D. Das, S. Mukhopadyay, S. Vishveshwara, and P. M. Goldbart, e-print quant-ph/0405162.

15. "Quantifying multipartite entanglement", T.-C. Wei, J. B. Altepeter, D. Das, M. Ericsson, P. M. Goldbart, S. Mukhopadyay, W. J. Munro, and S. Vishveshwara, to appear in the Proceedings of the 7th international conference on quantum communication, measurement and computing.